ARO 24626.209-PH-UIR

The CECOM Center for Night Vision and Electro-Optics

AD-A233 779

OPTOELECTRONIC WORKSHOPS

XXVII

SEMICONDUCTOR LASERS AND THEIR APPLICATIONS

December 17, 1990

sponsored jointly by

ARO-URI Center for Opto-Electronic Systems Research
The Institute of Optics, University of Rochester

91 4 01 010

REPORT DOCUMENTATION PAGE

Form Approved
OMB No. 0704-0188

Public reporting burden for this collection of information is estimated to average 1 hour per response, including the time for reviewing instructions, searching existing data sources, gathering and maintaining the data needed, and completing and reviewing the collection of information. Send comments regarding this burden estimate or any other aspect of this collection of information, including suggestions for reducing this burden, to Washington Headquarters Services, Directorate for Information Operations and Reports, 1215 Jefferson Davis Highway, Suite 1204, Arlington, VA 22202-4302, and to the Office of Management and Budget, Paperwork Reduction Project (0704-0188), Washington, DC 20503.

1. AGENCY USE ONLY *(Leave blank)*

2. REPORT DATE
12/17/90

3. REPORT TYPE AND DATES COVERED
Interim Technical

4. TITLE AND SUBTITLE
Optoelectronic Workshop XXVII: Semiconductor Lasers and Their Applications

5. FUNDING NUMBERS
DAAL03-86-K-0173

6. AUTHOR(S)
Govind Agrawal and C. Ward Trussell

7. PERFORMING ORGANIZATION NAME(S) AND ADDRESS(ES)
The Institute of Optics
University of Rochester
Rochester, NY 14627

8. PERFORMING ORGANIZATION REPORT NUMBER

9. SPONSORING/MONITORING AGENCY NAME(S) AND ADDRESS(ES)
U. S. Army Research Office
P. O. Box 12211
Research Triangle Park, NC 27709-2211

10. SPONSORING/MONITORING AGENCY REPORT NUMBER
ARO 24626.209-PH-UIR

11. SUPPLEMENTARY NOTES
The view, opinions and/or findings contained in this report are those of the author(s) and should not be construed as an official Department of the Army position, policy, or decision, unless so designated by other documentation.

12a. DISTRIBUTION/AVAILABILITY STATEMENT
Approved for public release; distribution unlimited.

12b. DISTRIBUTION CODE

13. ABSTRACT *(Maximum 200 words)*

This workshop on "Semiconductor Lasers and Their Applications" represents the twenty-seventh of a series of intensive academic / government interactions in the field of advanced electro-optics, as part of the Army sponsored University Research Initiative. By documenting the associated technology status and dialogue it is hoped that this baseline will serve all interested parties towards providing a solution to high priority Army requirements. Responsible for program and program execution are Dr. Nicholas George, University of Rochester (ARO-URI), and Dr. Rudolf Buser, CCNVEO.

14. SUBJECT TERMS
Optoelectronic workshop; semiconductor; lasers

15. NUMBER OF PAGES

16. PRICE CODE

17. SECURITY CLASSIFICATION OF REPORT	18. SECURITY CLASSIFICATION OF THIS PAGE	19. SECURITY CLASSIFICATION OF ABSTRACT	20. LIMITATION OF ABSTRACT
UNCLASSIFIED	UNCLASSIFIED	UNCLASSIFIED	UL

NSN 7540-01-280-5500

Standard Form 298 (Rev 2-89)
Prescribed by ANSI Std Z39-18
298-102

The CECOM Center for Night Vision and Electro-Optics

OPTOELECTRONIC WORKSHOPS

XXVII

SEMICONDUCTOR LASERS AND THEIR APPLICATIONS

December 17, 1990

sponsored jointly by

ARO-URI Center for Opto-Electronic Systems Research
The Institute of Optics, University of Rochester

A-1

OPTOELECTRONIC WORKSHOP

ON

SEMICONDUCTOR LASERS AND THEIR APPLICATIONS

Organizer: ARO-URI -University of Rochester and CECOM Center for Night Vision and Electro-Optics

1. INTRODUCTION

2. SUMMARY -- INCLUDING FOLLOW-UP

3. VIEWGRAPH PRESENTATIONS

   CECOM Center for Night Vision and Electro-Optics
   Organizer -- C. Ward Trussell

   ARO-URI Center for Opto-Electronic Systems Research
   Organizer -- Govind Agrawal

   Welcome and Overview
   C. Ward Trussell, CCNVEO

   Dynamics of Semiconductor Lasers and Amplifiers
   Govind Agrawal, ARO-URI

   Laser Diode Array Research at Night Vision Lab
   David Caffey, CCNVEO

   MBE Growth for Visible and Near-Infrared Lasers
   Gary Wicks, ARO-URI

   Intensity-Phase Coupling in Semiconductor Lasers
   Thomas Brown, ARO-URI

   High-Power Laser Diode Array Measurements
   Vernon King, CCNVEO

   Intensity and Phase Noise in Semiconductor Lasers
   George Gray, ARO-URI

   Diode-Pumped Solid-State Laser Amplifiers
   Richard Utano, CCNVEO

   Quantum-Well Dynamics
   Mark Biermann, ARO-URI

4. LIST OF ATTENDEES

1. INTRODUCTION

This workshop on "Semiconductor Lasers and Their Applications" represents the twenty-seventh of a series of intensive academic / government interactions in the field of advanced electro-optics, as part of the Army sponsored University Research Initiative. By documenting the associated technology status and dialogue it is hoped that this baseline will serve all interested parties towards providing a solution to high priority Army requirements. Responsible for program and program execution are Dr. Nicholas George, University of Rochester (ARO-URI), and Dr. Rudolf Buser, CCNVEO.

2. SUMMARY AND FOLLOW-UP

The workshop on "Semiconductor Lasers and Their Applications" was organized jointly by Prof. Govind Agrawal of the University of Rochester and Dr. C. Ward Trussell of CECOM Center for Night Vision and Electro-Optics. It was held on December 17, 1990 at Fort Belvoir and was attended by 20 people, including 9 from the University of Rochester. The agenda consisted of 9 technical presentations of about 20-25 minutes with about 10 minutes devoted to scientific discussions at the end of each presentation. A final 30-minute session was devoted to a general discussion aimed at finding areas of potential collaborations.

Dr. C. Ward Trussell opened the workshop with an overview of the laser-diode programs at the CCNVEO. The talk was particularly useful to the scientists from the University of Rochester as it gave a clear indication of the objectives and the thrust behind the laser-diode research at CCNVEO.

The presentation by Prof. Govind Agrawal focused on the dynamic performance of semiconductor lasers. He presented the details of a model based on the generalized rate equations. The model takes into account both interband and intraband gain saturation and is particularly suited for a fundamental understanding of the limitations on the output power under current modulation. Dr. Trussell indicated that the model can be useful for the 1.5 μm laser program at CCNVEO.

The research on laser-diode arrays at CCNVEO was summarized by Mr. David Caffey. He indicated the program goals and discussed the current status. Basic steps behind the fabrication of laser diode arrays were presented in a clear way. He also mentioned the research on external-cavity lasers as it can be used to combine the output of multiple diodes coherently with a narrow spectrum.

Prof. Gary Wicks reviewed the status of the growth of III-V materials and devices by using the molecular-beam epitaxy (MBE) machine at the University of Rochester. The CCNVEO group was particularly interested if we were able to grow InGaAsP material in the wavelength range 1.5-1.6 μm. There is a possibility of future collaboration in this field.

The next talk by Prof. T. G. Brown discussed the intensity-phase coupling in semiconductor lasers. Such a coupling is governed by the linewidth enhancement factor. The emphasis of the presentation was to study how the linewidth enhancement factor may depend on the device structure and geometry, particularly in the case of distributed feedback lasers.

Mr. Vernon King presented the measurement techniques and the data used to quantify the material and device characteristics of laser diode arrays. The light-current curves, the near and far fields, and the optical spectrum were among the many measurements made to characterize such arrays.

The noise characteristics of semiconductor lasers were discussed by Dr. George Gray of the Institute of Optics. He mentioned how spontaneous emission leads to intensity and phase fluctuations in semiconductor lasers. The issues discussed were the relative intensity noise, mode-partition noise, frequency noise, and the laser linewidth. The laser linewidth was found to be considerably enhanced by the presence of a weak side mode due to cross-saturation effects.

Mr. Richard Utano of CCNVEO discussed how diode pumping can be used to produce high-efficiency Q-switched lasers and amplifiers. He presented the data on several diode-pumped Nd-ion lasers with different host materials. The role of fluorescence lifetime on the storage efficiency was considered and issues related to its optimization were discussed.

The final presentation of the workshop by Mr. Mark Biermann of the Institute of Optics focused on the quantum-well devices. In particular, he discussed how the subband structure is affected when two narrow quantum wells are brought closer. He has developed a sophisticated computer model to analyze the electrical and optical properties of coupled quantum-well devices.

After the formal presentations a concluding session followed in which all participants discussed various aspects of semiconductor lasers and their use for pumping solid-state lasers. The purpose of this technical discussion was to identify the follow-up items. Three possible areas were identified.

The material research related to the growth of InGaAsP material in the wavelength region 1.5-1.6 μm is of considerable interest to CCNVEO because of its applications in laser radars and range finders. Prof. Gary Wicks of the University of Rochester and Dr. Dave Caffey of CCNVEO will follow-up on this topic. The numerical modeling capability of Prof. Agrawal's group is of interest to CCNVEO for the purpose of exploring the power limitation on 1.5-μm InGaAsP lasers imposed by interband and intraband gain saturation. Prof. Agrawal of the University of Rochester and Dr. Trussell of CCNVEO intend to follow-up on this topic. There is some interest in the work on semiconductor-laser noise since it may relate to the coherent laser radar. Further technical discussions will continue to explore this topic.

The workshop ended at about 3:30 pm and was followed by a tour of various laboratories in the Lasers and Photonics Division.

CECOM CENTER FOR NIGHT VISION AND ELECTRO-OPTICS
LASER DIODE PROGRAMS OVERVIEW

LASER DIODE PROGRAMS OVERVIEW

Dr. C. Ward Trussell
Directed Energy Team
Laser Division

U. S. Army CECOM
Center for Night Vision & Electro-Optics

OCT 31 1990

CECOM CENTER FOR NIGHT VISION & ELECTRO-OPTICS

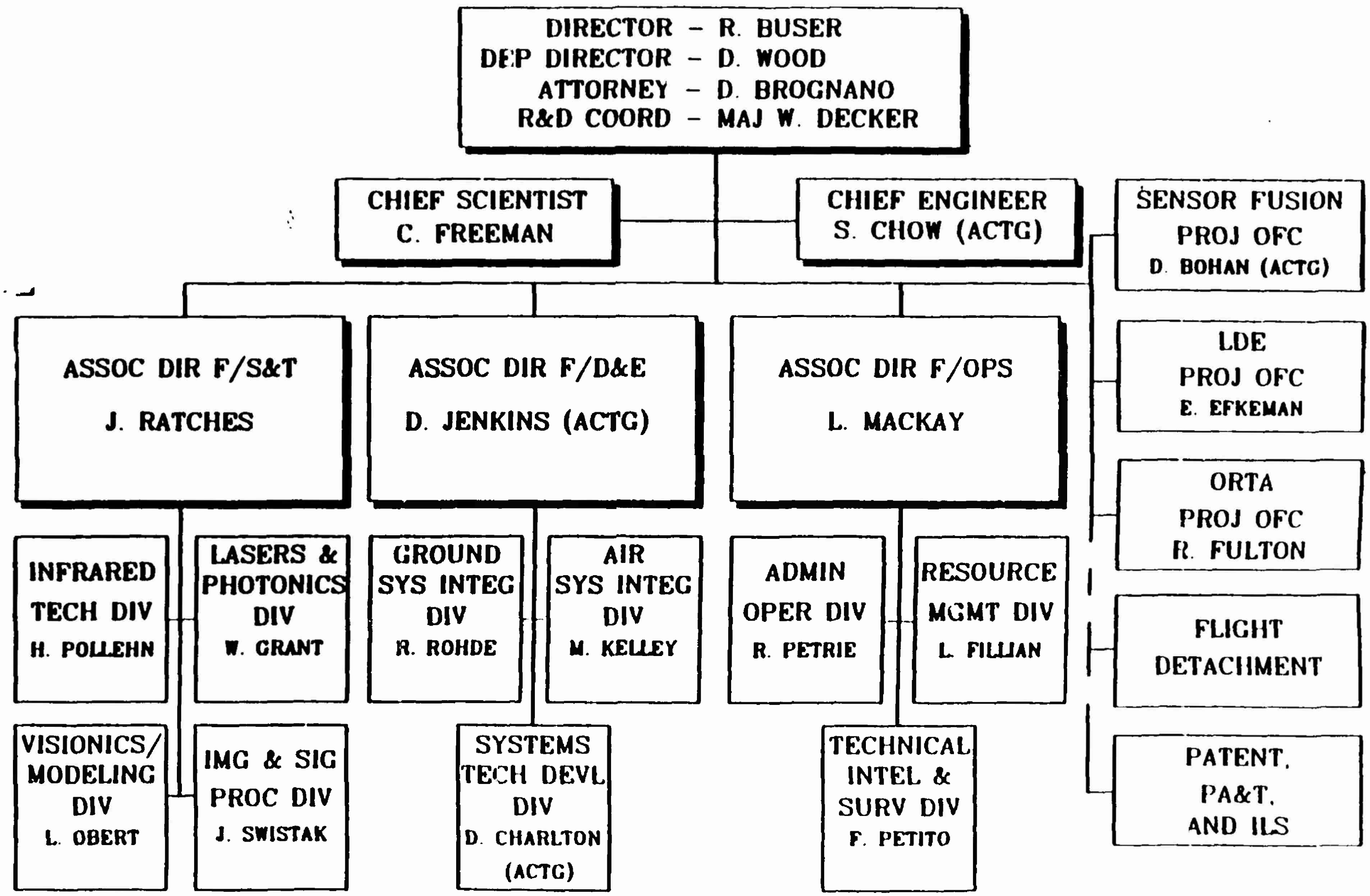

DIRECTED ENERGY TEAM

MAJOR PROJECTS

- LASER MATERIALS RESEARCH
- LASER DIODE ARRAYS
- DIODE PUMPED SOLID STATE LASERS
- FREQUENCY CONVERSION
- EYESAFE LASERS

LASER DIODE ARRAY PRODUCIBILITY PROGRAM

- JOINT ARMY, NAVY, AIR FORCE PROGRAM
- FUNDED BY BALANCED TECHNOLOGY INITIATIVE
- OBJECTIVE IS LOW COST, HIGH PERFORMANCE LASER ARRAYS FOR PUMPING SOLID STATE LASERS
- PRIMARY THRUST-STACKED ARRAYS-PHASE I
    1. Spectra Diode Laboratories
    2. McDonnell Douglas
    3. Advanced Optoelectronics
- SECONDARY THRUSTS - (SERVICE FUNDED)-PHASE I
    1. 2-D MONOLITHIC ARRAYS - TRW
    2. MBE GROWTH - NESI
- PHASE II - AWARDED AUGUST 1990 - SDL & AO

LASER DIODE ARRAY PRODUCIBILITY
PHASE I RESULTS

COMPANY	EFFICIENCY *	DELIVERIES	HIGHLIGHTS
Spectra Diode Lab	32% to 40% 36% Ave	2 20-bar 8 10-bar 5 5-bar 8.7 KWatt total	High Duty Factor, Low Cost Package High Yield
McDonnell Douglas	34% to 47% 42% Ave	7 25-bar 7 4-bar 10 KWatt total	High Efficiency High Uniformity Low Cost Package
Advanced Optoelect.	16% to 38% 27% Aver	1 20-bar 20 4-bar 5 KWatt total	Great Progress in Phase I High Vol.Potential

*Arrays tested by CNVEO

LDA PRODUCIBILITY

PHASE II PROGRAM

- FABRICATE 150 BARS - 807 nm. - SDL, AO
- FABRICATE 150 BARS - 785 nm. - SDL, AO
- DESIGN PACKAGE FOR 785 nm. ROD PUMP - SDL, AO
- ADVANCED ARRAY ANALYSIS FOR 20% DUTY - SDL, AO
  FABRICATE ARRAY TO VALIDATE DESIGN
- BACK COOLED CW ARRAY ANALYSIS - SDL
  FABRICATE ARRAY TO VALIDATE DESIGN
- IMPROVE YIELD, PERFORMANCE, THROUGHPUT - SDL
- OPTION FOR 1000 EACH 785 nm. BARS - SDL

LASER DIODE ARRAYS
FOR SOLID STATE LASER PUMPING

WAVELENGTH	MATERIAL	SS LASER
785 nm.	GaAlAs QW	Tm:YAG
795 nm.	GaAlAs QW	Nd:YLF
808 nm.	GaAlAs QW	Nd:YAG/Glass
970 nm.	GaInAs SL QW	Er:Glass/YAG

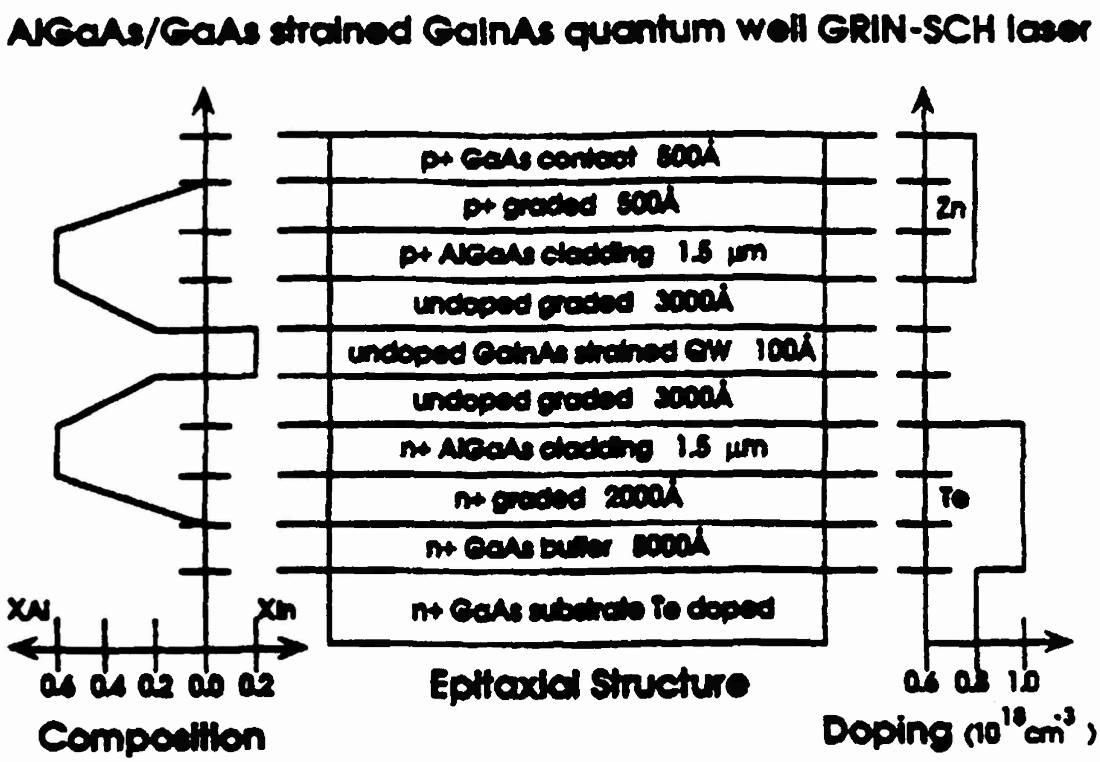

Figure 1. GRIN-SCH diode epitaxial structure (not to scale). The actual indium concentration in the quantum well is estimated to be 22%.

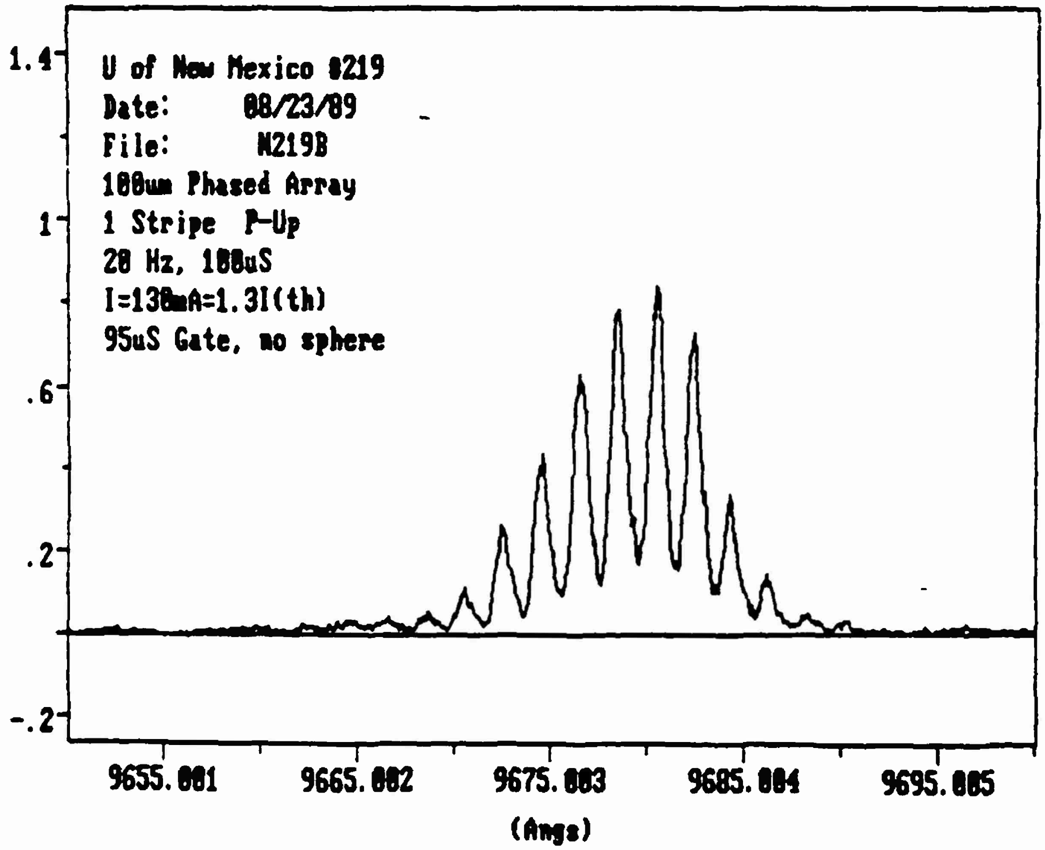

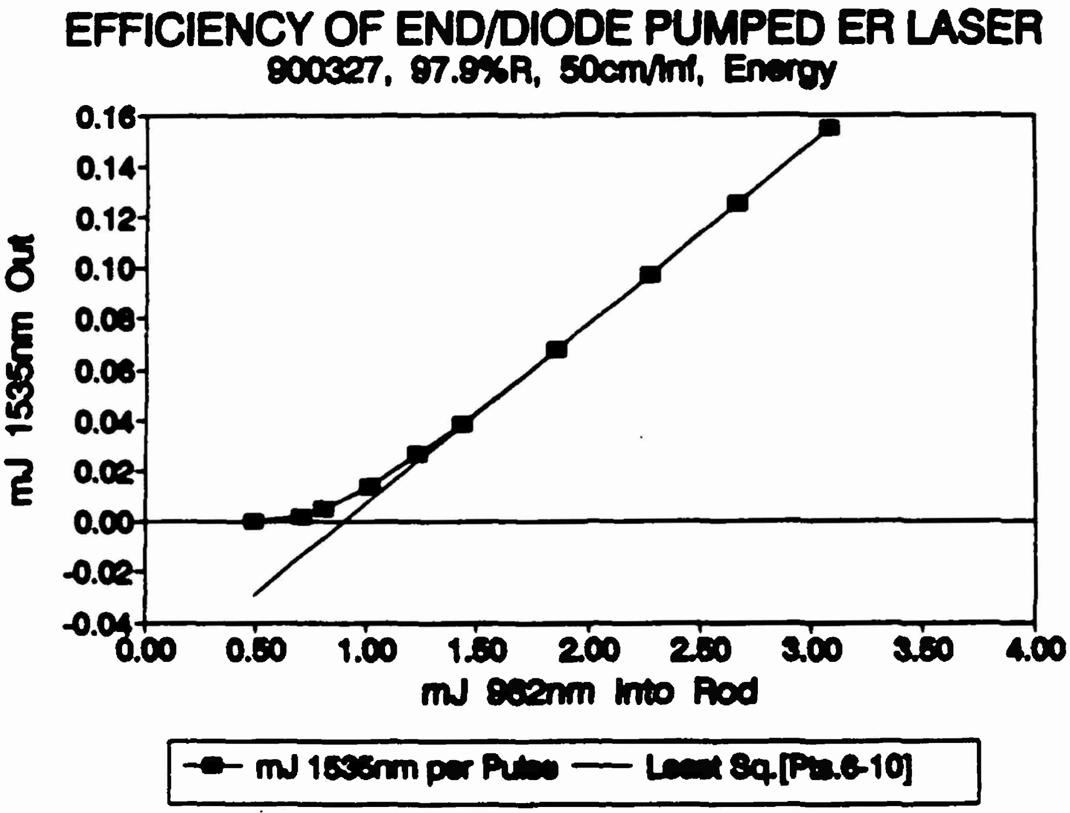

REFLECTIVITY OF OUTPUT COUPLER (%R)	99.4	97.9
ENERGY EFFICIENCY DIFFERENTIAL (SLOPE) EFFICIENCY (%) THRESHOLD (mJ @ 962nm)	 2.6 0.86	 7.1 0.90
PEAK POWER EFFICIENCY DIFFERENTIAL (SLOPE) EFFICIENCY (%) THRESHOLD (mW @ 962nm)	 2.7 69	 7.7 75

Er^{3+} $^4I_{13/2}$ FLUORESCENCE 7.58ms

CENTER FOR OPTO-ELECTRONIC SYSTEMS RESEARCH
DYNAMICS OF SEMICONDUCTOR LASERS AND AMPLIFIERS

Dynamics of Semiconductor Lasers and Amplifiers

Govind P. Agrawal
The Institute of Optics
University of Rochester

- Introduction
- Semiconductor Laser Dynamics
- Nonlinear Gain
- Modified Rate Equations
- Modulation and Noise Characteristics
- Semiconductor Optical Amplifiers
- Concluding Remarks

INTRODUCTION

- Electrical pumping through p-n junction

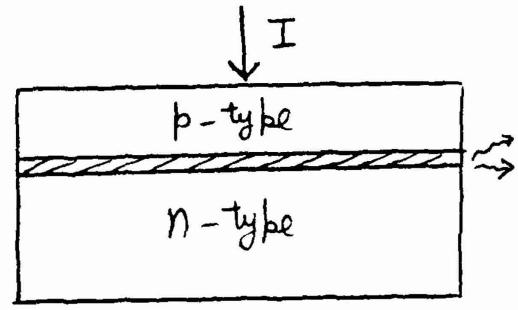

- population inversion through high carrier density in the active region ($\sim 10^{18}\,cm^{-3}$)

- Spontaneous and stimulated emission through electron-hole recombination

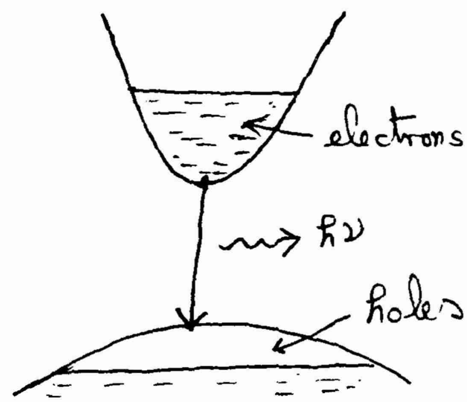

- Clamping of carrier density above laser threshold (interband gain saturation)

- Optical field can modify carrier distribution within the band at high intensities

- Intraband gain saturation affects laser dynamics

SEMICONDUCTOR LASER DYNAMICS

- Carrier lifetime $\tau_c \sim 1\text{-}3$ ns
  - radiative recombination (electron-hole recombination)
  - nonradiative recombination (impurities, Auger effects)
- Photon lifetime $\tau_p \sim 1\text{-}2$ ps
  - Small cavity length ($L = 0.2\text{-}0.3$ mm)
  - High loss (facet reflectivity $R \sim 30\%$)
- Polarization relaxation time $\tau_{in} \sim 0.1$ ps
  - Intraband carrier scattering
- Rate-equation approximation

$$\frac{dP}{dt} = \left(G - \frac{1}{\tau_p}\right)P + R_{sp}$$

$$\frac{dN}{dt} = \frac{I}{q} - \frac{N}{\tau_c} - GP$$

with $G(N) = G_N(N - N_0)$

AMPLITUDE-PHASE COUPLING

- A change in electron population N changes not only the gain but also the refractive index.
- Changes in the amplitude of the optical field produce simultaneous changes in the phase (via δN)
- Rate equation for the optical phase

$$\frac{d\phi}{dt} = \Delta\omega(t) = \frac{1}{2}\alpha_0\left(G - \frac{1}{\tau_p}\right)$$

where

$$\alpha_0 = \frac{\partial\chi_r/\partial N}{\partial\chi_i/\partial N} \qquad (\chi = \chi_r + i\chi_i)$$

- Consequences of amplitude-phase coupling
  - frequency chirp under modulation
  - broadening of the laser linewidth

α_0 – linewidth enhancement factor

Semiconductor-Laser Rate Equations

$$\frac{dP}{dt} = \left(G - \frac{1}{\tau_p}\right)P + R_{sp}$$

$$\frac{dN}{dt} = \frac{I}{q} - \frac{N}{\tau_c} - GP$$

$$\frac{d\phi}{dt} = \frac{1}{2}\alpha_0\left(G - \frac{1}{\tau_p}\right)$$

where $G = G_N(N - N_0)$.

- How good are the rate equations?

$$I(t) = I_b + I_m f(t)$$

I_b — Bias current

I_m — Modulation current

$f(t)$ — current pulse shape

Super-Gaussian pulse shape

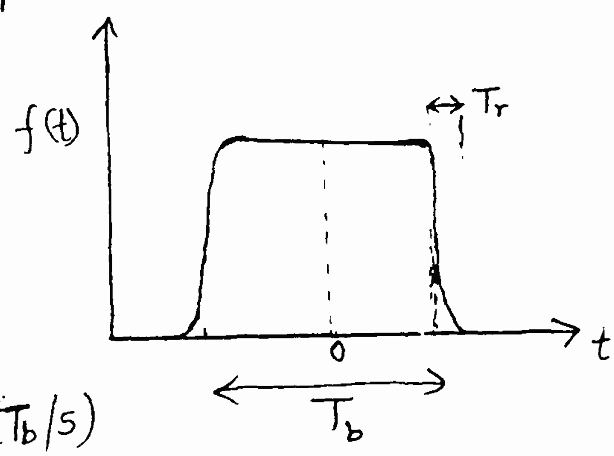

$$f(t) = \exp\left[-\left(\frac{2t}{T_b}\right)^{T_b/T_r}\right]$$

$T_b = \frac{1}{B}$ — pulse duration

T_r — rise or fall time $(T_b/5)$

LARGE-SIGNAL MODULATION

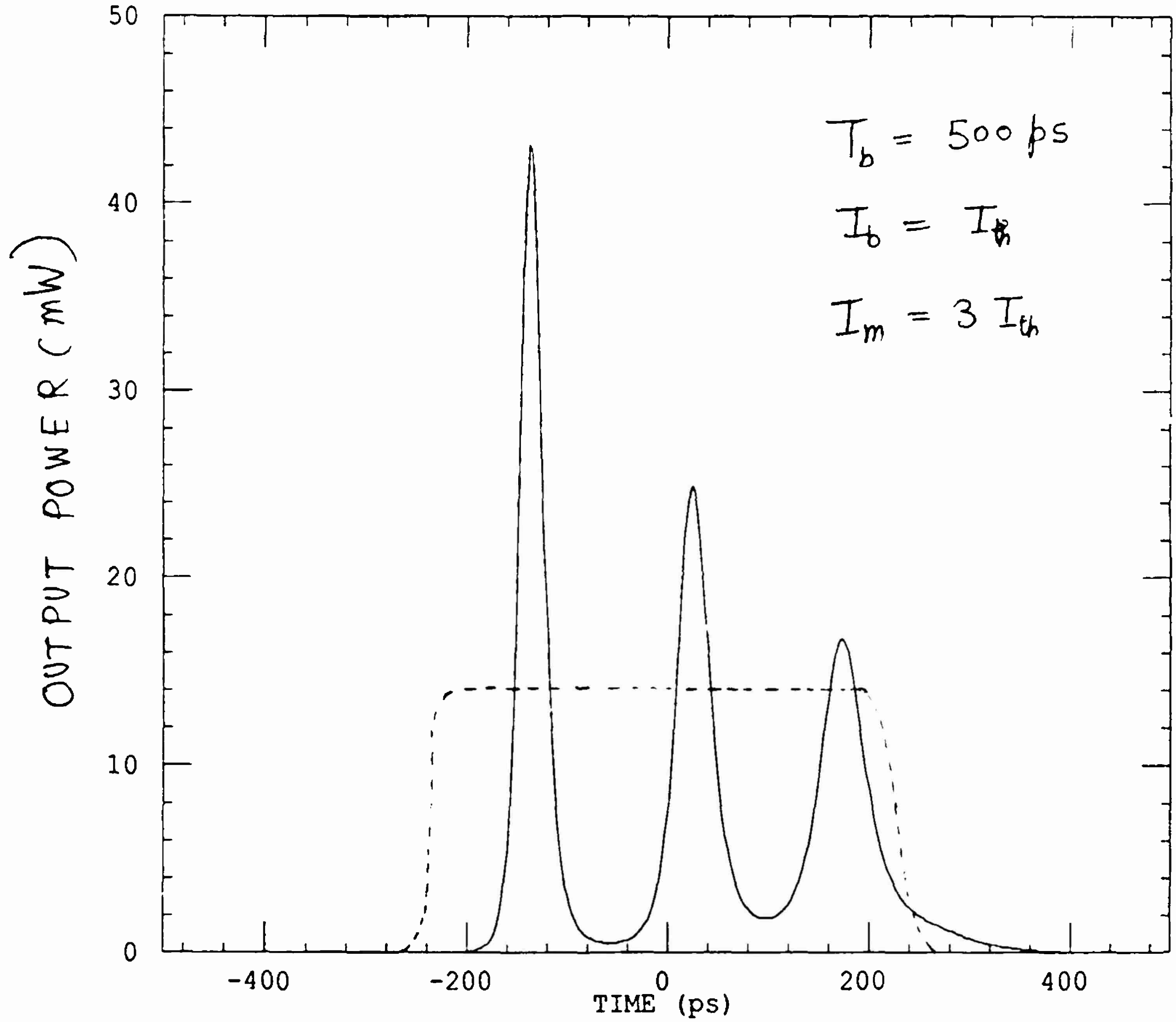

- Multiple optical pulses due to relaxation oscillations
- The predicted behavior is far from the experiments

NONLINER GAIN

- Intensity-dependent gain

$$G = G_N(N - N_0)(1 - \epsilon_{NL} P)$$

- For InGaAsP lasers

$$\epsilon_{NL} \sim 0.01 \ mW^{-1}$$

(1% gain reduction at 1 mW output power)

- Laser dynamics affected significantly
- Relaxation oscillations heavily damped

Small-signal analysis:

$$\Gamma = \frac{R_{sp}}{P} + \epsilon_{NL} P \frac{1}{\tau_p}$$

- For $\tau_p \sim 1$ ps, $\epsilon_{NL} P \sim 0.01$,

damping time $\Gamma^{-1} \sim 100$ ps

- $\Gamma^{-1} \sim 1\text{-}3$ ns without the nonlinear gain

Effect of Nonlinear Gain

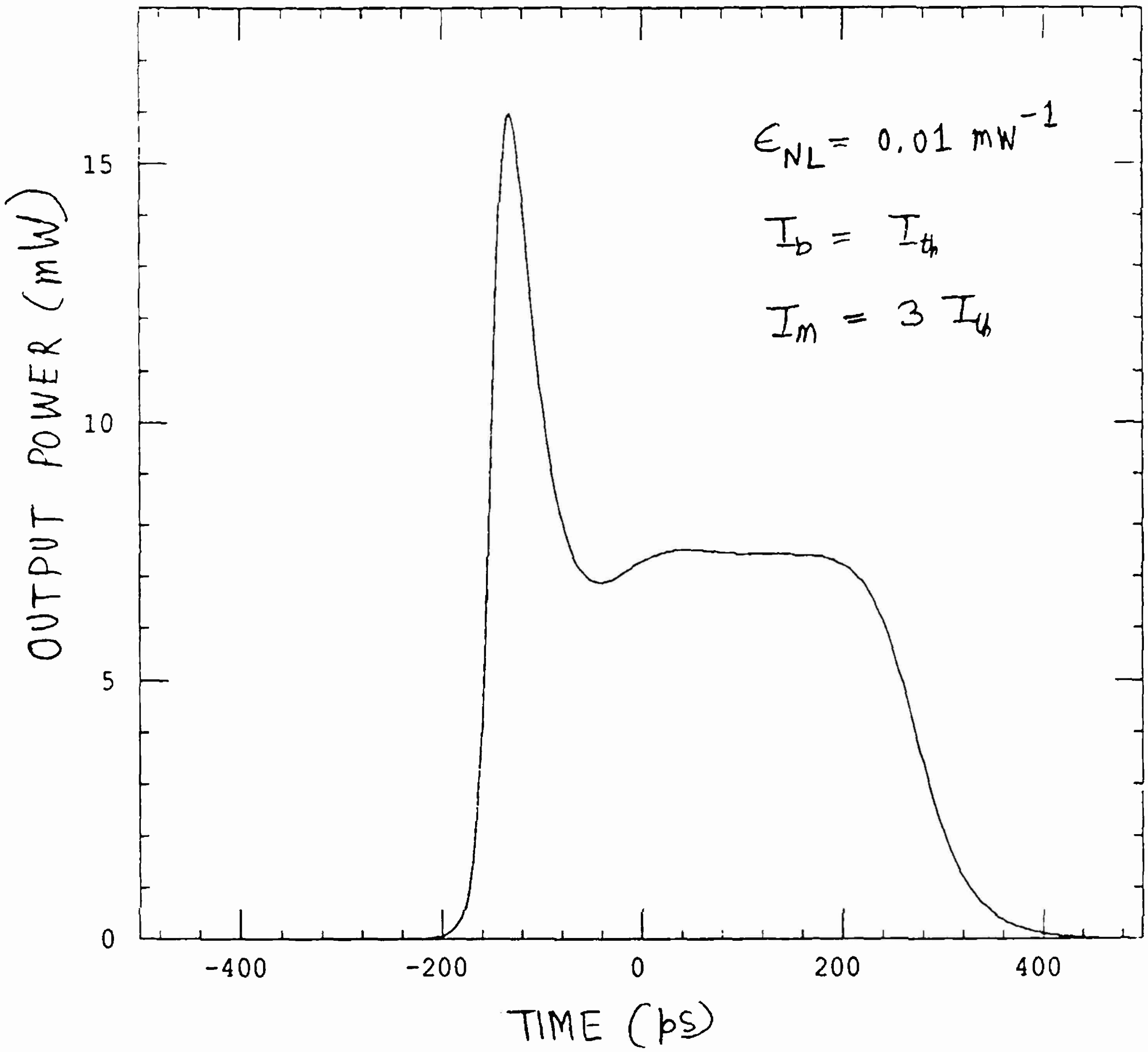

- Optical pulse shape in agreement with experiments
- Nonlinear gain must be included in the rate equations

NONLINER GAIN AT HIGH POWERS

- Phenomenological model

$$G = G_N (N - N_0)(1 - \epsilon_{NL} P)$$

Valid only at low powers ($\epsilon_{NL} P << 1$)

- What is the functional form of the nonlinear gain?
- Two-level atom analogy

$$G(N, P) = \frac{G_N (N - N_0)}{1 + P/P_s}$$

- Validity for semiconductor lasers questionable!
- What is the physical origin of nonlinear gain?
  - gain saturation due to electron-hole recombination is already included in the rate equations
- Answer: Intraband gain saturation

GAIN SATURATION

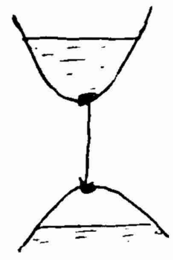

- Two distinct saturation processes
  - Stimulated emission changes the electron and hole populations as a result of electron-hole recombination. The gain saturation is due to interband processes. The rate equation

$$\frac{dN}{dt} = \frac{I}{q} - \frac{N}{\tau_c} - GP$$

includes interband gain saturation (the last term)

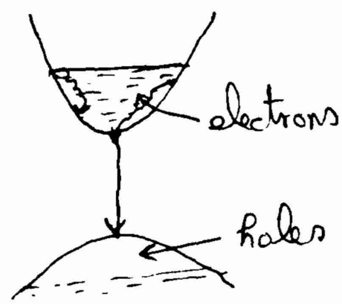

- The optical field can change the distribution of electrons within the conduction band. Intraband relaxation processes try to restore the equilibrium distribution at a time scale $\tau_{in} \sim 0,1$ ps

- At high intensities ($\Omega \tau_{in} \sim 1$), the gain is reduced since electron distribution is modified significantly. This is <u>intraband gain saturation</u>. It is not included in the rate equations.

GAIN and INDEX NONLINEARITIES

$$\chi_{NL} = 2n\left(\Delta n_{NL} - i\,\frac{g_{NL}}{2k_0}\right)$$

$$\Delta n_{NL} = \frac{\beta g_L}{2k_0}\,\frac{I}{1+\sqrt{1+I}}$$

$$g_{NL} = -\frac{g_L\, I}{\sqrt{1+I}\,(1+\sqrt{1+I})}$$

Total Gain

$$g = g_L + g_{NL} = \frac{g_L}{\sqrt{1+I}}$$

- Modification in the rate equations:

$$G = \Gamma V_g\, g = \frac{G_N (N - N_0)}{\sqrt{1 + P/P_s}}$$

Saturation photon number

$$P_s = \frac{\epsilon_0\, n\, n_g\, V}{\hbar\,\omega_0\,\Gamma}\, I_s$$

- Include Δn_{NL} in the phase equation

MODIFIED RATE EQUATIONS

$$\frac{dP}{dt} = \left(\frac{G_N(N-N_0)}{\sqrt{1+P/P_s}} - \frac{1}{\tau_p}\right) P + R_{sp}$$

$$\frac{dN}{dt} = \frac{I}{q} - \frac{N}{\tau_c} - \frac{G_N(N-N_0)P}{\sqrt{1+P/P_s}}$$

$$\frac{d\phi}{dt} = \frac{\alpha}{2}\left(G_N(N-N_0) - \frac{1}{\tau_p}\right) - \underbrace{\frac{\beta}{2}\,\frac{G_N(N-N_0)\,P/P_s}{1+\sqrt{1+P/P_s}}}_{\text{index nonlinearities}}$$

- Small-signal modulation
  - relaxation oscillations
  - 3-dB modulation bandwidth
- Large-signal modulation
  - pulse shape, rise and fall times
  - frequency chirp, gain switching
- Noise characterestics
  - Laser linewidth
  - Relative intensity noise

RELAXATION OSCILLATIONS

- Linear stability analysis of the modified rate equations
- Oscillatory approach to the steady state

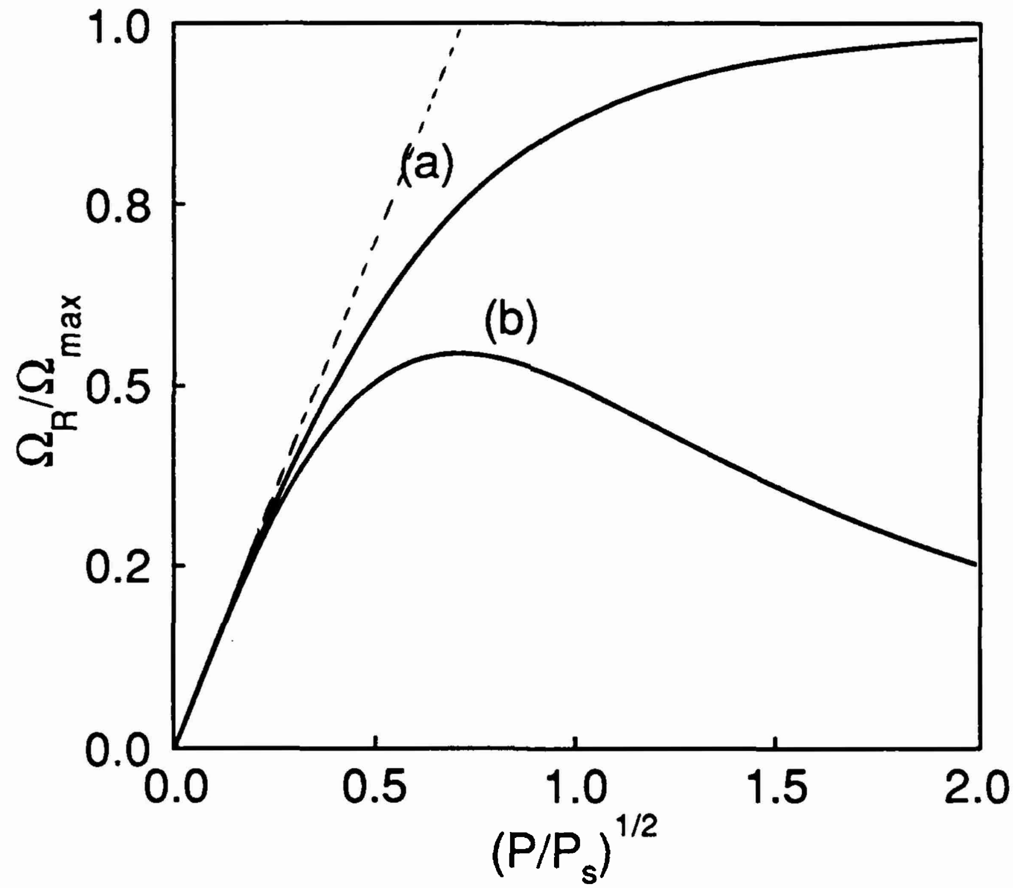

- Power dependence of the relaxation-oscillation frequency

(a) $G(N, P) = \dfrac{G_N(N-N_0)}{\sqrt{1+P/P_s}}$

(b) $G(N, P) = \dfrac{G_N(N-N_0)}{(1+P/P_s)}$

DAMPING RATE OF RELAXATION OSCILLATIONS

$$\Gamma'_R \simeq \frac{1}{4\tau_p} \frac{P/P_s}{(1+P/P_s)^{3/2}}$$

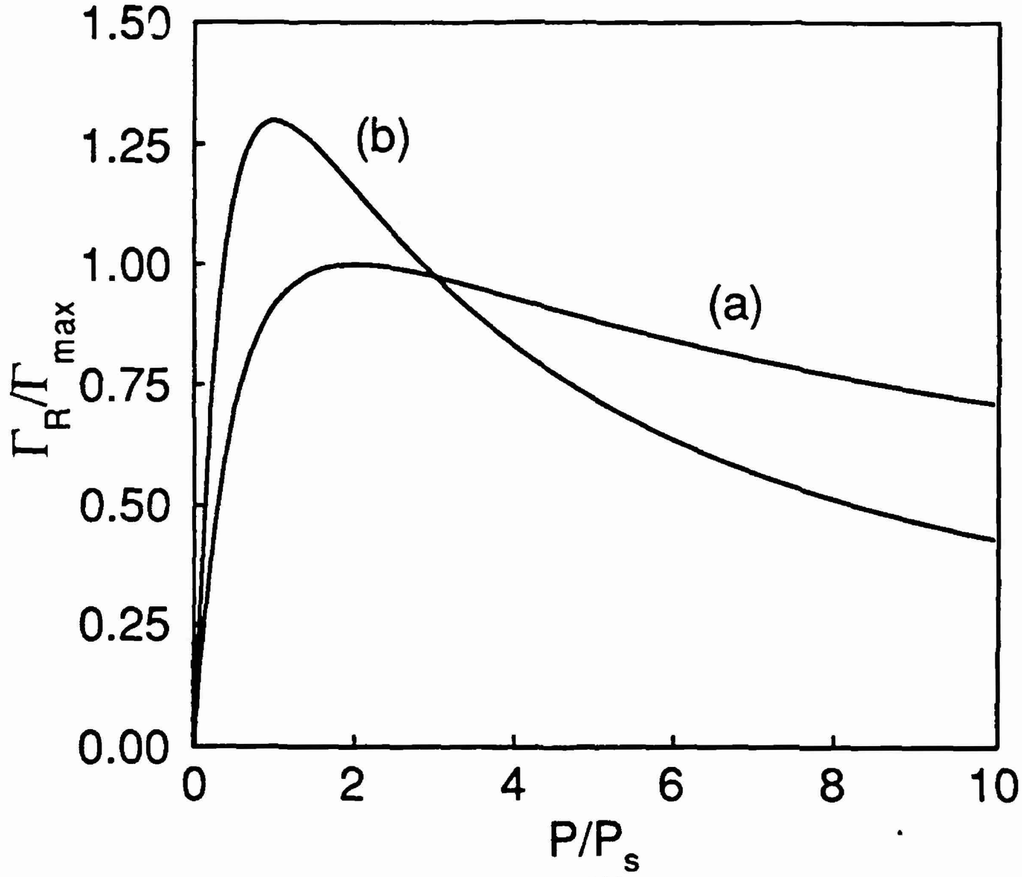

(a) $G(N, P) = \dfrac{G_N(N-N_0)}{\sqrt{1+P/P_s}}$

(b) $G(N, P) = \dfrac{G_N(N-N_0)}{1+P/P_s}$

$$\Gamma'_{max} \simeq \frac{1}{10\tau_p} \qquad (\tau_p \sim 1-2\ ps)$$

SMALL-SIGNAL MODULATION

- Solve the modified rate equations with

$$I(t) = I_b + I_m \exp(i\omega_m t), \qquad I_m \ll I_b - I_{th}$$

- Modulation Response

$$\delta P(\omega_m) = \frac{G_N P (I_m/q)(1+P/P_s)^{-1/2}}{(\Omega_R - i\Gamma_R + \omega_m)(\Omega_R + i\Gamma_R - \omega_m)}$$

- 3-dB modulation bandwidth f_{3dB}

$$\frac{\delta P(f_{3dB})}{\delta P(0)} = \frac{1}{2}$$

$$f_{3dB} = \frac{1}{2\pi}\left\{\Omega_R^2 - \Gamma_R^2 + 2\left[\Omega_R^2(\Omega_R^2+\Gamma_R^2)+\Gamma_R^4\right]^{1/2}\right\}^{1/2}$$

- In the absence of intraband gain saturation

$$f_{3dB} \propto \sqrt{P}$$

- In the presence of intraband gain saturation f_{3dB} saturates

$$f_{3dB}^{max} = \frac{1}{2\pi}\left(\frac{3}{2}\frac{G_N P_s}{\tau_p}\right)^{1/2}$$

$$f_{3dB}^{max} = \left[\frac{3\epsilon_0 n n_g \hbar^2 V G_N}{8\pi^2 \hbar \omega_0 \mu^2 \Gamma \tau_{in}(\tau_c+\tau_r)}\right]^{1/2}$$

MODULATION BANDWIDTH

- f_{3dB} depends on the bias power and other device parameters

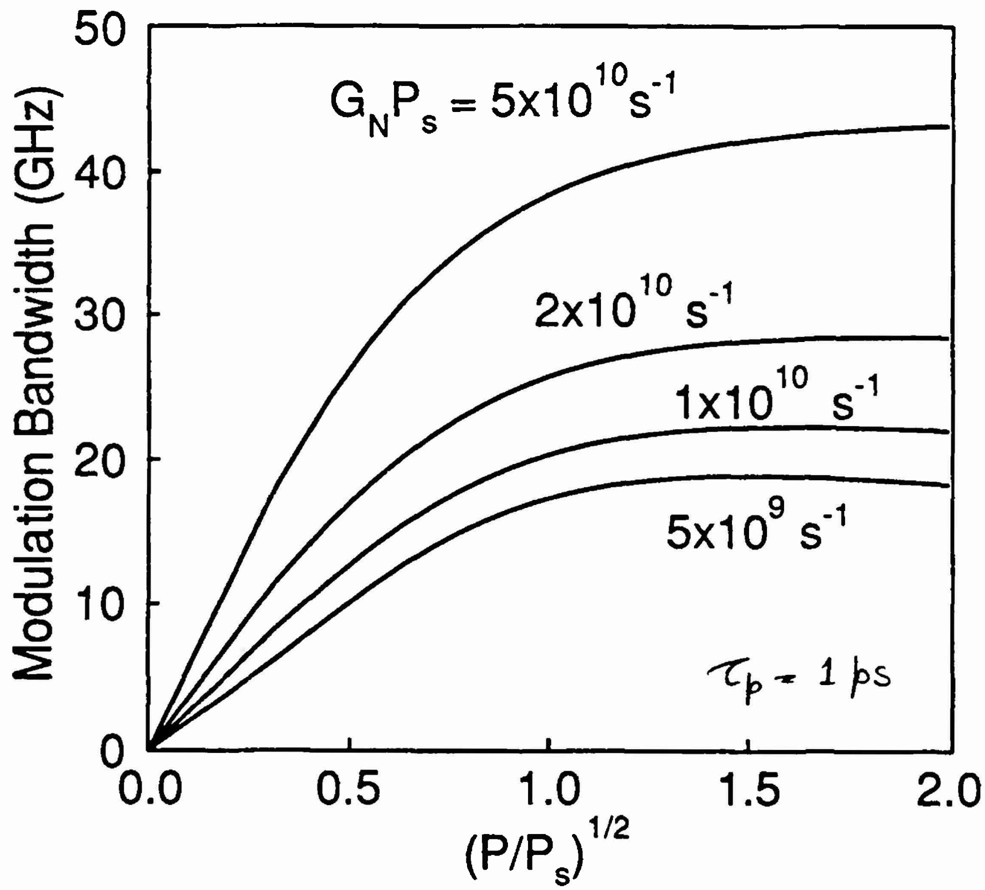

$$f_{3dB}^{max} \sim 20-40 \text{ GHz} \quad \text{for InGaAsP lasers}$$

- Can be enhanced for quantum-well lasers (G_N larger)

LARGE-SIGNAL MODULATION

- Direct current modulation ($I_b = I_{th}$)

$$I(t) = I_b + I_m f(t)$$

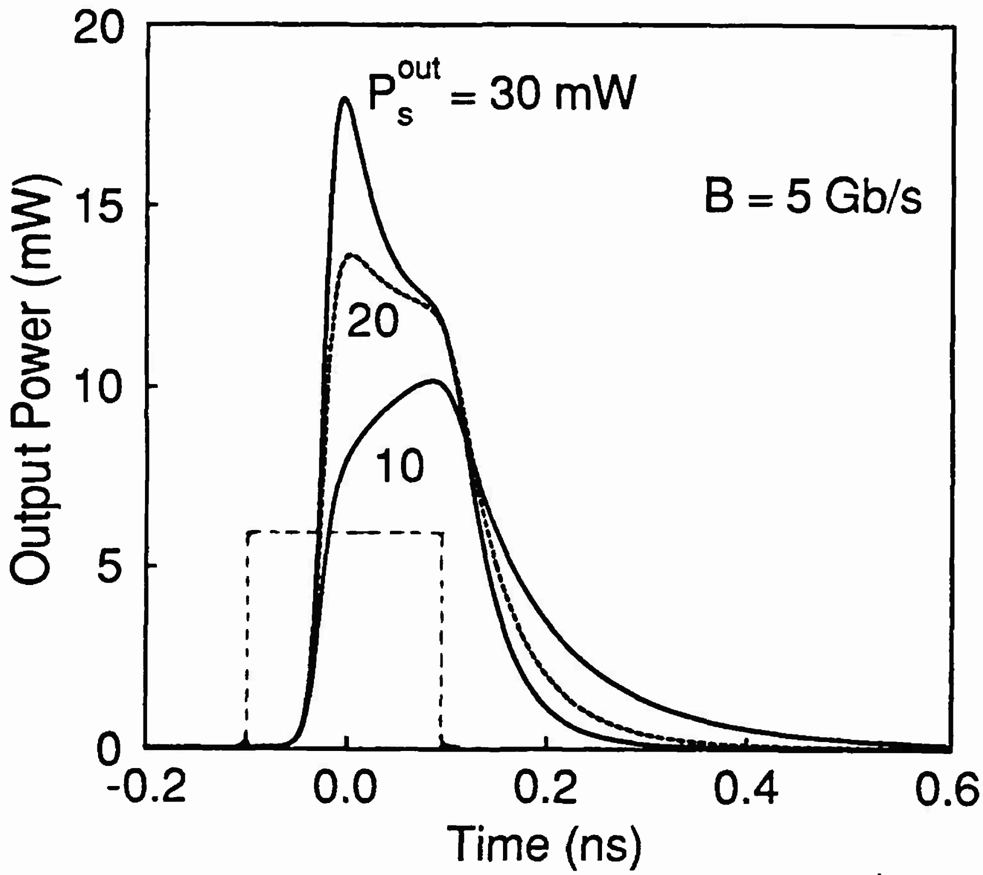

- Rise and Fall times increase when $P^{out} \sim P_s^{out}$
- Intersymbol interference in communication systems

LASER LINEWIDTH

- Add Langevin noise sources to the modified rate equations
- Solve the stochastic rate equations by linearizing them around the steady-state average values
- Calculate the spectrum by taking the Fourier transform of the autocorrelation function
- Lorentzian spectrum with FWHM

$$\Delta\nu \simeq \frac{R_{sp}}{4\pi P}\left(1 + \alpha_{eff}^2\right)$$

$$\alpha_{eff} = \alpha_0\sqrt{1+I} + \beta\,\frac{I(1+I)}{(2+I)}$$

where $$I = \frac{|E|^2}{I_s} = \frac{P}{P_s}$$

- In the absence of intraband gain saturation $\alpha_{eff} = \alpha_0$ and $\Delta\nu \propto 1/P$.
- Linewidth saturates to a limiting value ($\sim$ 1-10 MHz) because of intraband gain saturation

SPECTRAL LINEWIDTH

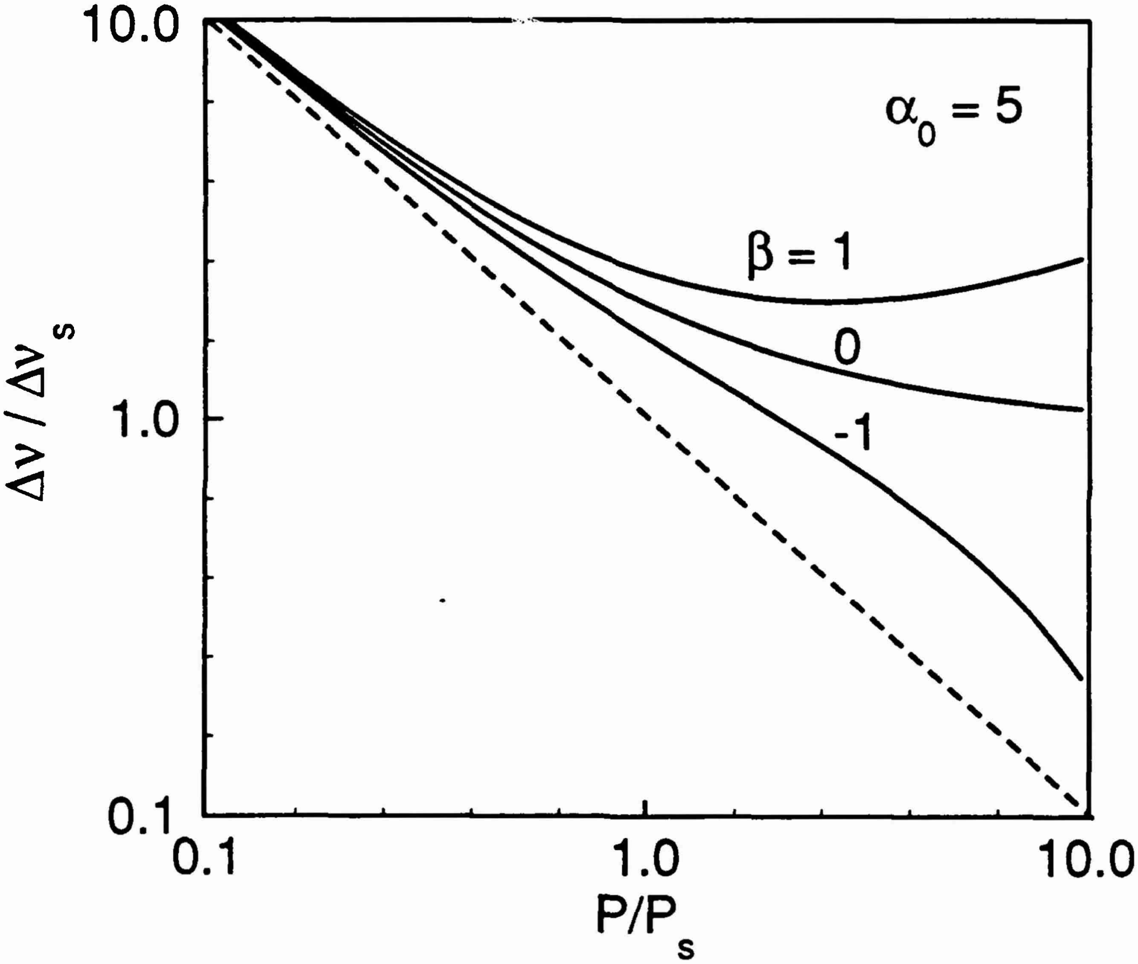

G. P. Agrawal, IEEE J. Quantum Electron. (to be published).

- Rebroadening of the linewidth can occur for lasers oscillating away from the gain peak because of index nonlinearities ($\beta \neq 0$).

SEMICONDUCTOR LASER AMPLIFIERS

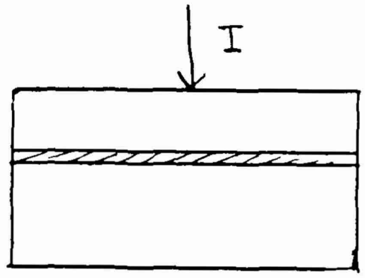

- Traveling-wave amplifier

  AR facet coatings ($< 10^{-3}$ reflectivity)

- Rate equations must include spatial variation of the optical field

$$\frac{\partial A}{\partial z} + \frac{1}{v_g}\frac{\partial A}{\partial t} = \frac{1}{2}(1 - i\alpha)\, g A - \frac{1}{2}\alpha_{int} A$$

- Gain dispersion

$$\tilde{g}(\omega) = g_p\left[1 - T_2^2(\omega - \omega_0)^2\right]$$

$$g = g_p\left[1 + T_2^2 \frac{\partial^2}{\partial t^2}\right]$$

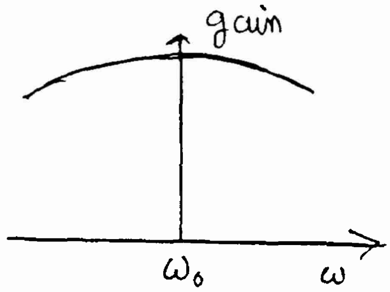

- Peak gain $\quad g_p = \Gamma a (N - N_0)\big/\left(1 + |A|^2/P_s\right)^{1/2}$

$$\frac{\partial N}{\partial t} = \frac{I}{qV} - \frac{N}{\tau_c} - \frac{g_p |A|^2}{\mathcal{E}_{sat}}$$

interband saturation energy $\quad \mathcal{E}_{sat} = \hbar\omega_0(\sigma/a)$

- Gain dispersion leads to carrier-induced index dispersion
- Gain saturation leads to self-phase modulation

Carrier-Induced Group-Velocity Dispersion

- $$\frac{\partial A}{\partial z} + \frac{1}{v_g}\frac{\partial A}{\partial t} = \frac{1}{2}(1-i\alpha)\, g_p \left(A + T_2^2 \frac{\partial^2 A}{\partial t^2}\right)$$

  Define $\tau = (t - z/v_g)/T_0$

- $$\frac{\partial A}{\partial z} - \frac{1}{2}(1-i\alpha)\, g_p \left(\frac{T_2}{T_0}\right)^2 \frac{\partial^2 A}{\partial \tau^2} = \frac{1}{2}(1-i\alpha)\, g_p$$

  Dispersion length $L_D = \dfrac{T_0^2}{\beta_2^{\text{eff}}} = \dfrac{T_0^2}{\alpha g_p T_2^2}$

  GVD parameter $\beta_2^{\text{eff}} = \alpha g_p T_2^2$

- Pulse broadening and compression

$$A(0,\tau) = A_0 \exp\left[-(1+iC)\frac{\tau^2}{2}\right]$$

$$A(L,\tau) = \frac{A_0 \exp[(1-i\alpha) g_0 L/2]}{(1+Q)^{1/2}} \exp\left[-\frac{1+iC}{1+iQ}\frac{\tau^2}{2}\right]$$

$$Q = \left(\frac{T_2}{T_0}\right)^2 g_0 L\, (1-i\alpha)(1+iC)$$

- Pulse broadening for $C \geqslant 0$
- Pulse compression for $C < 0$

Broadening Factor for Chirped Gaussian Pulses

- Amplifier gain 30 dB

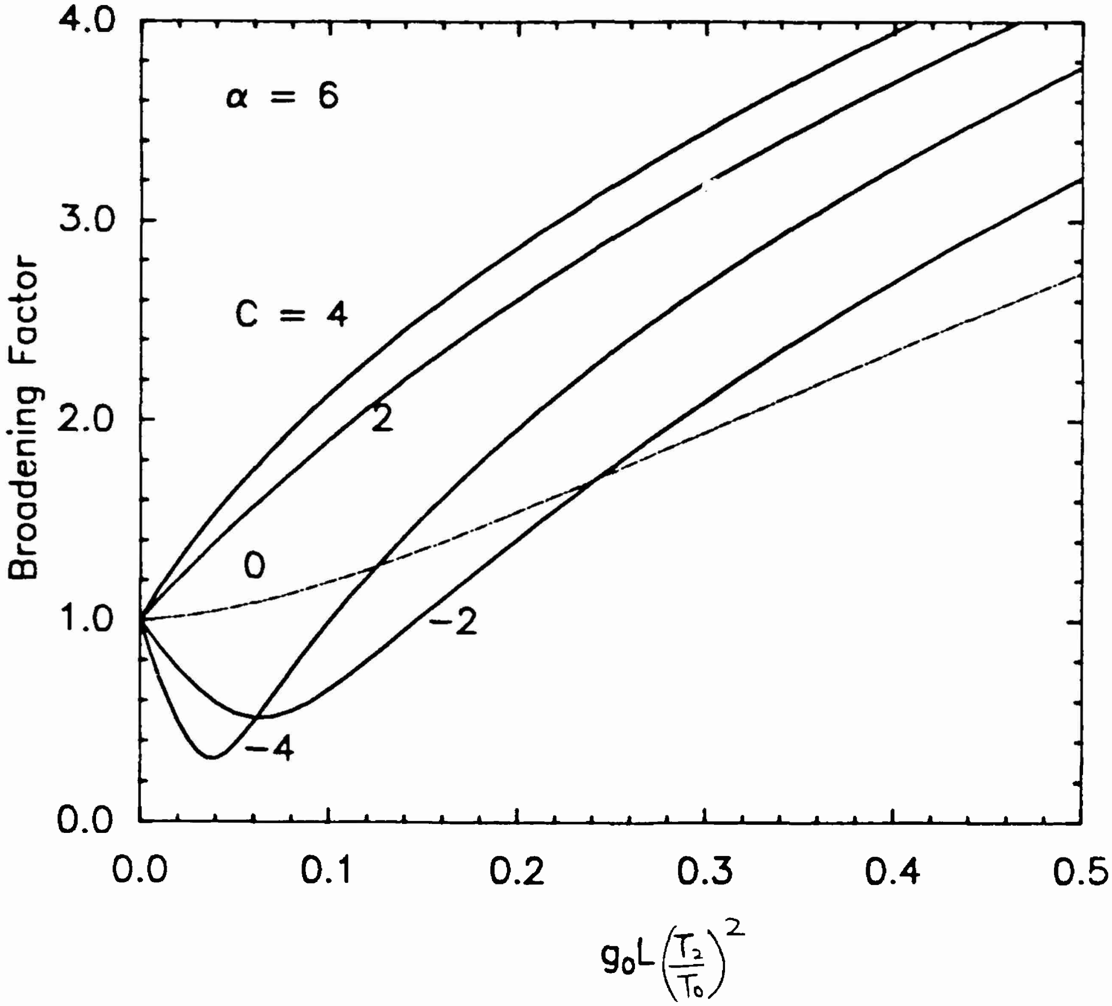

- Pulse compression possible for $C < 0$
- C is negative for pulses emitted by semiconductor lasers

Carrier-Induced Nonlinearity

- Refractive index in semiconductor laser amplifiers depends on the injected carrier density.
- Gain saturation leads to intensity-dependent variations in the carrier density.
- Refractive index becomes intensity dependent as a result of gain saturation
- Self-phase modulation due to carrier-induced nonlinearity.
- Amplified pulse develops a nearly linear frequency chirp.
- Chirped pulse can be compressed by passing through a dispersive-delay line.
- Significant chirp can occur for input pulse energies as small as 0.1 pJ.

SPM-INDUCED SPECTRAL DISTORTION

Gaussian input pulse: $P_{in}(\tau) = P_0 \exp(-\tau^2/\tau_0^2)$

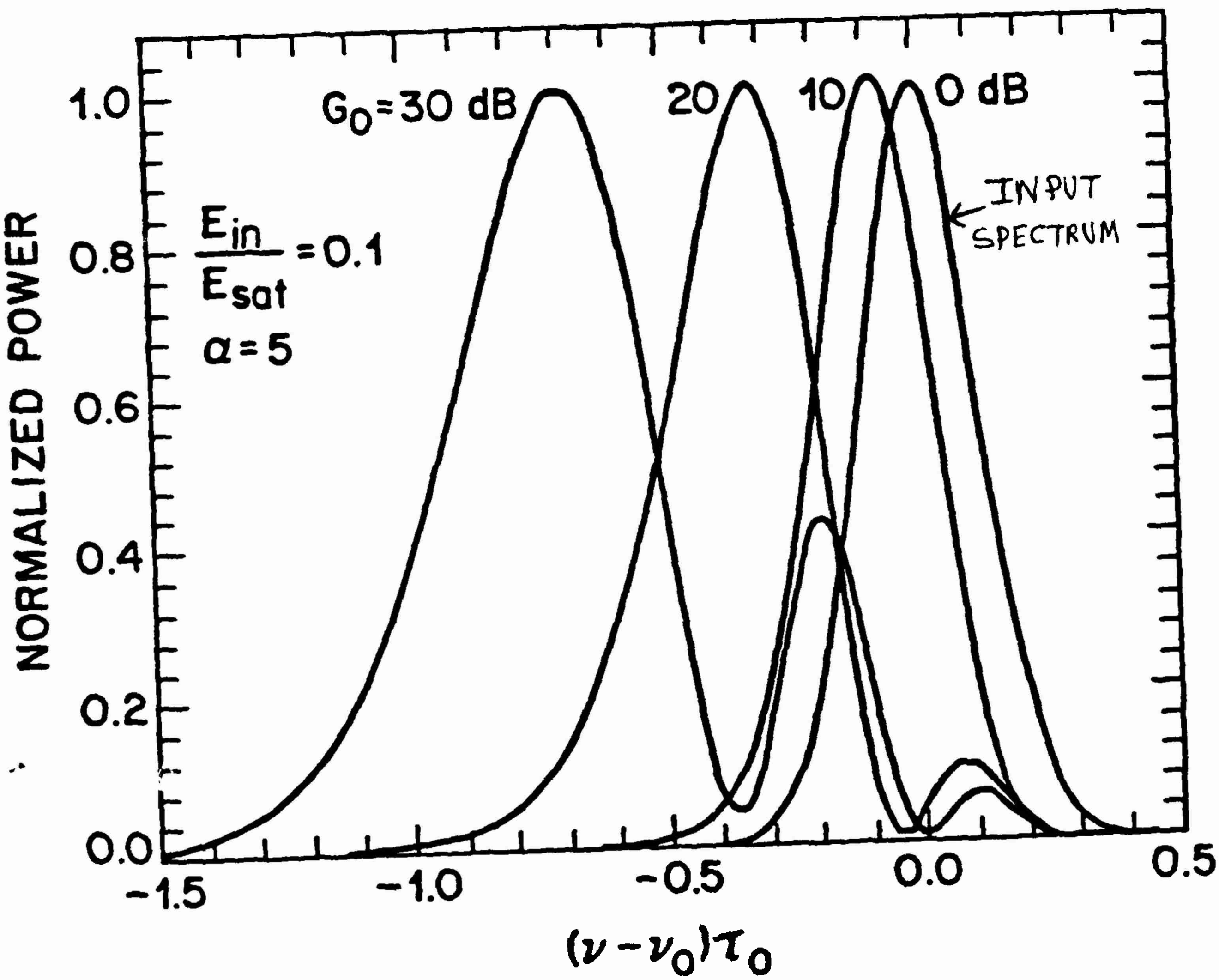

- Spectral red shift and broadening
- Asymmetric multipeak structure

Concluding Remarks

- Rate equations can model the laser dynamics quite well.
- Intraband gain saturation must be considered for a realistic description of semiconductor lasers.
- Nonlinear gain limits the modulation bandwidth of semiconductor lasers in the neighborhood of 30 GHz.
- Carrier-induced dispersion is important for semiconductor optical amplifiers. It can lead to pulse compression under certain conditions.
- Spectrum of the amplified pulse is considerably modified by gain-induced self-phase modulation.

CECOM CENTER FOR NIGHT VISION AND ELECTRO-OPTICS
LASER DIODE PROGRAMS OVERVIEW

LASER DIODE ARRAY

Internal Program

David Caffey

Vernon King

Neal Bambha

Bill Lyndon, SAIC

PROGRAM GOALS

- Support BTI producibility program
- Develop low-cost, high performance arrays
- Support in-house research
- Improve performance of basic device

SOURCES OF WAFER MATERIAL

- University of New Mexico — 785nm
- NIST — 970nm
- Advanced Optoelectronics — 808nm
- NESI — 808nm

BASIC FABRICATION STEPS

1. *Coat epi-side of wafer with SiO2*
2. *Pattern SiO2 using PR*
3. *Metallize epi-side*
4. *Thin wafer*
5. *Metallize n-side*
6. *Cleave wafer into bars*
7. *Coat cleaved facets*
8. *Bond bars to heatsinks*

785 nm. LASER DIODE ARRAYS STATUS

- Bar Bonder (SEC) set up and operating
- New fixtures developed for bar AR/HR coatings
- High Density bar process developed
- Indium coating improved using new vacuum system
- New 785 nm. wafers ordered from U. New Mexico
  2 - GRINSCH single quantum well
  2 - GRINSCH SQW narrow divergence
  1 - GaInAlAs quantum well

ORTEL, INC.

Phase II SBIR Goals

- High power arrays
- Window laser structures
- Post-growth processing
- Re-growth process

Started 05/89

SUPPORT IN-HOUSE RESEARCH

- Provide pump arrays at 785, 808, 970nm for end-pumped and microchip lasers

- Provide specialized devices for external cavity operation

LASER DIODE ARRAYS
FOR SOLID STATE LASER PUMPING

WAVELENGTH	MATERIAL	SS LASER
785 nm.	GaAlAs QW	Tm:YAG
795 nm.	GaAlAs QW	Nd:YLF
808 nm.	GaAlAs QW	Nd:YAG/Glass
970 nm.	GaInAs SL QW	Er:Glass/YAG

External Cavity Laser Diode

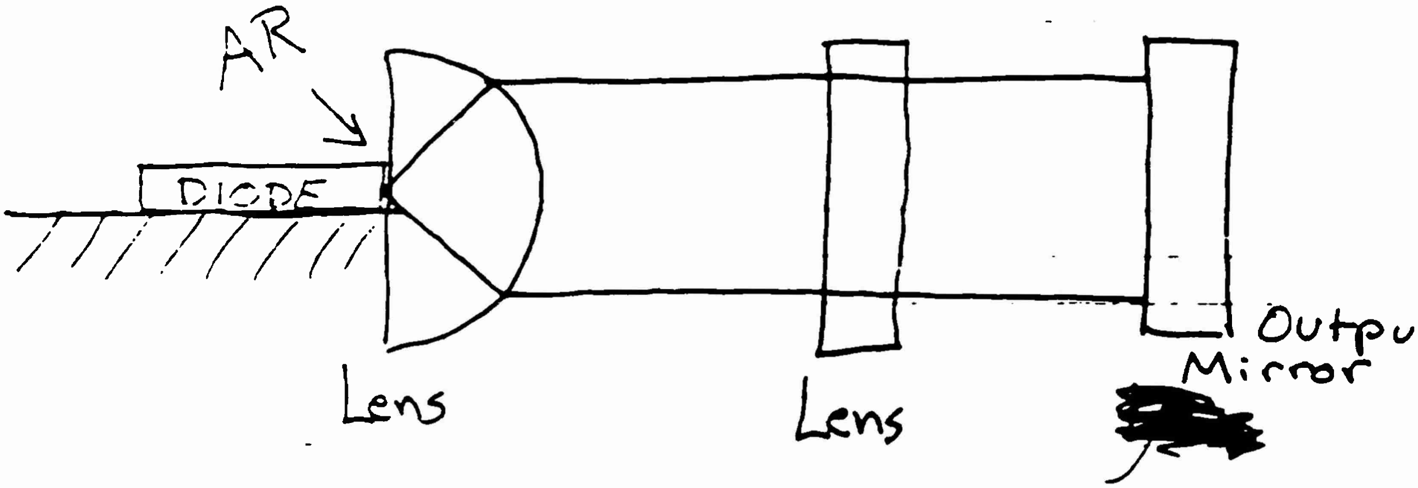

- Spectral narrowing $\Delta\nu = \dfrac{\Delta\nu_0}{(1+\sqrt{\eta})^2}$

  η: power feedback ratio

- Diffration limited output

- Ability to combine multiple diodes coherently in one cavity

U of New Mexico & C2NVEO

UNM #204, 100um Broad, 8 Stripes,500um c–c

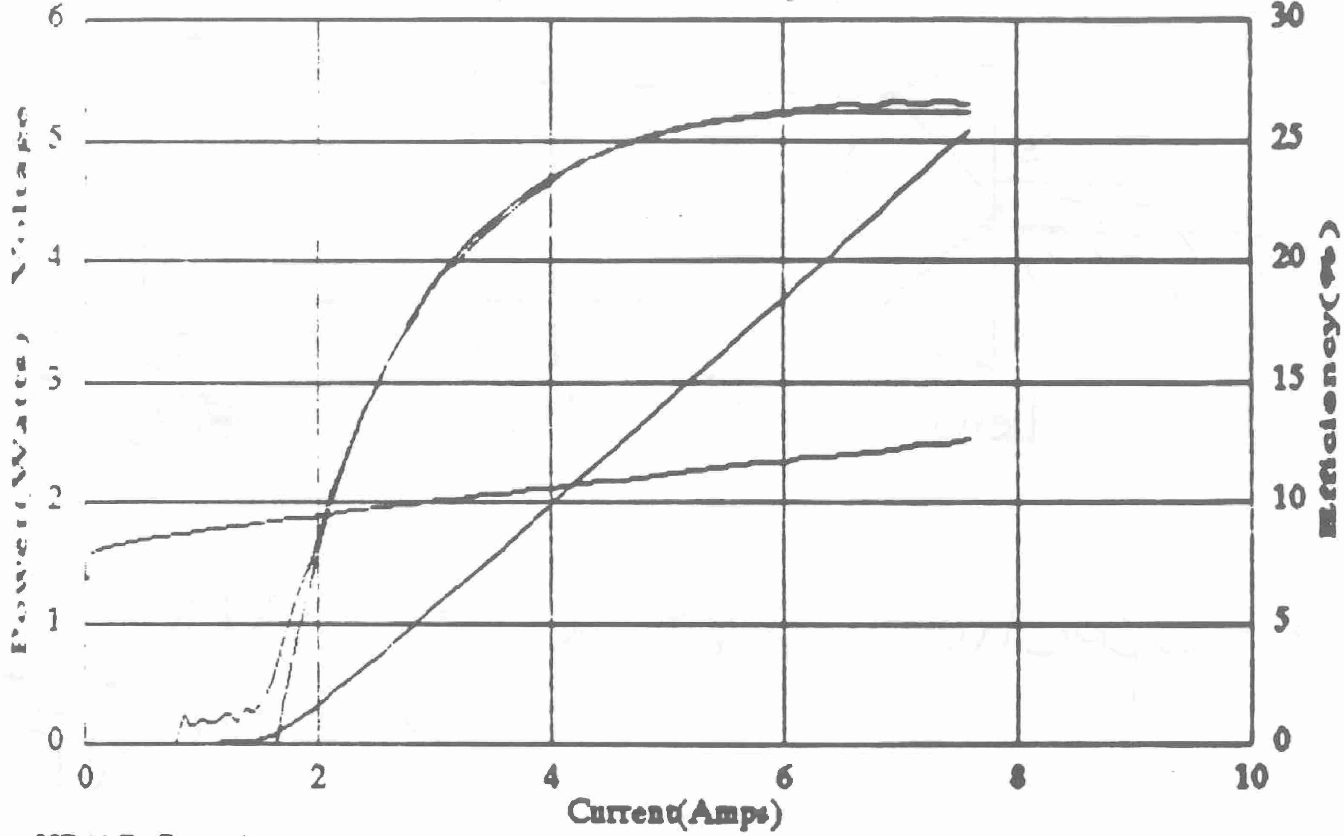

HR/AR Coated
Ref'd P6063B, 6LC

File Name:	M204E3P.DTA		Thresh.=	1.64	Amps
File Date:	03-Apr-90		J(th)=	325	A/cm2
Device Size	1	junction(s)	Slope=	0.843	W/A
Length	630	µm	Slope/Jct=	0.843	W/A
Active Width	800	µm	Resistance=	0.1131	Ohms
Pulse Width	200	µS	Resist./Jct=	0.1131	Ohms
Rep. Rate	50	Hz	Diff. Q.E.=	52	%
Wavelength	779	nm	V(c)=	1.672	Volts
Current Min.	2	Amps	Water Temp:	20	°C
Power Max.	4	Watts	Printed:	10/12/90	

U of New Mexico & C2NVEO

UNM #206, 100um Phased, P-Down, 1 Stripe

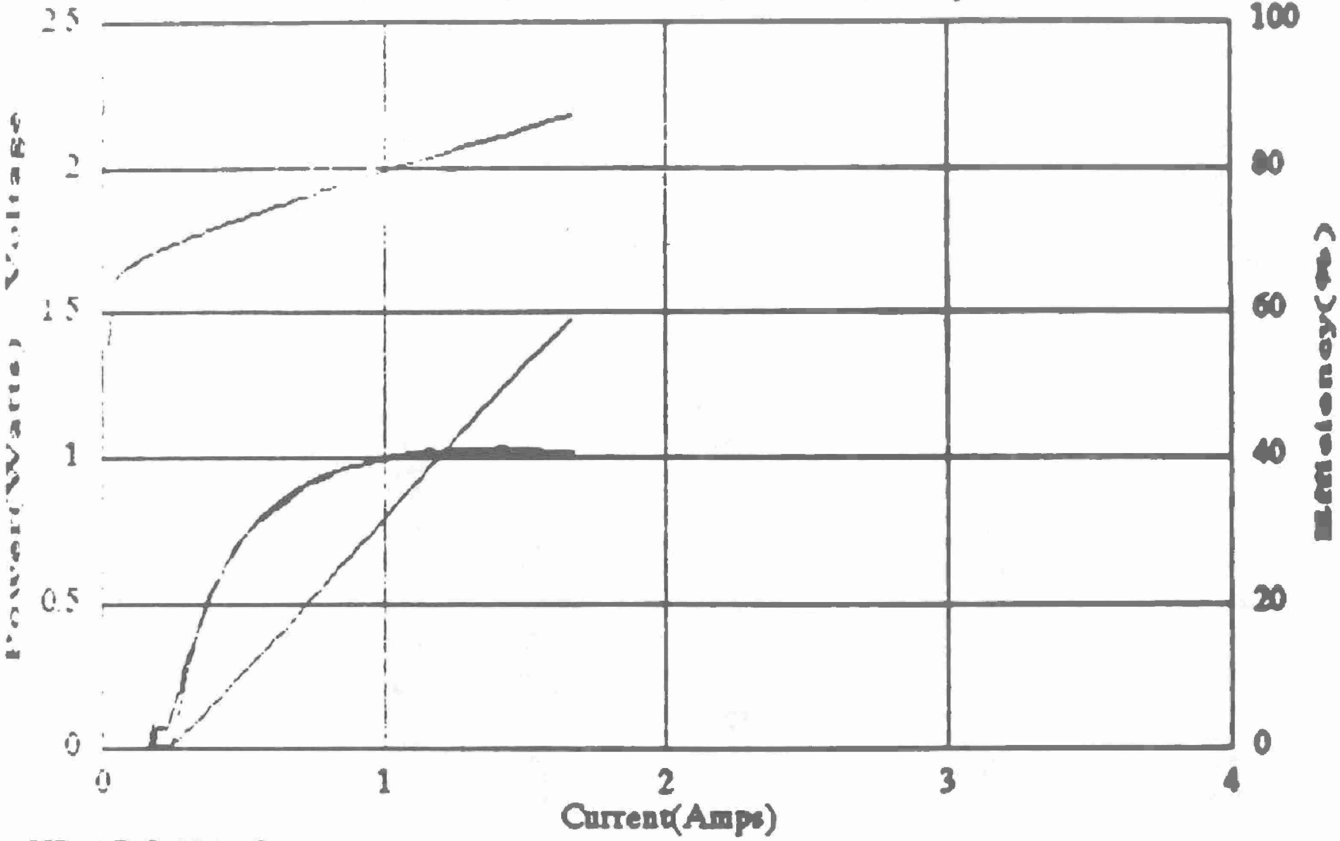

HR/AR Sulfide Coating
Ref'd Dir,6LC

File Name:	N206K1P.DTA	Thresh.=	0.249 Amps
File Date:	01-Mar-90	J(th)=	383 A/cm2
Device Size	1 junction(s)	Slope=	1.052 W/A
Length	650 µm	Slope/Jct=	1.052 W/A
Active Width	100 µm	Resistance=	0.3224 Ohms
Pulse Width	200 µS	Resist./Jct=	0.3224 Ohms
Rep. Rate	50 Hz	Diff. Q.E.=	66 %
Wavelength	785 nm	V(c)=	1.663 Volts
Current Min.	0.3 Amps	Water Temp:	23 °C
Power Max.	1 Watts	Printed:	10/11/90

IMPROVE PERFORMANCE OF BASIC DEVICE

- *Device power is limited by COD to facets*

APPROACH

- *Use PL to characterize new facet coatings*
- *Work with NIST and UNM on advanced laser structures*

Run# 582 Structure
576

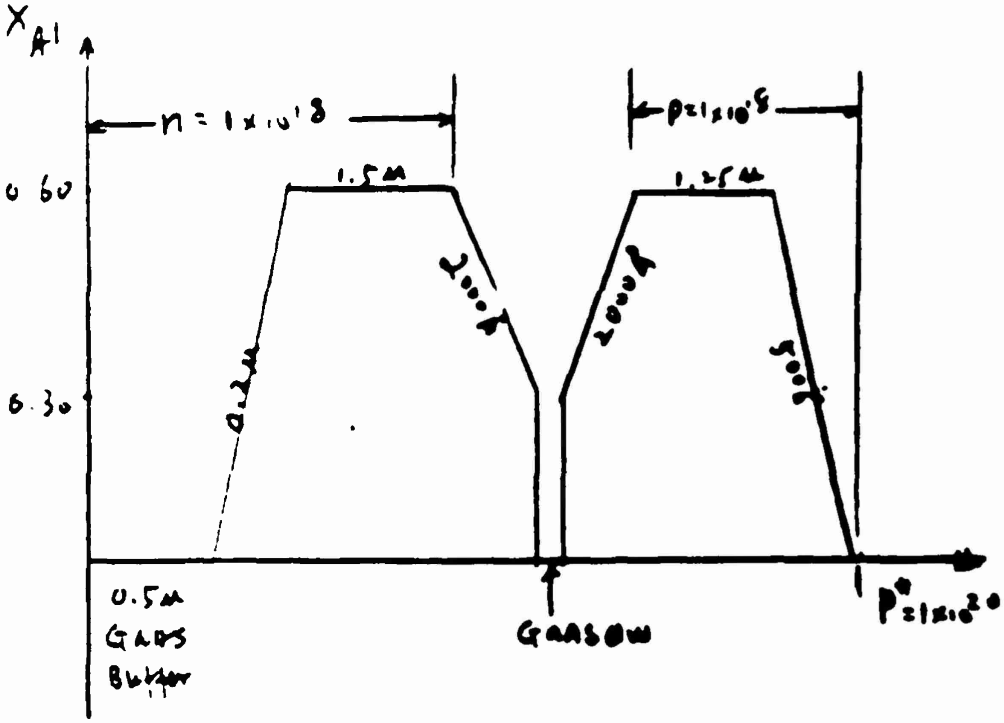

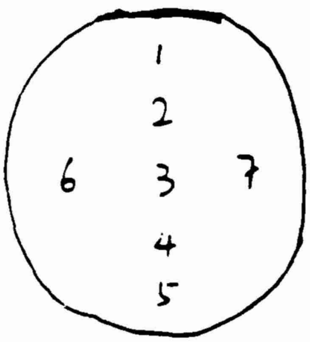

#1	782
#2	783
#3	783
#4	782
#5	781
#6	782
#7	781

$\bar{\lambda}_{pl} = 782$ nm

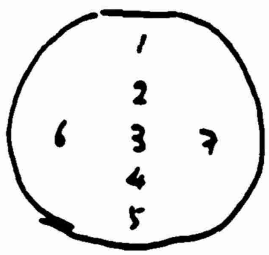

#1	781
#2	781
#3	781
#5	779
#6	781
#7	780

Run# 584, 585, 590 Structure

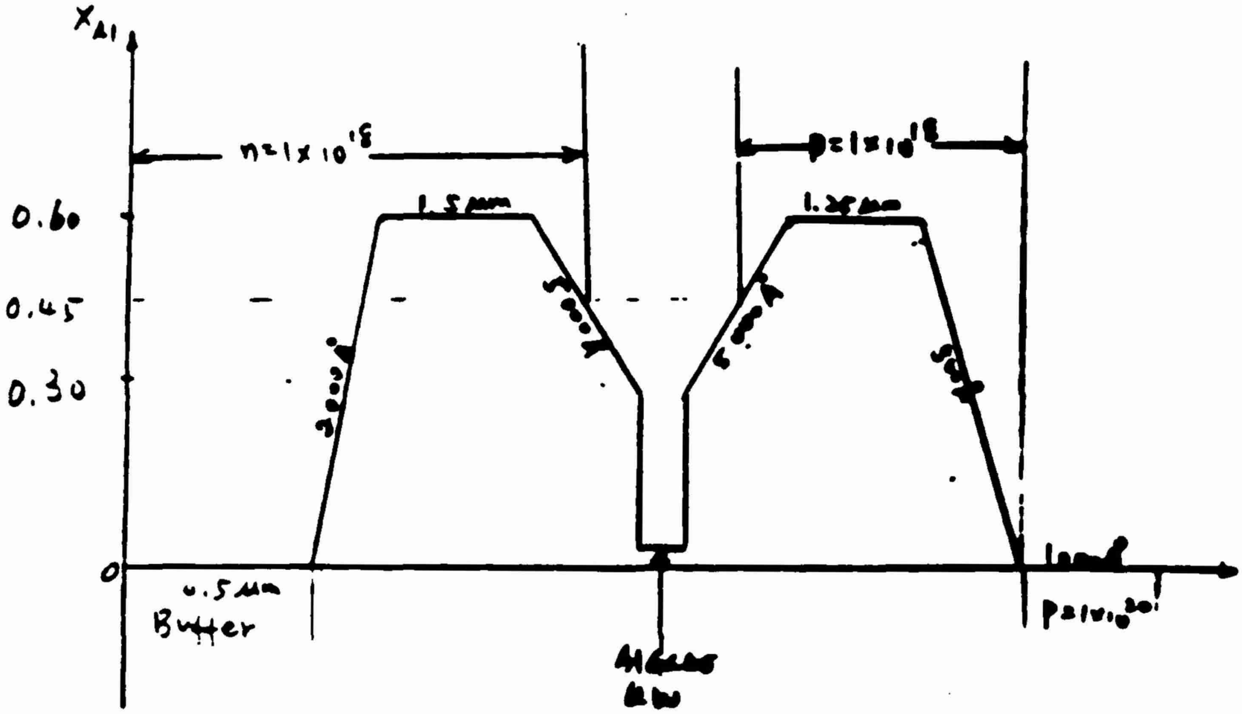

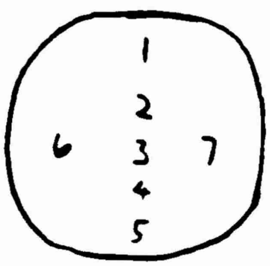

#1	781 nm
#3	783 nm
#5	782 nm
#6	782 nm
#7	782 nm
	782 nm

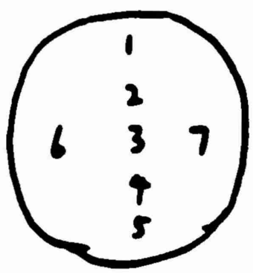

#1	782 nm
#2	783 nm
#3	783 nm
#4	783 nm
#5	783 nm
#6	783 nm
#7	783 nm
	783 nm

1.5μm High Power InGaAs/InGaAsP MQW Lasers

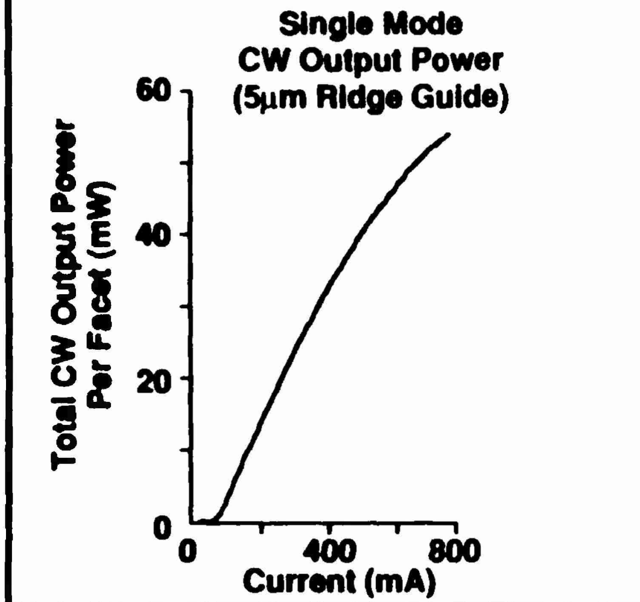

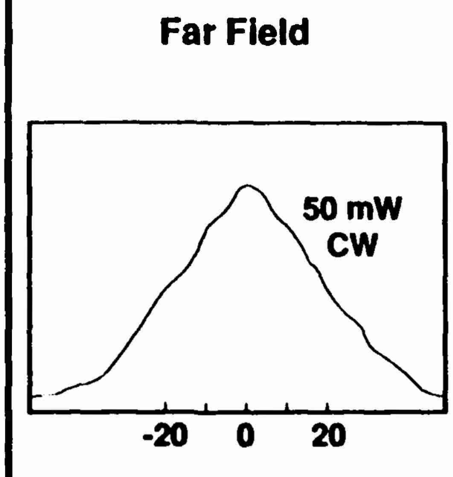

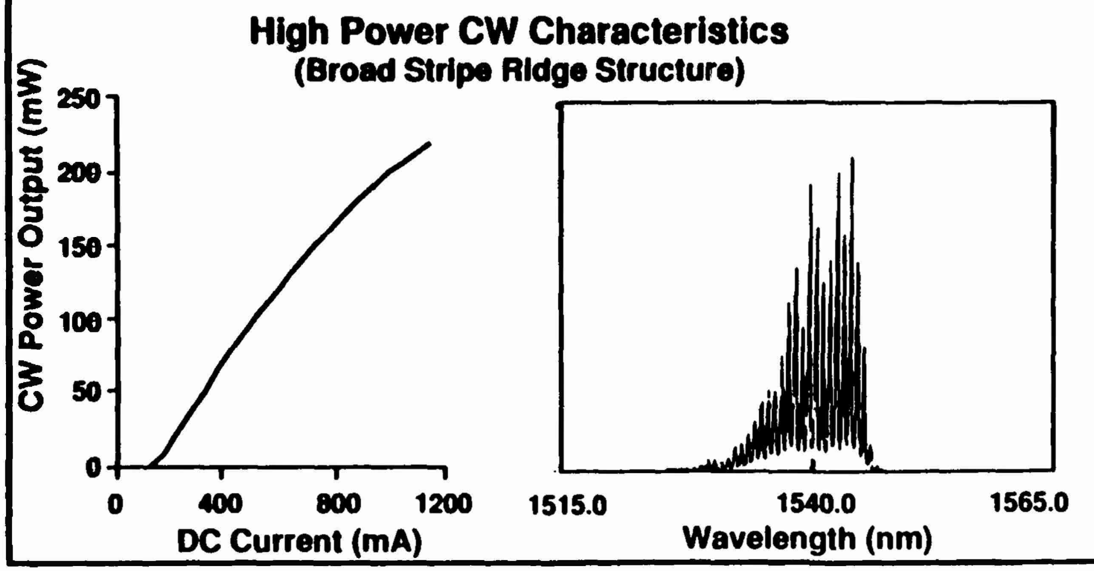

- High Power - 55 mW CW Per Facet, Index-Guided Ridge Guide Structure
- >200 mW CW from Broad Stripe (30μm) Ridge Structure
- High External Diff. Quantum Eff. from Multiple Quantum Well (MQW) Structure
- 1.5μm Eyesafe Wavelength
- High Reliability InGaAsP Materials

CENTER FOR OPTO-ELECTRONIC SYSTEMS RESEARCH
MBE GROWTH FOR VISIBLE AND NEAR-INFRARED LASERS

III-V Materials and Devices

Gary W. Wicks

I. FACILITIES AT UR

• **MOLECULAR BEAM EPITAXY (MBE)**

BEAMS AVAILABLE: III: Al, Ga, In
V: As_4, P_2
Dopants: Si, Be

MATERIALS: GaAs/AlGaAs/GaInAs on GaAs
GaInP/AlInP on GaAs
(GaInAs/AlInAs on InP)
(III-V's on Si substrate)

• **CHEMICALLY ASSISTED ION BEAM ETCHING**

Dry Etching of GaAs

• **RAPID THERMAL ANNEALERS**

Annealing of GaAs and Si

• **OPTICAL CHARACTERIZATION**

Raman Spectroscopy
Photoluminescence
Photoluminescence Excitation spectroscopy
Waveguide endfiring

• **DEVICE PROCESSING EQUIPMENT** (D. HALL)

Evaporators
Photolithography

III-V Materials and Devices

Gary W. Wicks

II. RESEARCH AREAS

- **III-V MATERIALS STUDIES**
  - – Vertical Superlattices/Quantum Wires
  - – GaInP/AlInP on GaAs Substrates
  - – (111) Quantum Wells

- **OPTO-ELECTRONIC EFFECTS AND DEVICES**
  - – Quantum Well Lasers
    - •visible ($\lambda \leq 660$ nm) AlGaInP materials
    - •IR (720 nm $\leq \lambda \leq 1.1$ µm) AlGaAs/GaInAs
    - •dry etching of laser mirrors for integration
  - – Optical Modulators
    - •new electrooptic effects
      - – enhanced e/o effects in {111} quantum wells
      - – field induced ionization of excitons in QW's
      - – coupled quantum wells
    - •MQW modulators in mismatched materials
      - – AlGaAs/GaAs on Si
      - – AlGaAs/GaInAs on GaAs

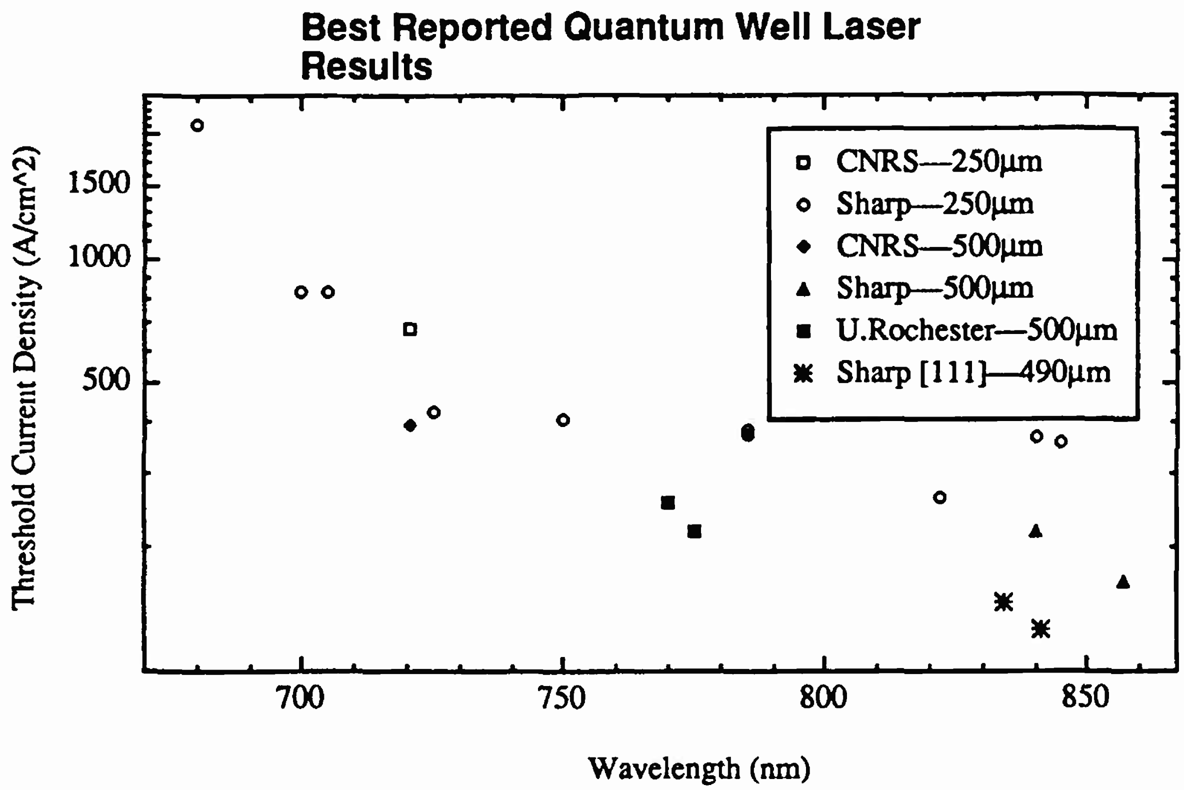

Best Reported Quantum Well Laser Results
Threshold Current Density (A/cm^2)
1500
1000
500
700
750
800
850
Wavelength (nm)
CNRS—250µm
Sharp—250µm
CNRS—500µm
Sharp—500µm
U.Rochester—500µm
Sharp [111]—490µm

III-V Compounds Lattice-matched to GaAs Substrates

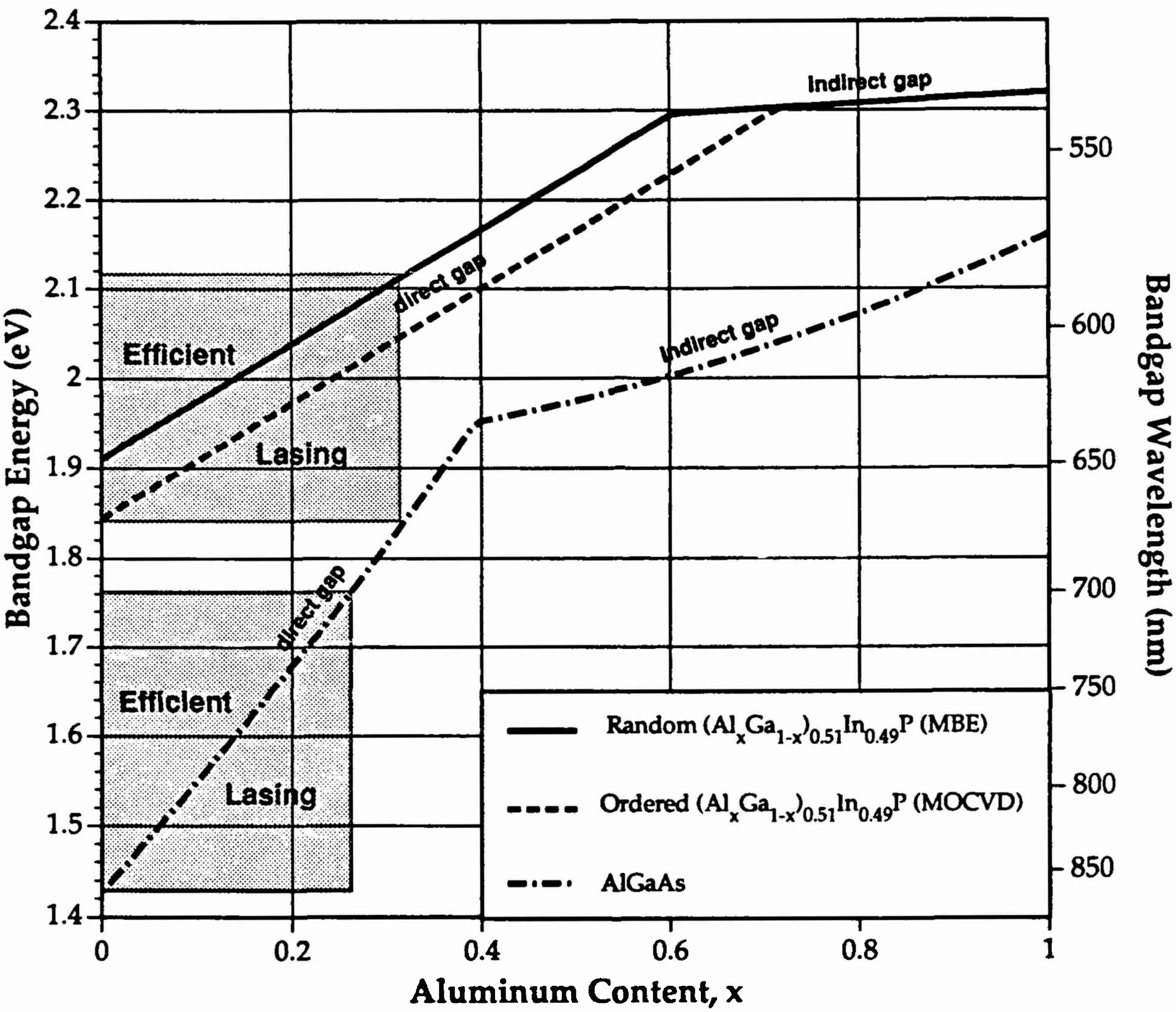

Conventional Solid Phosphorous Source

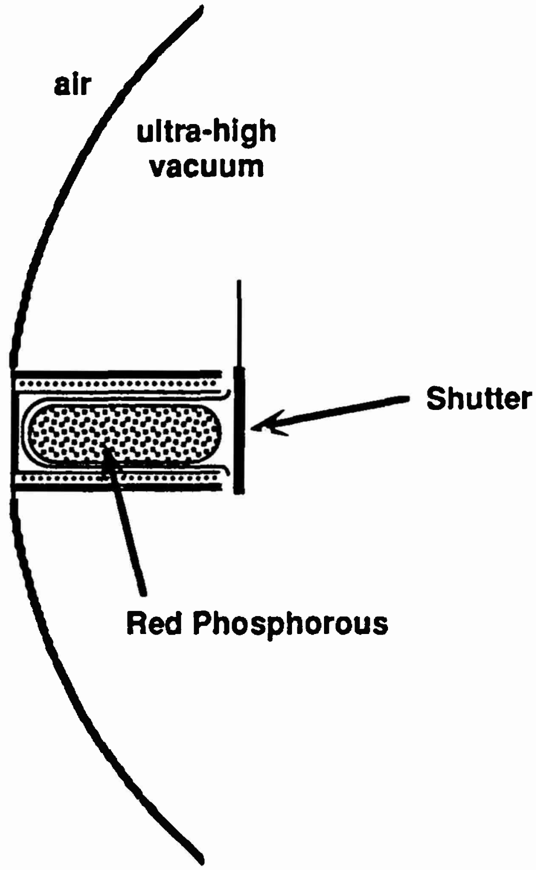

Problems:
- Small phosphorous charge
- Shutter clogging
- Loss of phosphorous during machine bake-out
- Beam stability/low operating temperature

Solutions:
- Phosphine Gas Source
  - ➵ Solves above problems, but is toxic and expensive
- Valved Cracker
  - ➵ Solves above problems, and is <u>safe</u> and <u>inexpensive</u>

Valved Solid Phosphorous Source

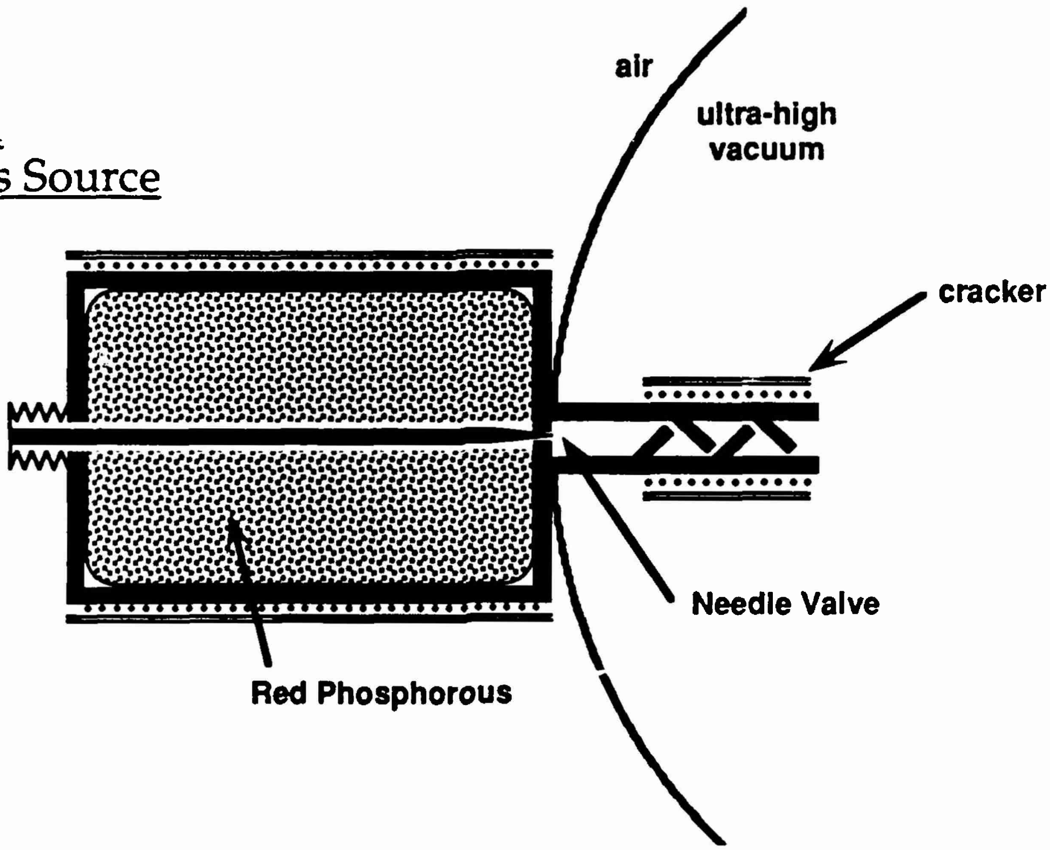

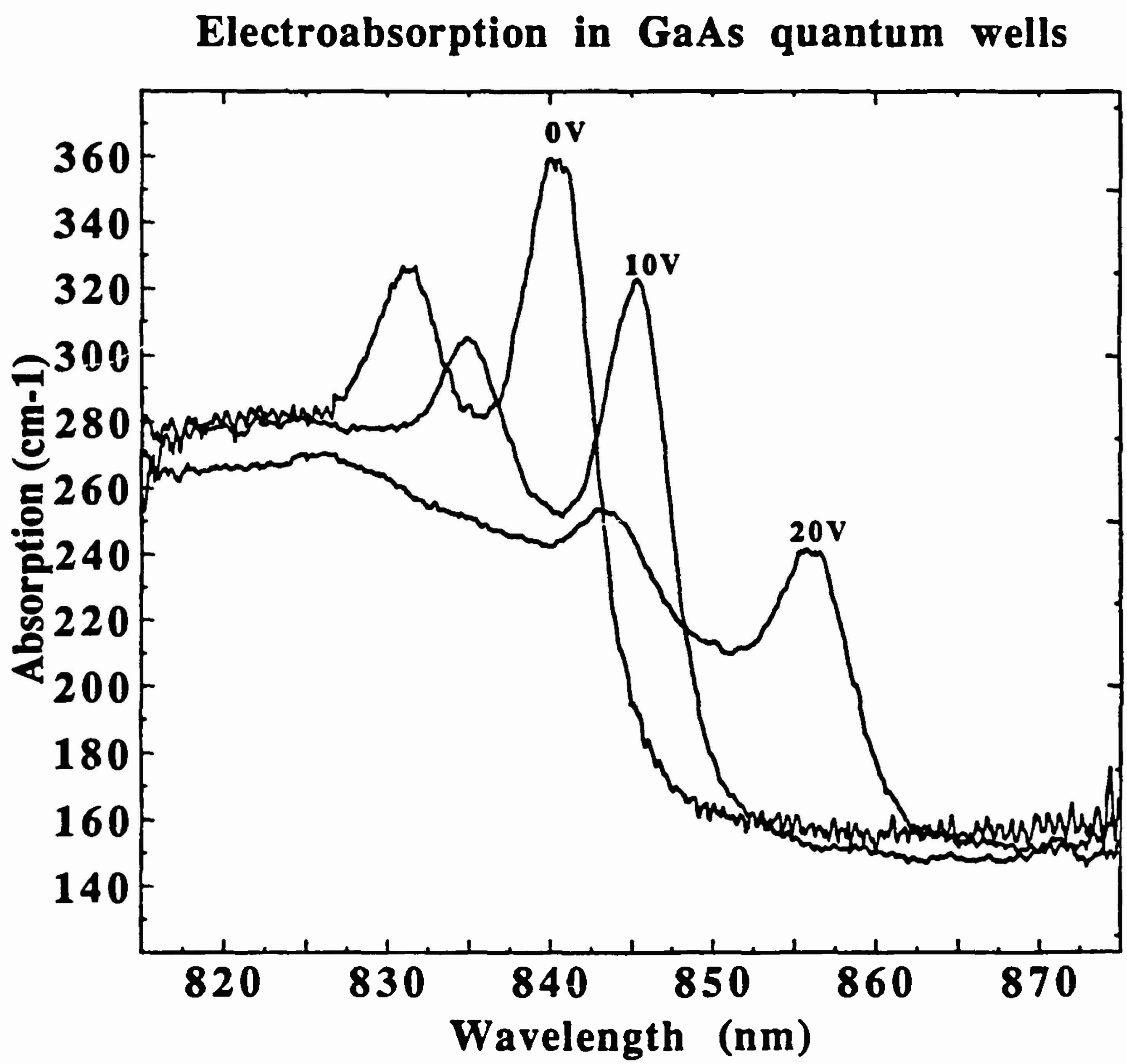
Electroabsorption in GaAs quantum wells
0V
10V
20V
360
340
320
300
280
260
240
220
200
180
160
140
Absorption (cm-1)
820
830
840
850
860
870
Wavelength (nm)

Enhanced Electrooptic Effects on Quantum Wells Grown on {111} Substrates

•Heavy hole effective mass:

→ in plane of QW: $m^*_{hh}(001) > m^*_{hh}(111)$

→ $\perp$ to plane of QW: $m^*_{hh}(111) > m^*_{hh}(001)$

Results — increased oscillator strength in QW's on {111} surfaces.

→ lasers: higher gain, lower threshold, higher speed
→ modulators: higher electroabsorption and electrorefraction, higher speed

•Piezoelectric effects

Vertical Superlattice:
Diagrams in real and reciprocal space.

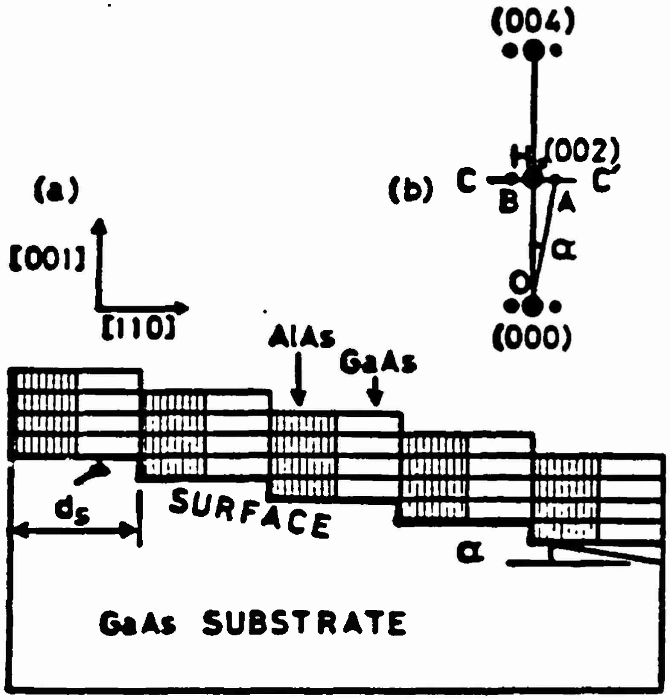

FIG. 1. (a) Idealized representation of an $(AlAs)_{0.5}(GaAs)_{0.5}$ fractional-layer superlattice grown on a (001) vicinal surface. The shaded and unshaded areas correspond to AlAs and GaAs layers, respectively. (b) X-ray diffraction position in reciprocal lattice space expected from ideal FLS structure.

For a substrate misorientation of $\alpha = 2$ degrees, the average terrace width d is 84 A.

(Appl. Phys. Lett. 50 (13), March 30, 1987 - Takashi Fukui)

Vertical Superlattice $\phi = 90°$ 9349

Siemens Analytical X-Ray Instruments Inc. 8-OCT-90

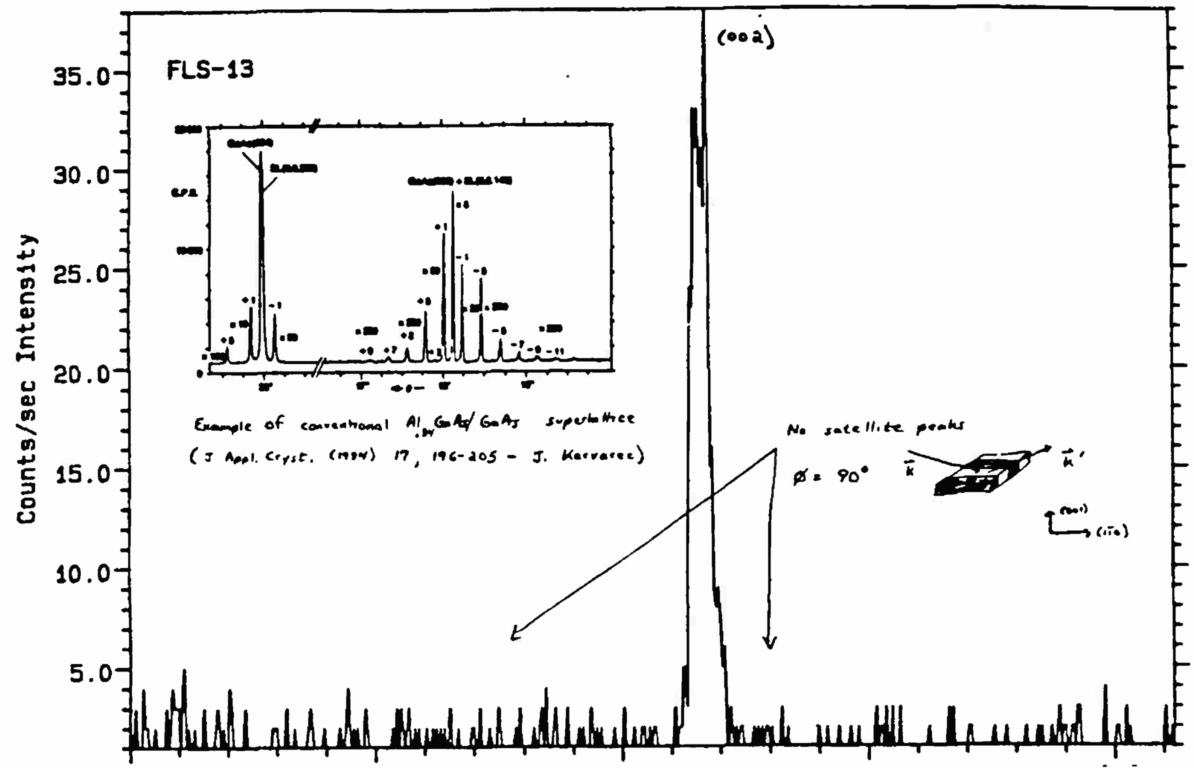

Vertical Superlattice $\phi = 0°$ 9349

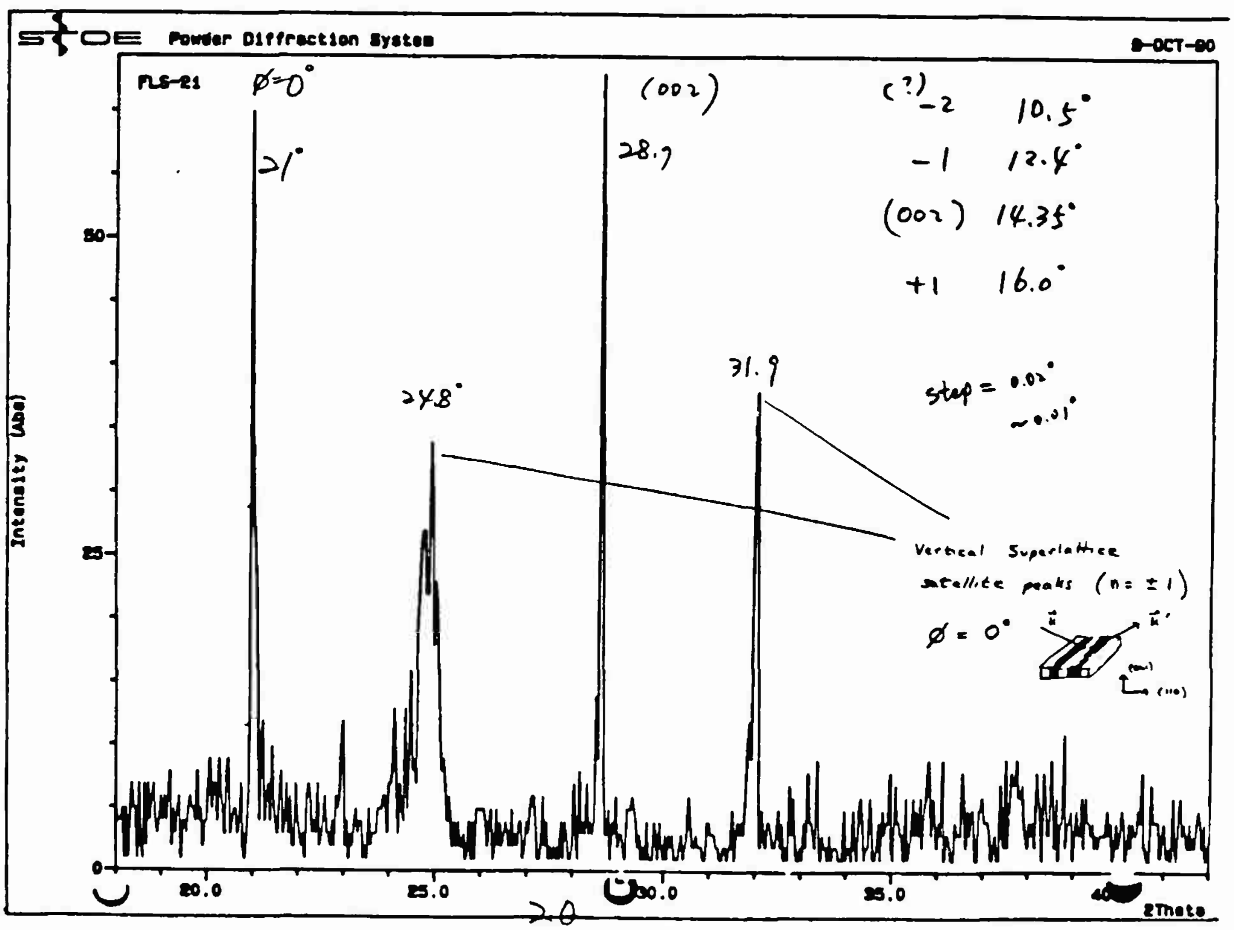

Concept:

Circular Grating Surface Emitting (CGSE) Laser:
A Special Case of a Circular Surface Emitting (CSE) Laser

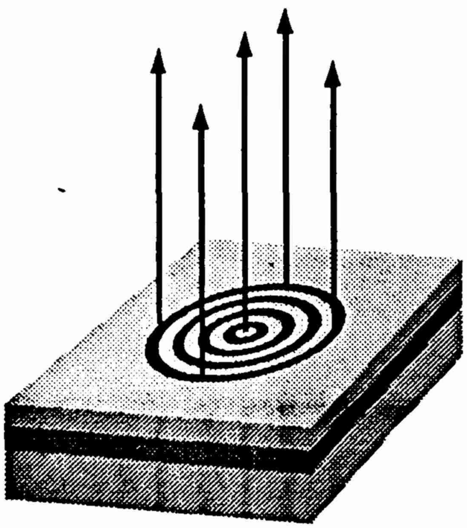

- ● Circular Beam
- ● Large Emission Aperture
  - ➡ Well-collimated Beam
  - ➡ High Power
- ★ Utilizes Planar Waveguide Modes
  - ➡ Light Confinement
  - ➡ Current Confinement

- ● 2 - Dimensional Array
- ★ Equal Phase-Locking in Both Dimensions

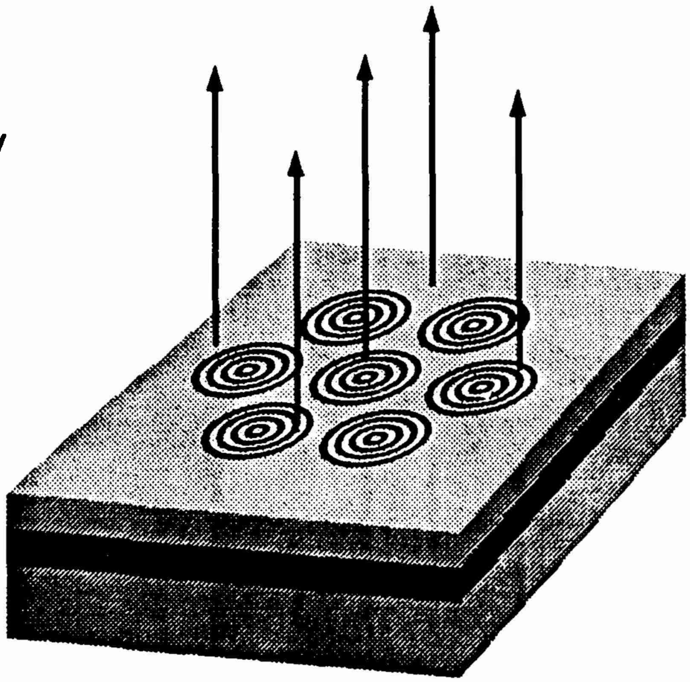

- ● General CSE (Including CGSE and Vertical Cavity SE)
- ★ Unique to Circular Grating Surface Emitting Laser

Possible Implementations
of a Circular Grating Surface Emitting Laser:

A Circular Distributed Feedback (DFB) Laser

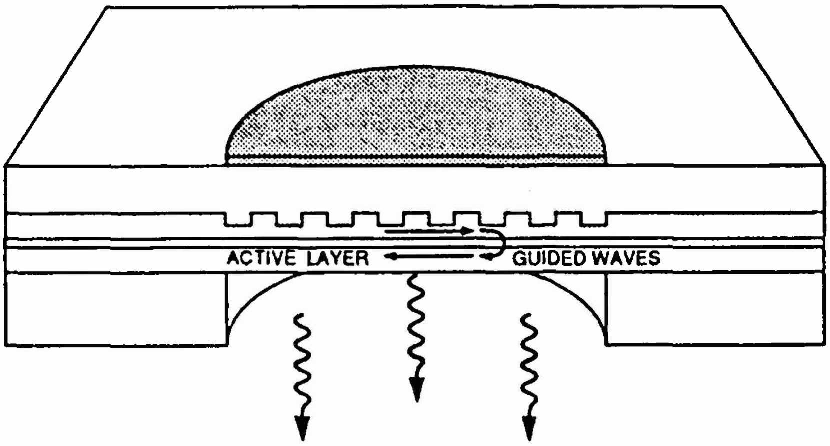

A Circular Distributed Bragg Reflector (DBR) Laser

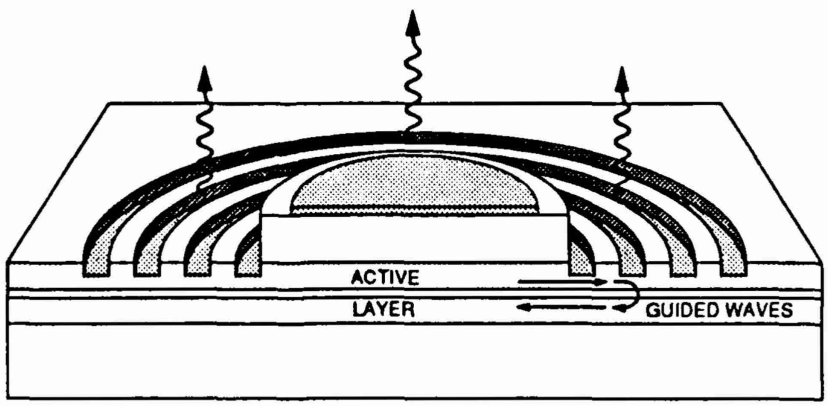

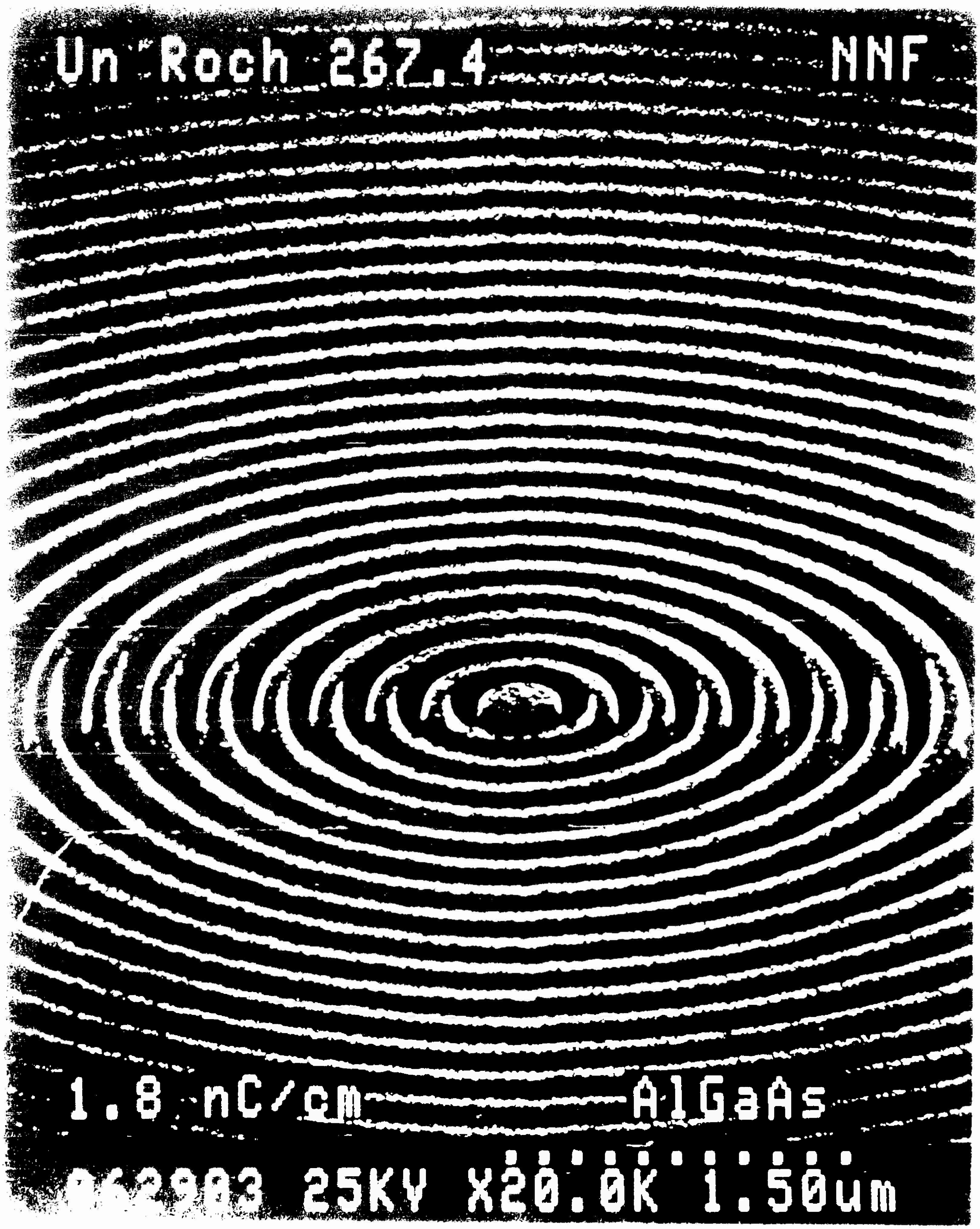
Un Roch 267.4
NNF
1.8 nC/cm
AlGaAs
25KV X20.0K 1.50um

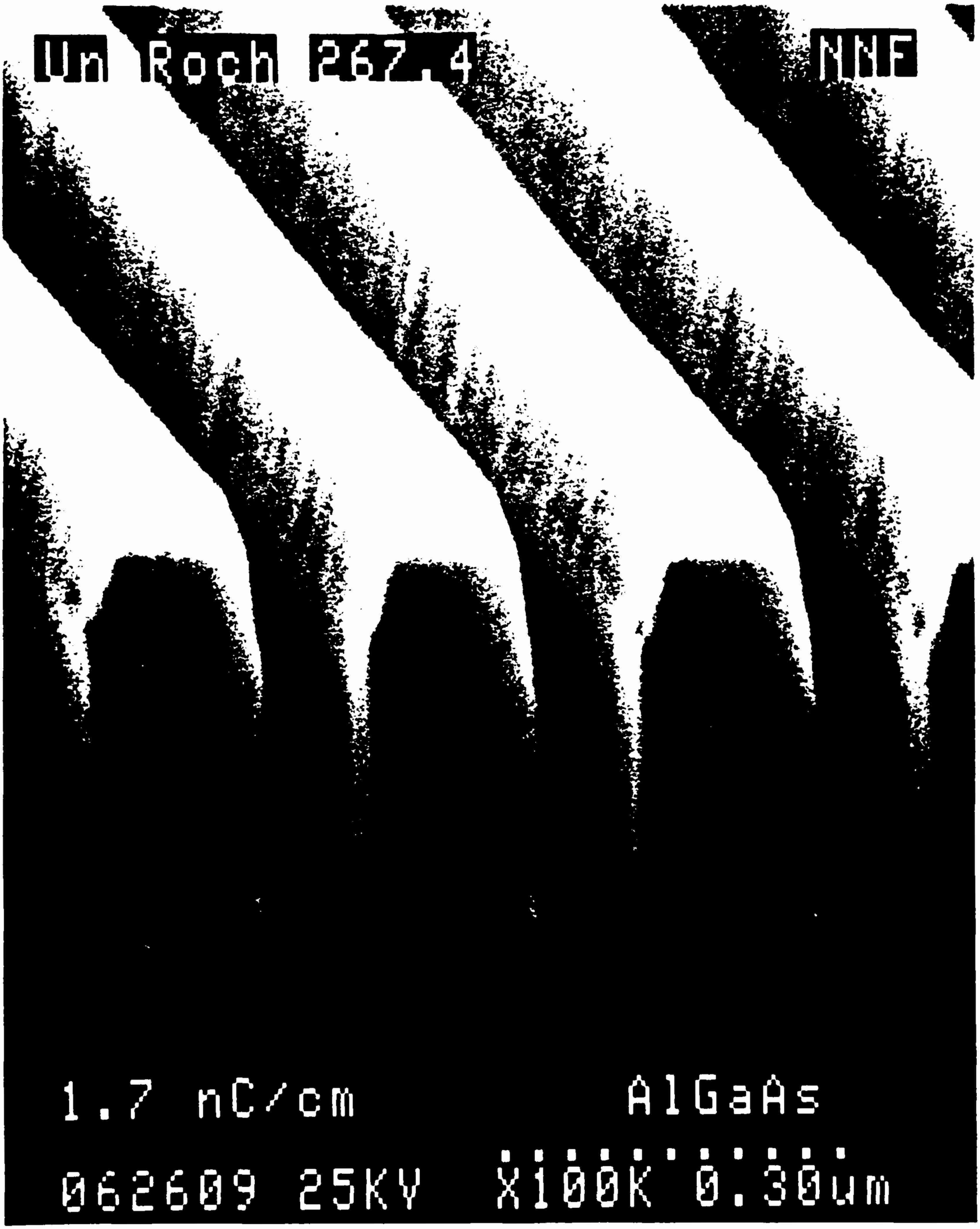

Un Roch 267.4
NNF
1.7 nC/cm
AlGaAs
062609 25KV X100K 0.30um

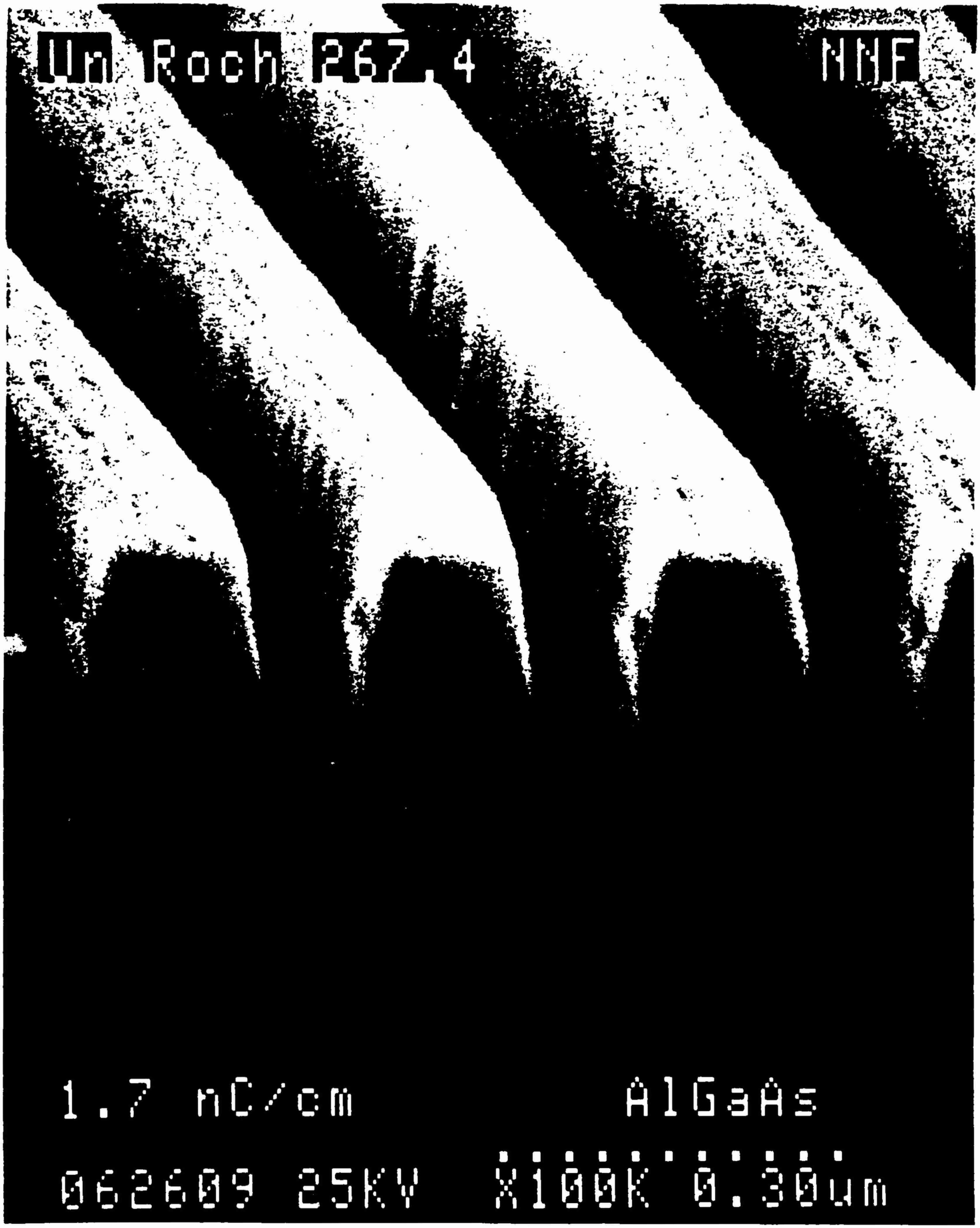
Un Roch 267.4
NNF
1.7 nC/cm
AlGaAs
062609 25KV X100K 0.30um

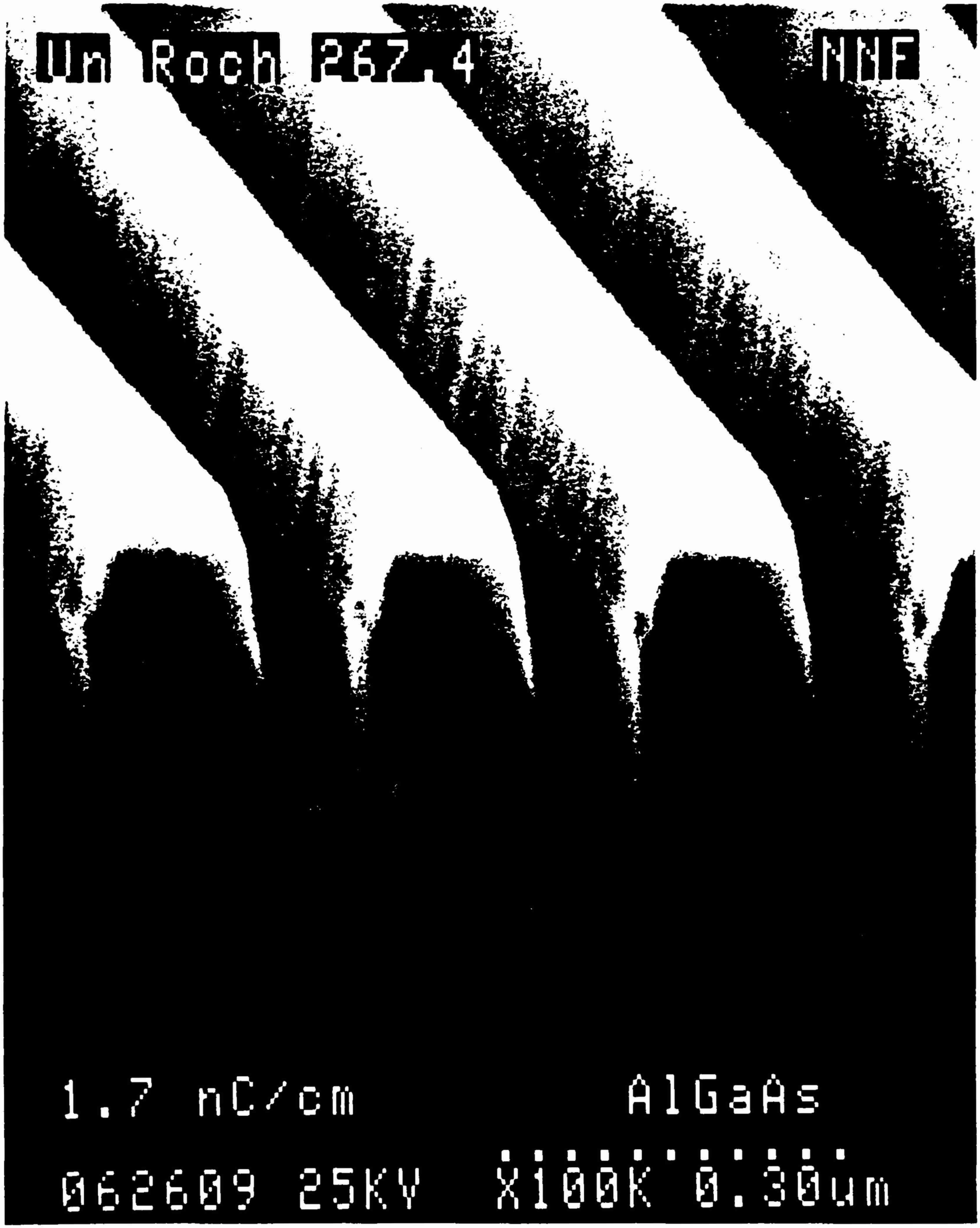
Un Roch 267.4
NNF
1.7 nC/cm
AlGaAs
062609 25KV X100K 0.30um

INTENSITY - PHASE COUPLING IN SEMICONDUCTOR LASERS*

T. G. BROWN

L. OLOFSSON, GRAD. STUDENT

* SUPPORTED IN PART BY THE NEW YORK STATE CENTER FOR ADVANCED OPTICAL TECHNOLOGY

WHY STUDY INTENSITY-PHASE COUPLING?

1. EXCESS LINE BROADENING

2. MODULATION-INDUCED FREQUENCY CHIRP.

3. REFLECTION-INDUCED INTENSITY NOISE AND COHERENCE COLLAPSE

Importance of Laser Linewidth

- Optical Communications

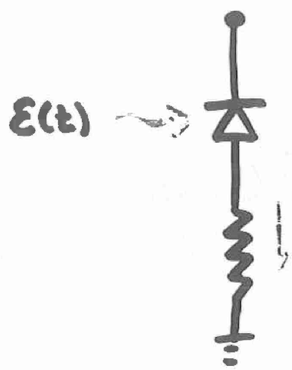

$i(t) \sim |\mathcal{E}(t)|^2$

Optical frequency/phase info. is lost!

How do we detect phase?

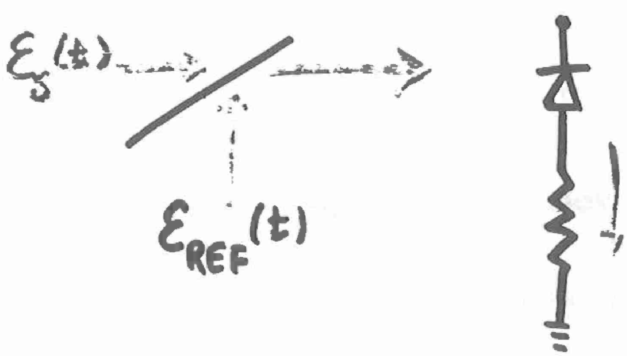

$$i(t) \sim |\mathcal{E}_s + \mathcal{E}_{REF}|^2$$

"Beat" signal

$$= |\mathcal{E}_s|^2 + |\mathcal{E}_{REF}|^2 + \boxed{2|\mathcal{E}_s \mathcal{E}_{REF}| \cos\phi(t}$$

$\phi(t) \equiv$ Dynamic Phase Difference

DIGITAL PHASE MODULATION — PHASE SHIFT KEYING

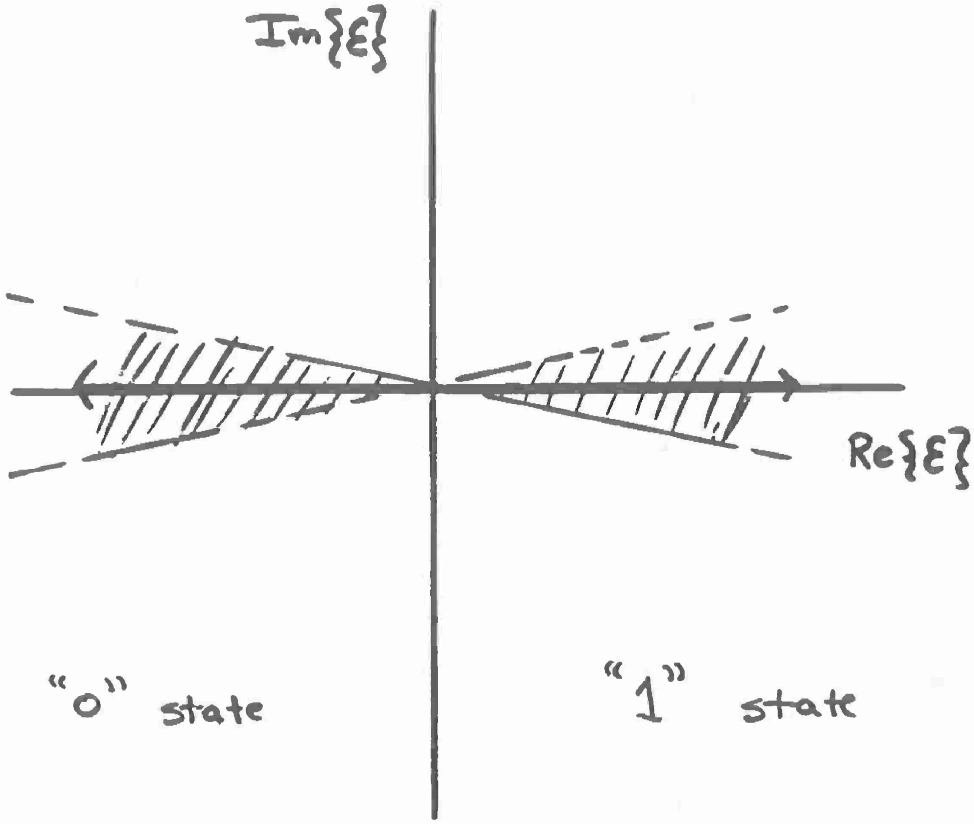

FOR ACCURATE PHASE DETECTION, WE NEED LOW PHASE NOISE – NARROW LINEWIDTH.

Spontaneous Emission

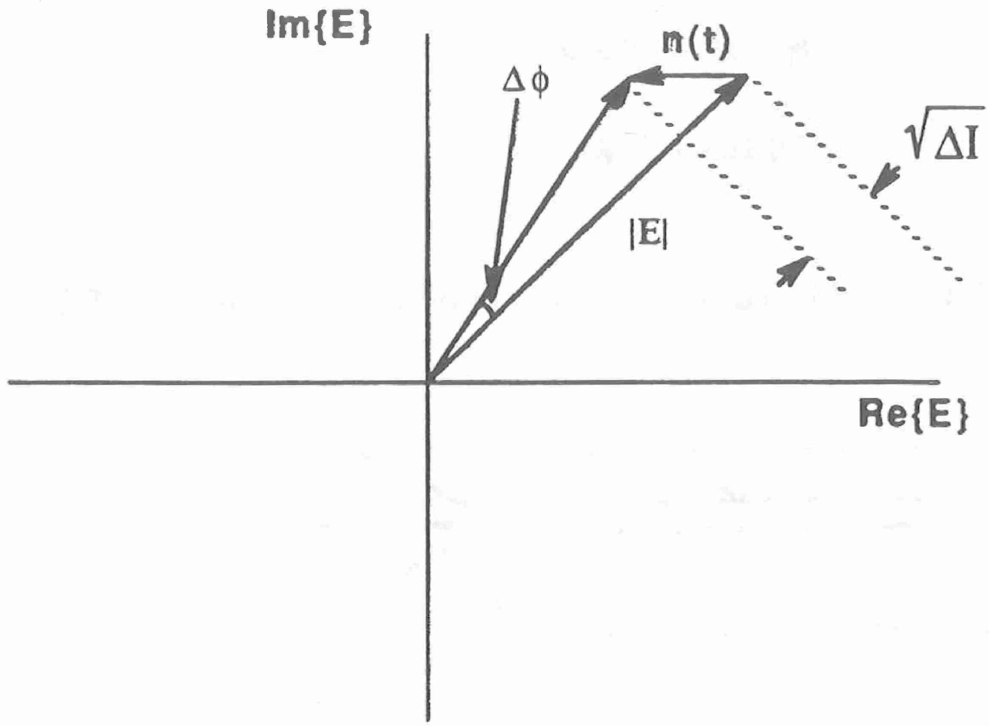

The spontaneous emission event perturbs both the intensity and phase of the optical signal.

$$\Delta\nu \propto \sigma_\phi^2$$

INFLUENCE OF LASER STRUCTURE ON LINEWIDTH

- WAVEGUIDE GEOMETRY
- GAIN MEDIUM
- * RESONATOR

GENERALIZED RESONATORS (WAVEGUIDE)

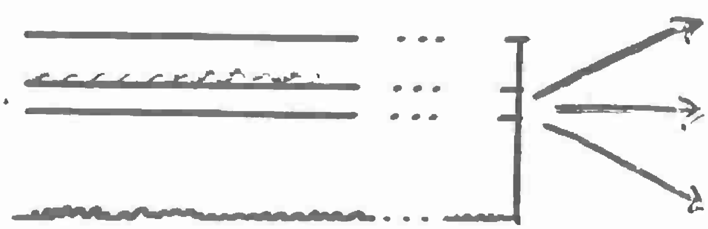

FABRY-PEROT (2 FACETS)

↓

DISTRIBUTED REFLECTORS (DFB & DBR)
USING PERIODIC CORRUGATION

↓

APERIODIC STRUCTURES

WEAKLY APERIODIC (CHIRPED) STRUCTURES

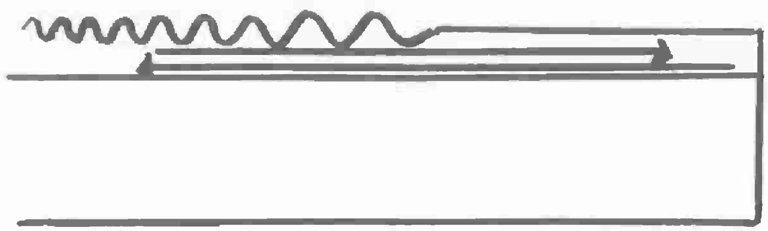

THE $\left\{\begin{array}{l}\text{OSCILLATION FREQUENCY}\\ \text{RESONANCE CONDITION}\end{array}\right\}$ IS DETERMINED BY THE ROUND TRIP PHASE SHIFT.

CAN THIS BE MADE INDEPENDENT OF REFRACTIVE INDEX?

$$\text{CHANGES IN } \left\{\begin{array}{l}\text{Temp.}\\ \text{Current}\\ \text{Carrier Density}\end{array}\right\} \longrightarrow \Delta n$$

LOOK AT PASSIVE RESONATORS FIRST

$$\text{Figure of Merit} \quad \alpha = \frac{Re\{\Delta n\}}{Im\{\Delta n\}}$$

Detuning

Gain

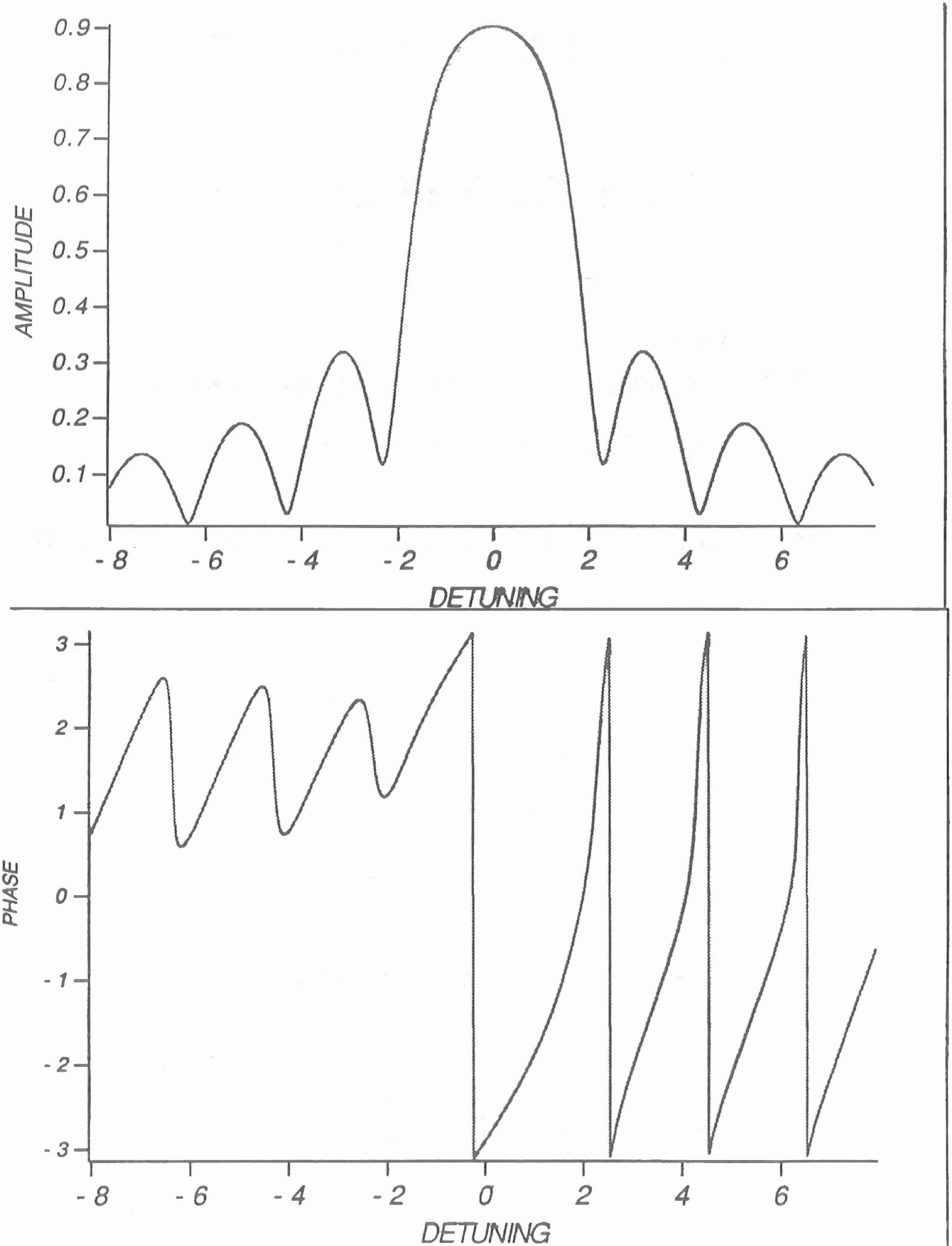
0.9
0.8
0.7
0.6
0.5
0.4
0.3
0.2
0.1
AMPLITUDE
- 8
- 6
- 4
- 2
0
2
4
6
DETUNING
3
2
1
0
- 1
- 2
- 3
PHASE
- 8
- 6
- 4
- 2
0
2
4
6
DETUNING

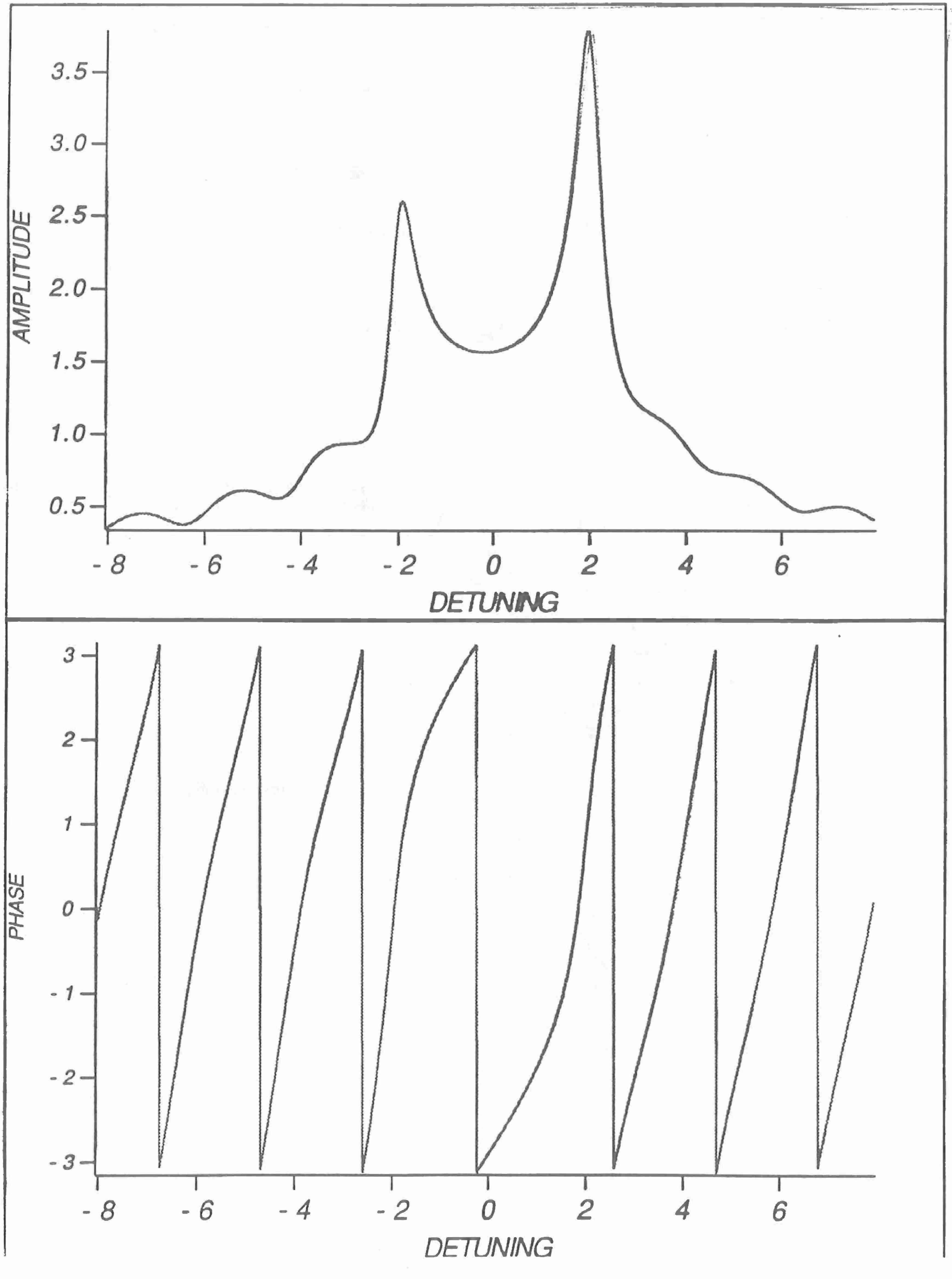
AMPLITUDE
3.5
3.0
2.5
2.0
1.5
1.0
0.5
- 8
- 6
- 4
- 2
0
2
4
6
DETUNING
PHASE
3
2
1
0
- 1
- 2
- 3
- 8
- 6
- 4
- 2
0
2
4
6
DETUNING

FUNDAMENTAL LOOK AT INTENSITY - PHASE COUPLING: FIGURES OF MERIT

① $\alpha_m \equiv \dfrac{\Delta n'}{\Delta n''}$ $\Delta n' \rightarrow$ DISPERSIVE, $\Delta n'' \rightarrow$ ABSORPTIVE

KRAMERS - KRONIG RELATIONS:

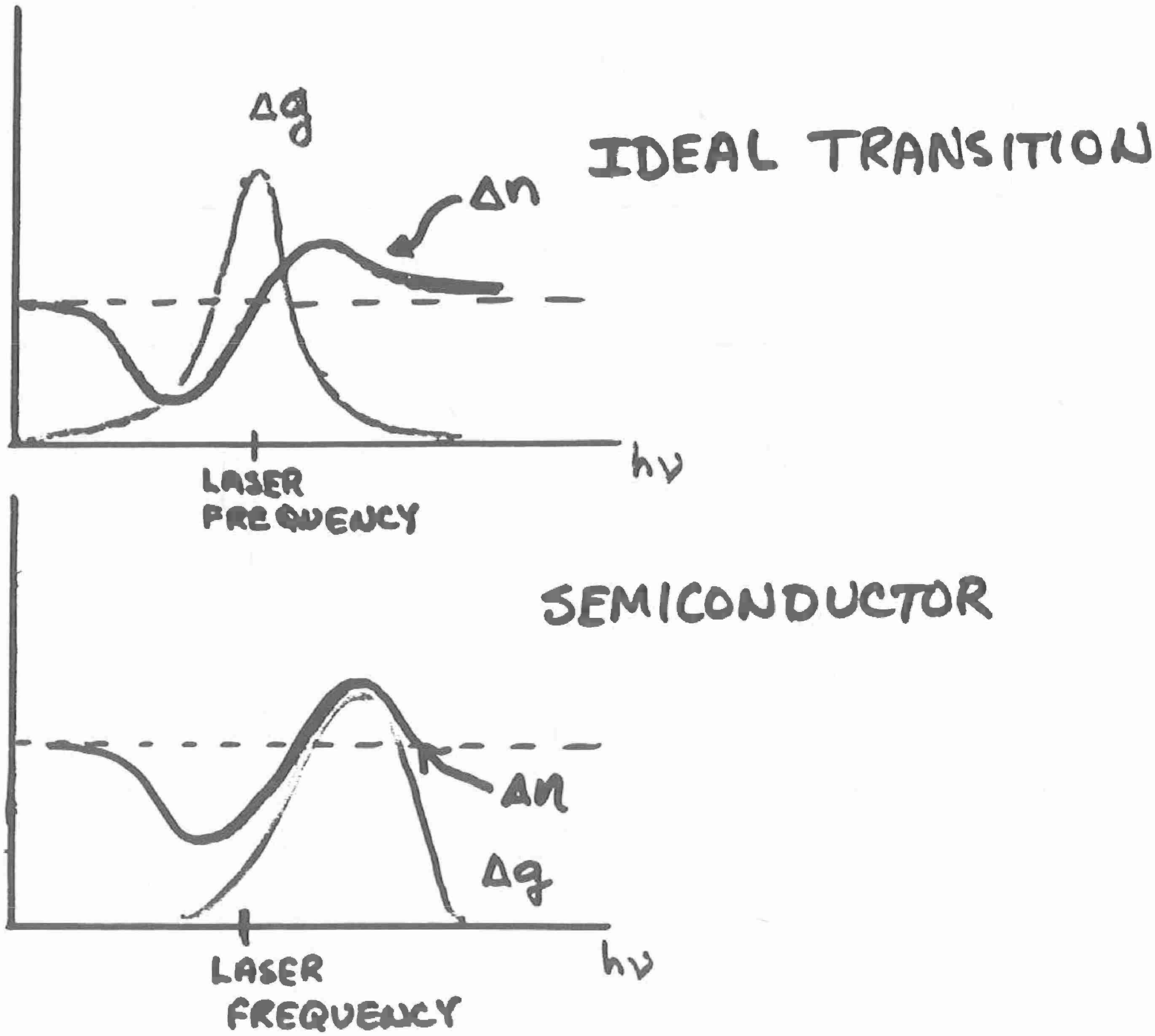

(2) $\alpha_{eff} \equiv 2 \cdot \dfrac{d\phi/dt}{d(\ln I)/dt}$ $\rightarrow$ PHASE PERTURBATION ; $\rightarrow$ INTENSITY PERTURBATION

FULL CAVITY PICTURE:

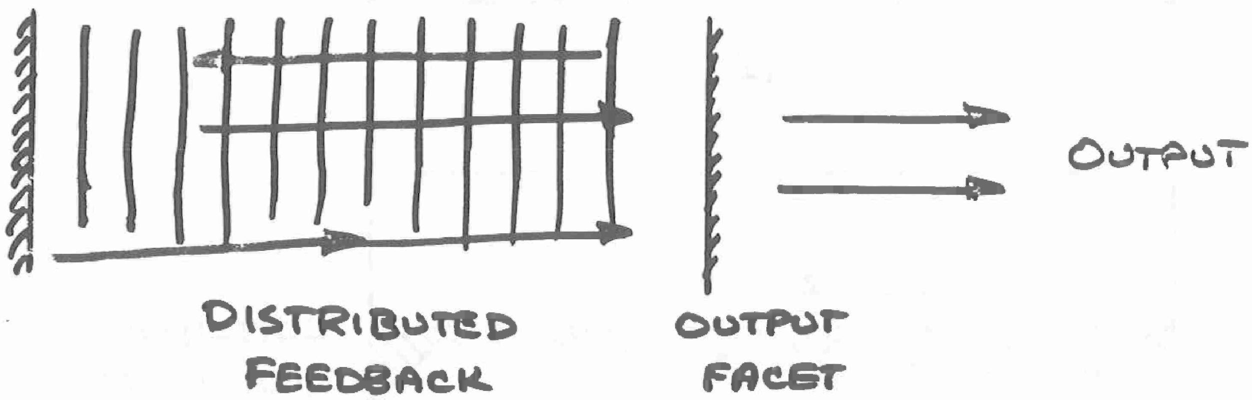

$$\frac{\partial^2 E}{\partial z^2} + \tilde{\beta}^2 E = -4\tilde{\beta} K \cos(2\beta_0 z) E$$

K → COUPLING CONSTANT (DISTRIBUTED FEEDBACK)

$\tilde{\beta}$ → COMPLEX PROPAGATION CONSTANT

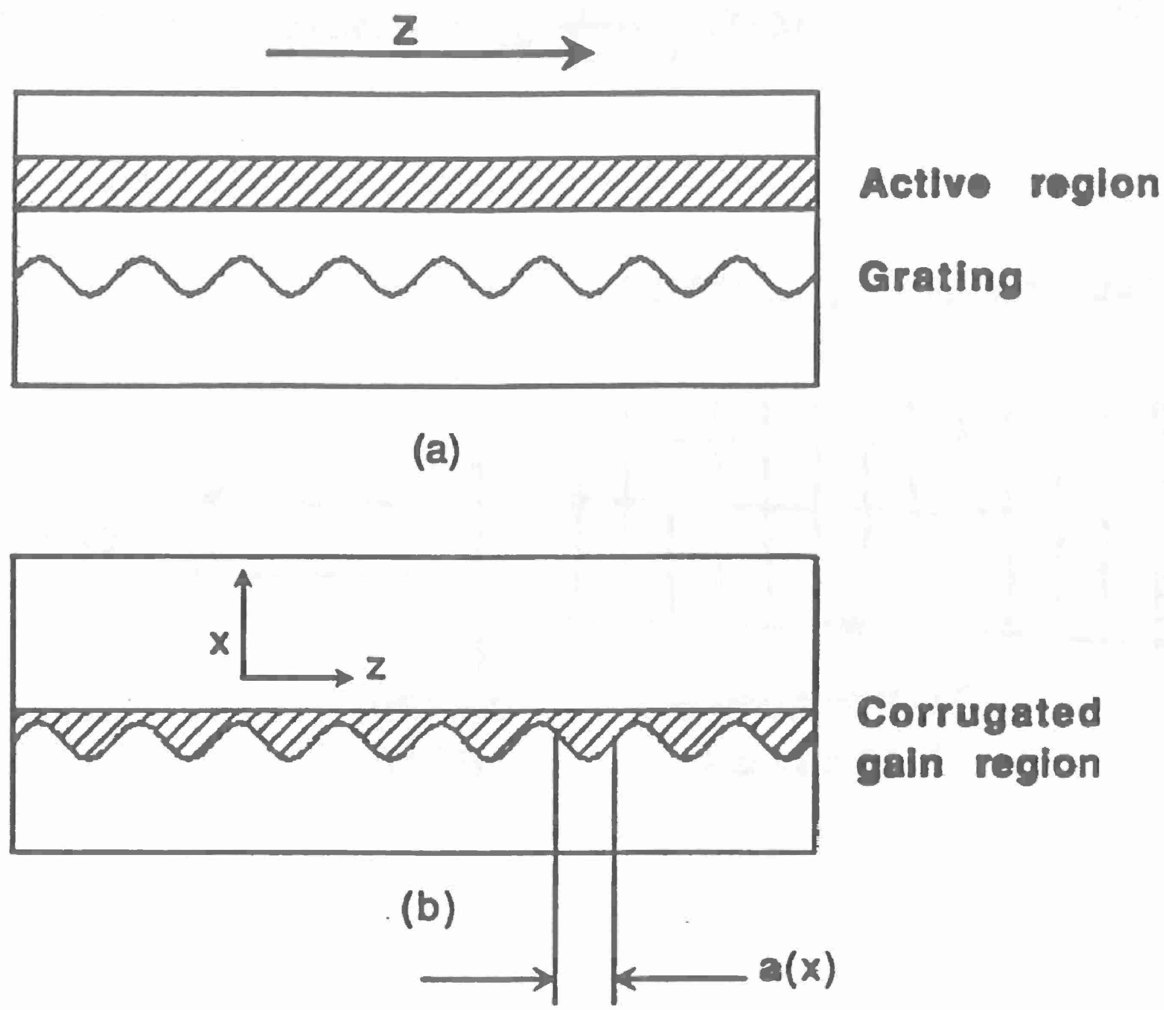
z
Active region
Grating
(a)
x
z
Corrugated
gain region
(b)
a(x)

INDEX COUPLING VS GAIN COUPLING

$Re\{\kappa\}$ ⟶ INDEX COUPLING

$Im\{\kappa\}$ ⟶ GAIN COUPLING

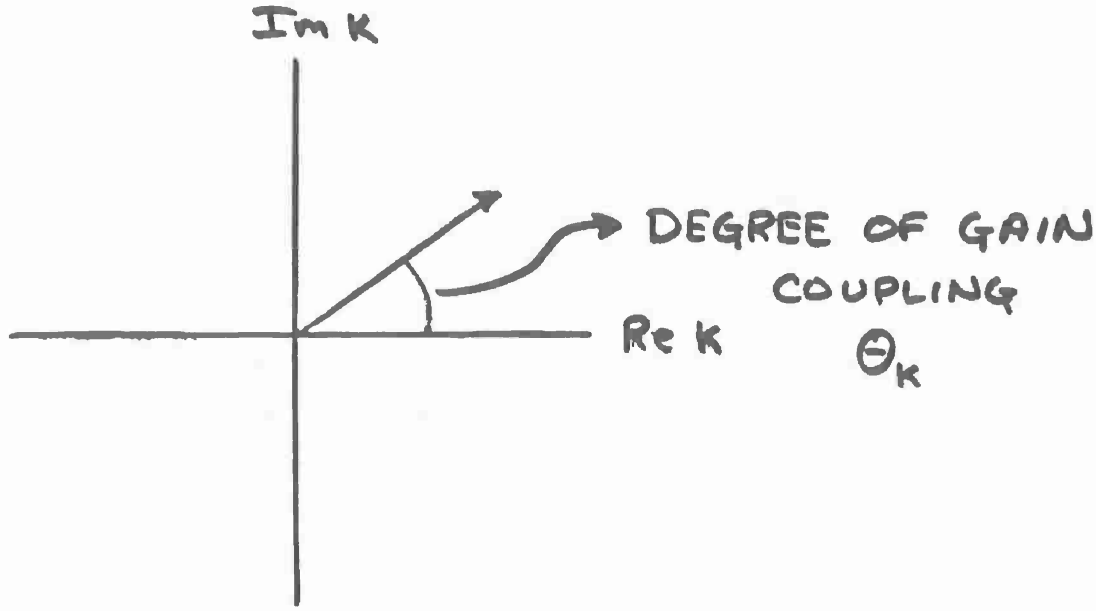

IF $\theta_K = 0, \pi$ THEN

$$\alpha_m = \alpha_{eff}$$

INTENSITY PHASE COUPLING IS INDEPENDENT OF THE LONGITUDINAL STRUCTURE!!

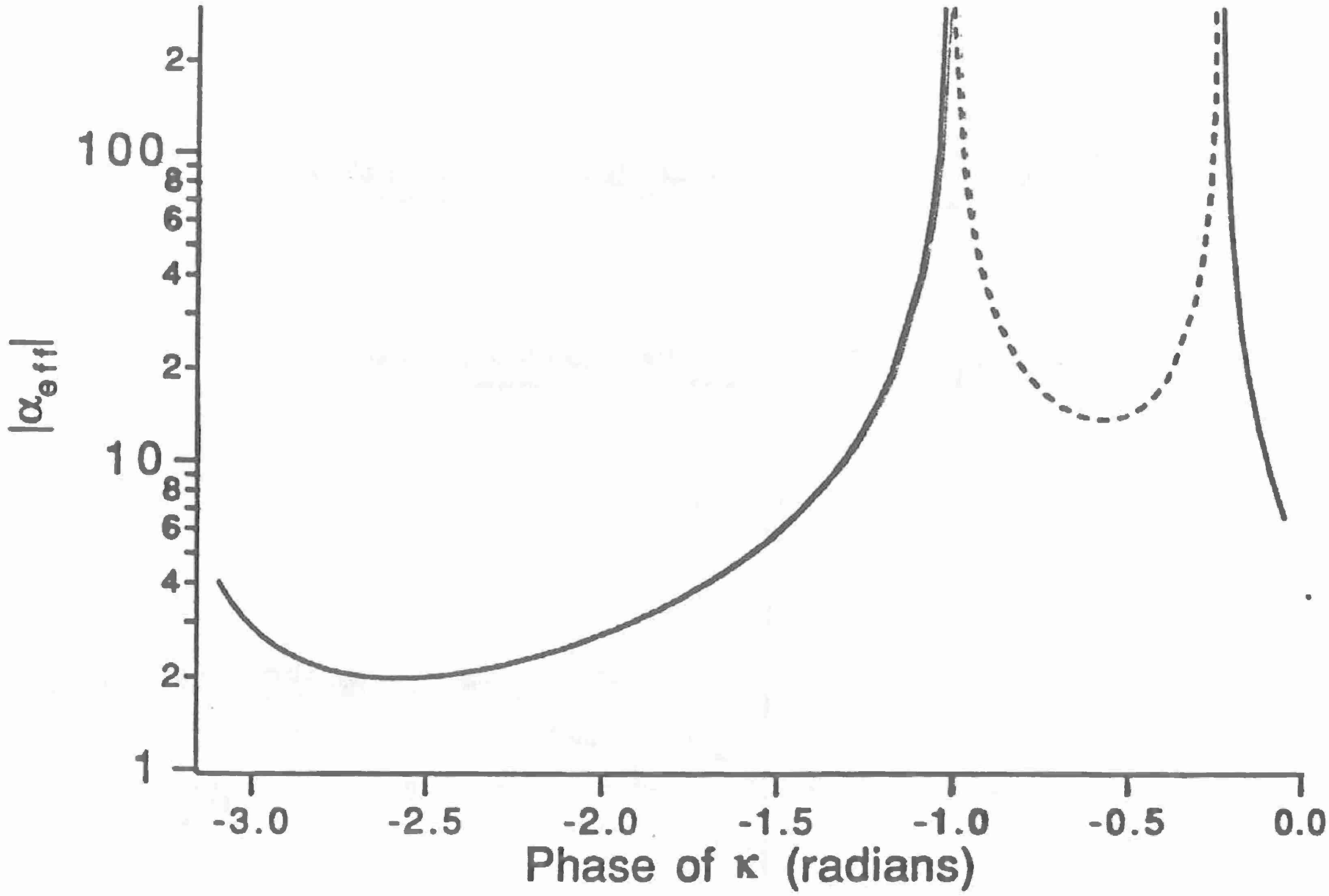

$|\alpha_{eff}|$
1
2
4
6
8
10
2
4
6
8
100
2
-3.0
-2.5
-2.0
-1.5
-1.0
-0.5
0.0
Phase of κ (radians)

CARRIER SCATTERING PARAMETER Q

$$Q \sim -\frac{\Delta K \text{ DUE TO } \Delta N}{\Delta g \text{ DUE TO } \Delta N}$$

$$\begin{tikzcd} & & \Delta \mathrm{Im}(K) & \\ \Delta N \arrow[r] & \Delta g \arrow[ur] \arrow[dr] & & \\ & & \Delta n \arrow[r] & \Delta \mathrm{Re}(K) \end{tikzcd}$$

IF $Q = 0$ THEN

$$\boxed{\alpha_{eff} = \alpha_m}$$

IN GENERAL, $-1 \leq Q \leq 1$

$Q = 0 \longrightarrow$ CORRUGATION SEPARATED FROM GAIN REGION

$Q = 1 \longrightarrow$ 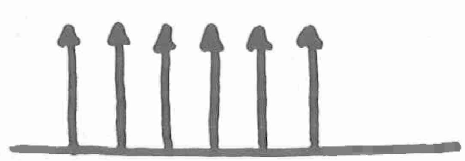

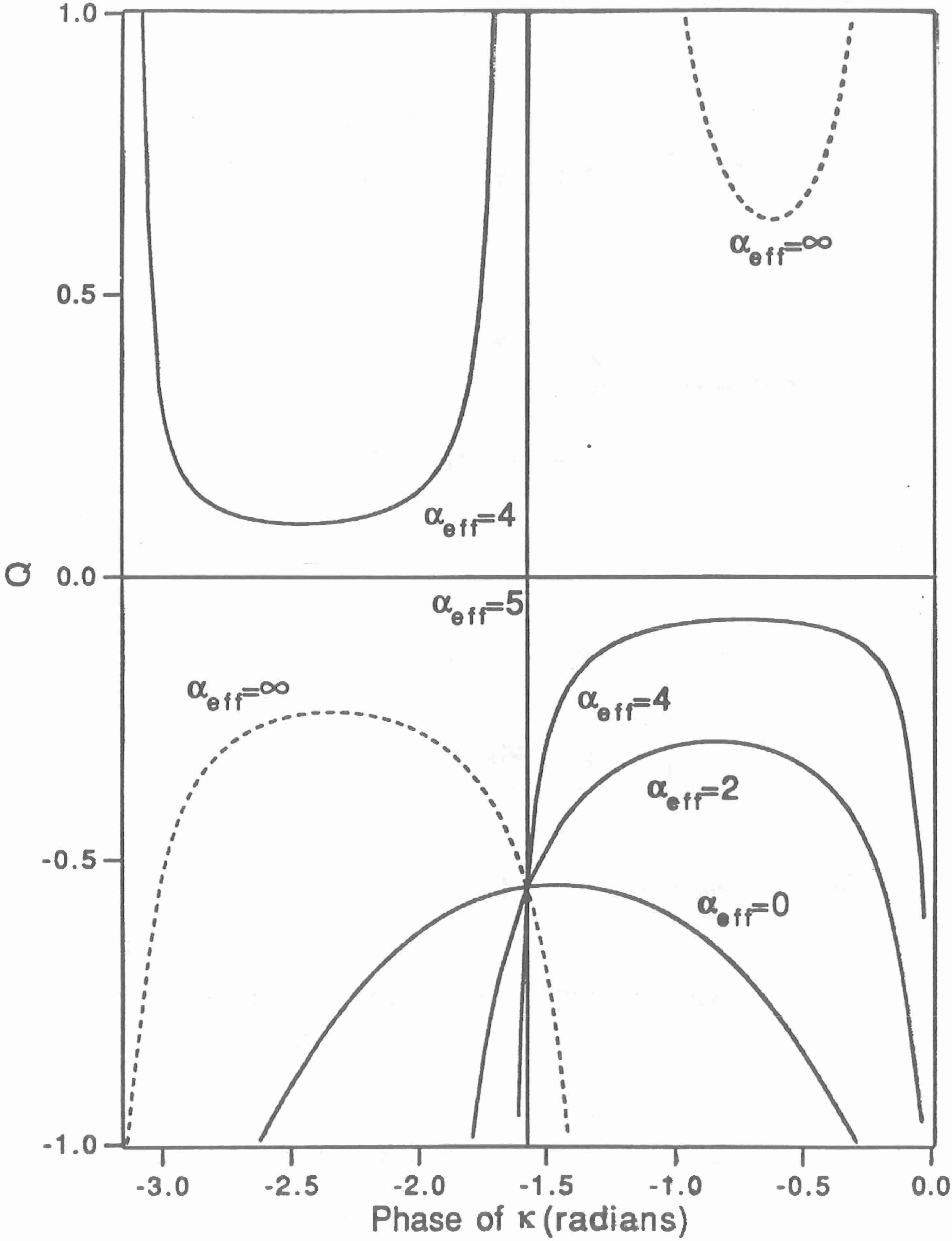

Olofsson and Brown Figure 4

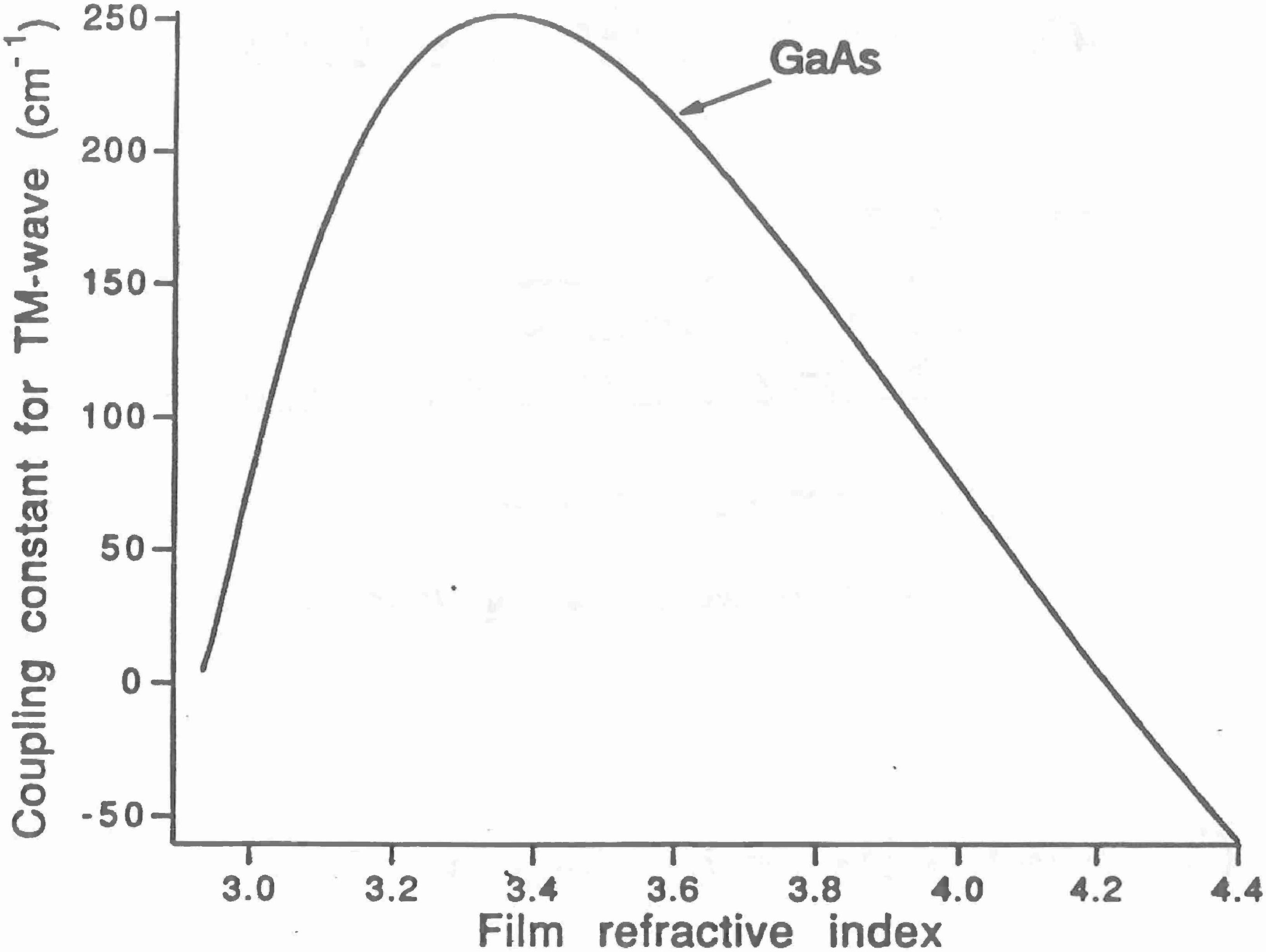

IS IT POSSIBLE FOR Q TO BE NEGATIVE?

YES, IF K DECREASES WITH AN INCREASE IN FILM INDEX.

GAIN-COUPLED LASER STRUCTURES

① Edge-Emitters

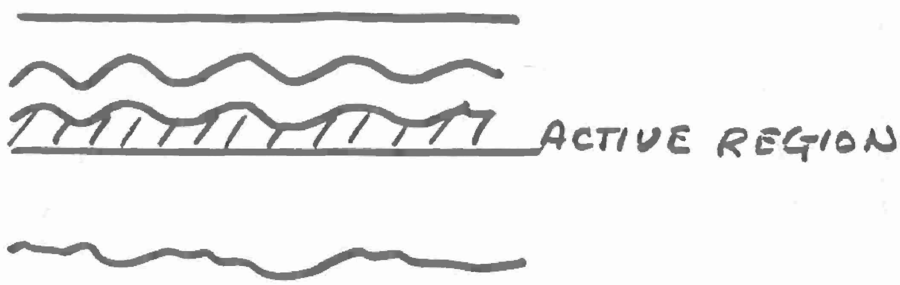

LUO et al, APL 56, 1620 (1990)

② Vertical Cavity Surface Emitters

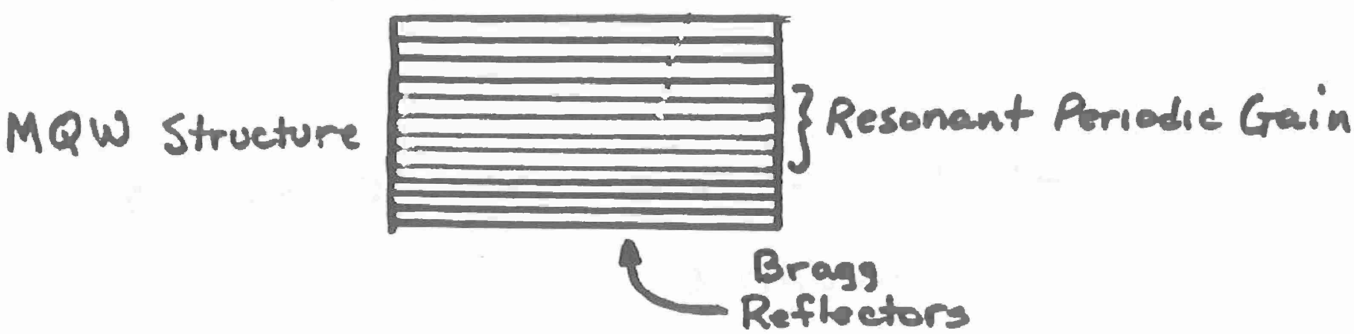

CECOM CENTER FOR NIGHT VISION AND ELECTRO-OPTICS
HIGH-POWER LASER DIODE ARRAY MEASUREMENTS

U of Rochester Workshop
Dec. 17, '90
Vernon King

MATERIAL CHARACTERISTICS

- Wafer Uniformity
- Internal quantum efficiency
- Differential gain
- Loss coefficient (alpha)
- Transparency current
- Wavelength
- Lifetime

DEVICE CHARACTERISTICS

- Wavelength
- Threshold current
- Threshold current density
- Slope efficiency
- Differential quantum efficiency
- Series Resistance
- Characteristic voltage
- Temperature coefficient - T_0
- Catastrophic mirror damage

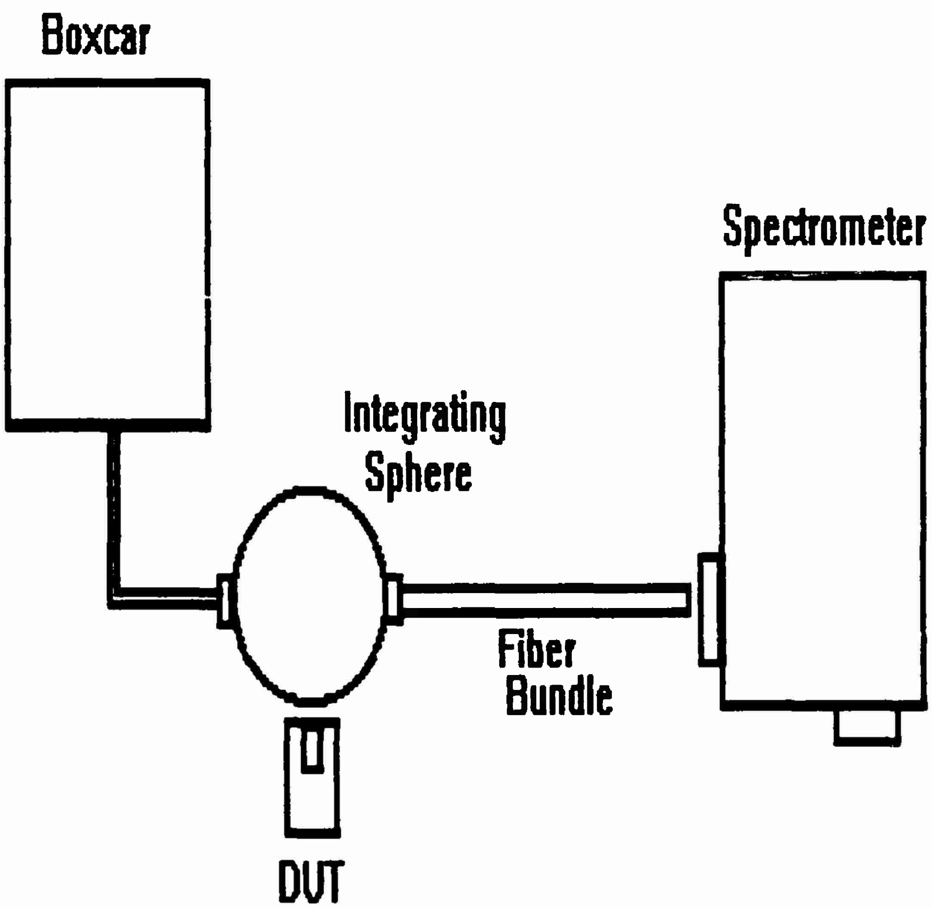
Boxcar
Spectrometer
Integrating
Sphere
Fiber
Bundle
DUT

UNM #219: P-Up: Data/Facet: Multi-Widths
50 Hz: Long Pulse

U of New Mexico & C2NVEO

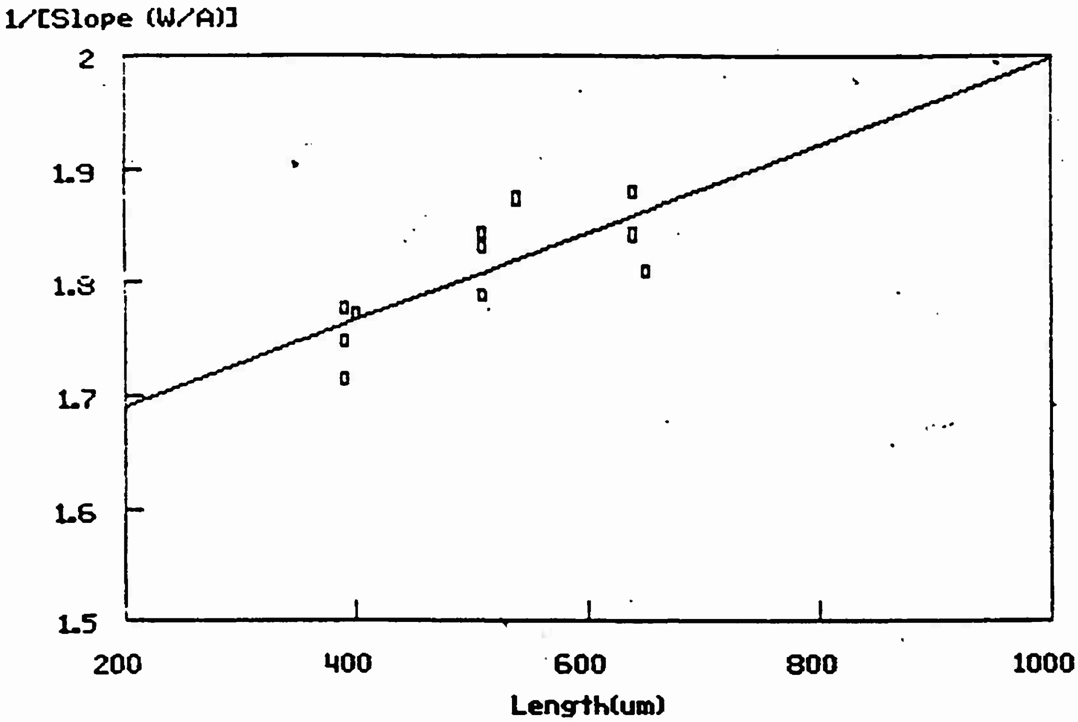

Regression Report:

Y Intercept (C0)	1.612953
Std Y Est Error	0.034923
R Squared [0..1]	0.595740
Number of Samples	11
Degrees of Freedom	9

η(i)=	0.83
αi=	2.7 /cm
V(c)=	1.49 Volts

X Coeffs (C1-Cn): 0.000384

Std Coeff Errors: 0.000105

Len. (um)	η(s)W/A	1/η
390	0.583	1.715265
390	0.572	1.748251
390	0.563	1.776198
400	0.564	1.773049
510	0.546	1.831501
510	0.542	1.845018
510	0.559	1.788908
540	0.534	1.872659
640	0.543	1.841620
640	0.532	1.879699
650	0.552	1.811594

C2NVEO Data
Spectra Diode Labs

	Max. Pwr. (W)	Max. Eff. (%)	I(th) (Amps)	Slope (W/A)	V(c) (Volts)	Resist. (Ohms)	Ctr. Wavel. (nm)	FWHM (nm)
S031 (5)	305	42.5	18.50	5.18	8.2	0.015	809.5	2.6
C2NVEO	290	34	18.75	4.46	8.16	0.023	809.4	2.6
NOSC								
NASA								
% Diff.		-20	1.40	-13.9	-0.5	53.3		0
S032 (10)	610	41	20.00	10	16	0.025	808	2.5
C2NVEO	584	36	20.42	9.24	16.43	0.032	806.8	2.2
NOSC								
NASA								
% Diff.		-12.2	2.10	-7.6	2.7	28		-12
S040 (20)	1220	41	21.00	19.5	31.5	0.043	808.5	2.4
C2NVEO	1110	36	21.80	18.4	33.1	0.055	810.1	2.1
NOSC								
NASA								
% Diff.		-12.2	3.80	-5.6	5.1	27.9		-12.5
S042 (10)	610	41	20.00	9.75	16	0.025	808.5	2.5
C2NVEO	580	36	21.20	9.35	16.6	0.036	807.4	2.2
NOSC								
NASA								
% Diff.		-12.2	6.00	-4.1	3.8	44		-12
S044 (10)	610	35	20.50	9.1	15	0.034	810	2.6
C2NVEO	560	33	21.60	8.4	14.8	0.051	808.4	2
NOSC		34	20.00	8.25				
NASA								
% Diff.		-5.7	5.40	-7.7	-1.3	50		-23.1
S046 (5)	308	41	20.00	5.1	8.2	0.015	807	2.9
C2NVEO	280	33	20.52	4.5	8.27	0.022	806.4	2.8
NOSC								
NASA								
% Diff.		-19.5	2.60	-11.8	0.9	46.7		-3.4
S047 (5)	307	39	20.00	4.58	8.4	0.01	808.5	3.1
C2NVEO	260	30	21.20	4.06	8.41	0.019	807.7	2.5
NOSC								
NASA								
% Diff.		-23.1	6.00	-11.4	0.1	90		-19.4

UNM #222,100um Phased, P-Up, (1 Stripe)
Ref'd P6063B, 6LC, HR/AR
U of New Mexico & C2NVEO

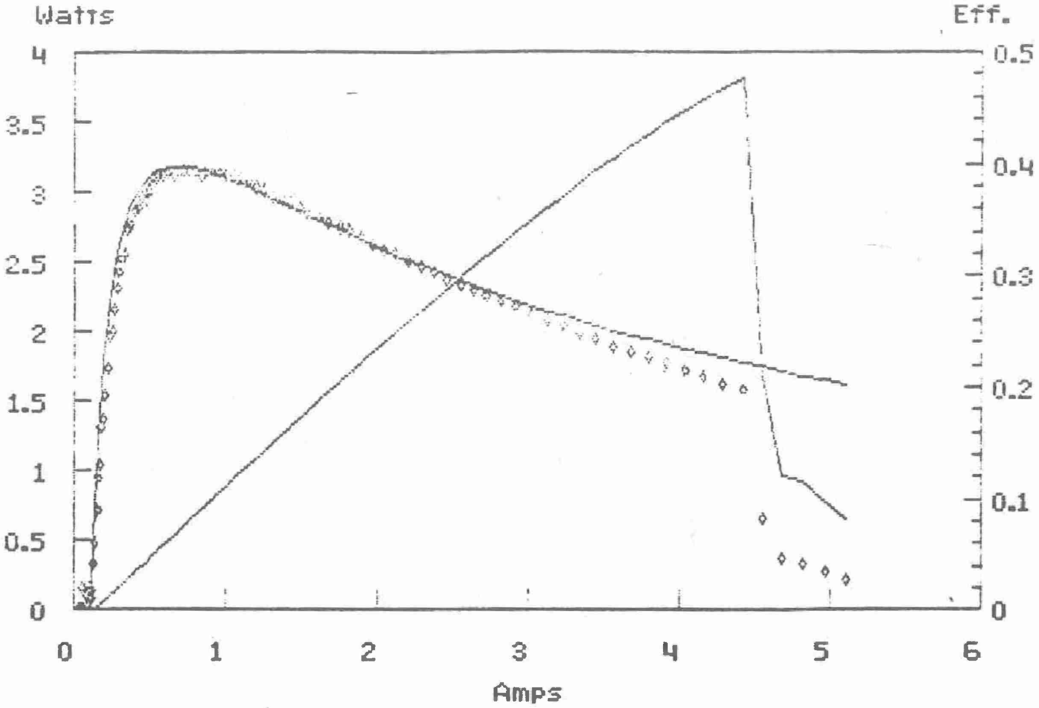

File Name:	N222B4P.DTA		Thresh.=	0.121 Amps
Date:	01-Mar-90		J(th)=	183 A/cm²
Length	660	µm	Slope=	0.996 W/A
Width	100	µm	Diff. Q.E.=	77 %
Pulse Width	200	µS	Resistance=	0.6161 Ohms
Rep. Rate	50	Hz	V(c)=	1.639 Volts
Wavelength	962	nm	Temp:	21 °C
End Points	0.50-2.50	Amps		

HNM #9A: Pkyeak Orrya: P-Hn xH RaA
DATA/FACET, 9 Stripes

U of New Mexico & CNVEO

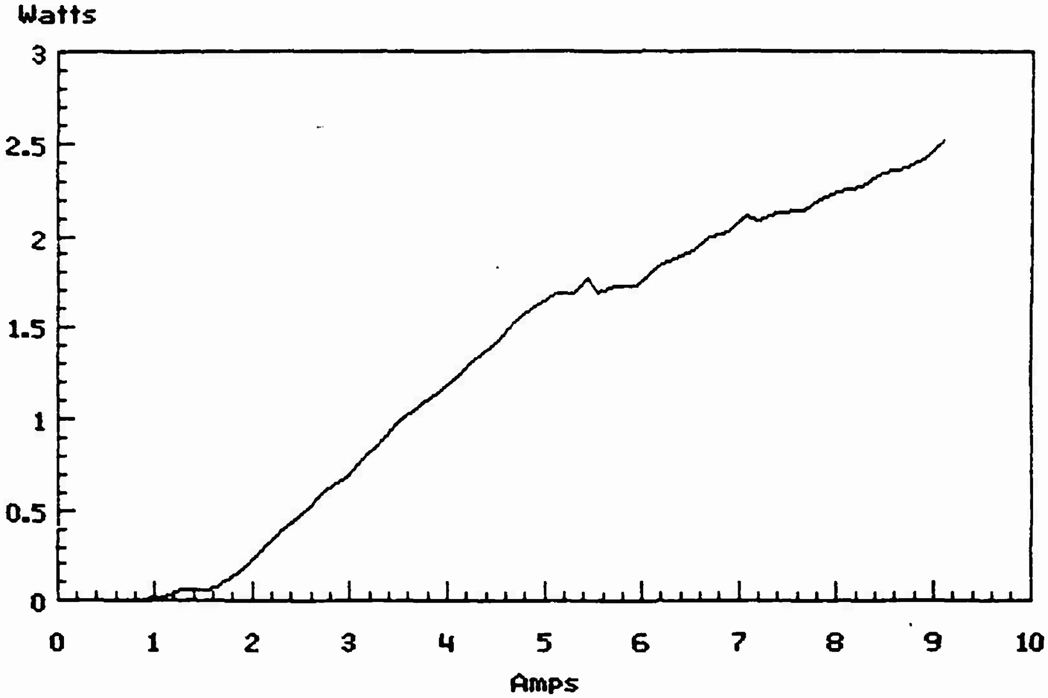

Length	600	μm
Width	900	μm
File	NOZ2001.PWR	
Thresh.=	1.467	Amps
J(th) =	271	A/cm²
Slope=	0.471	W/A
Diff Q.E.=	30	%
Pulse Width	100	μS

Rep. Rate	20	Hz
Wavelength	795	nm
End Points	2-4.5	Amps
Date	10/14/88	

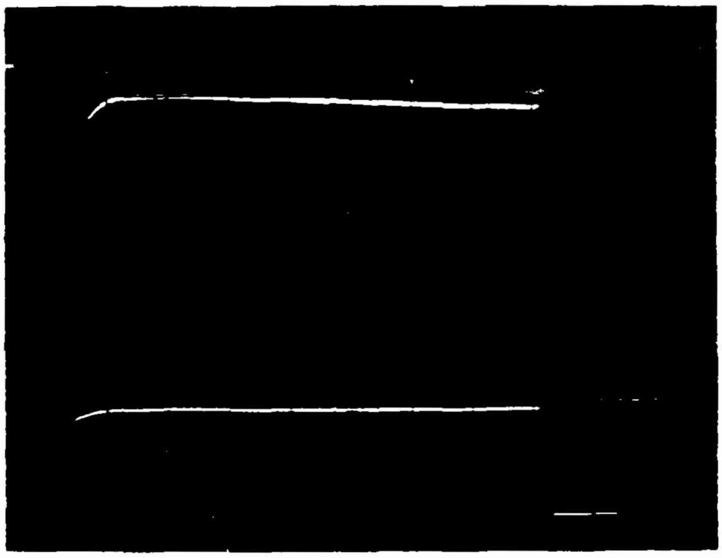

400 μSEC PW S047 Iop=85A 5/9/90

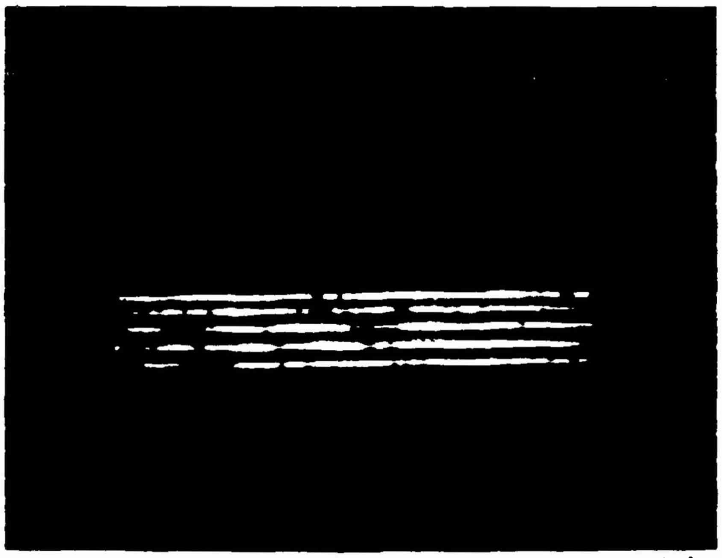

S047 5/9/90

WAVELENGTH CHANGE WITH REP RATE

1100 to 1200 Watts Peak Out (LDAI 170W)

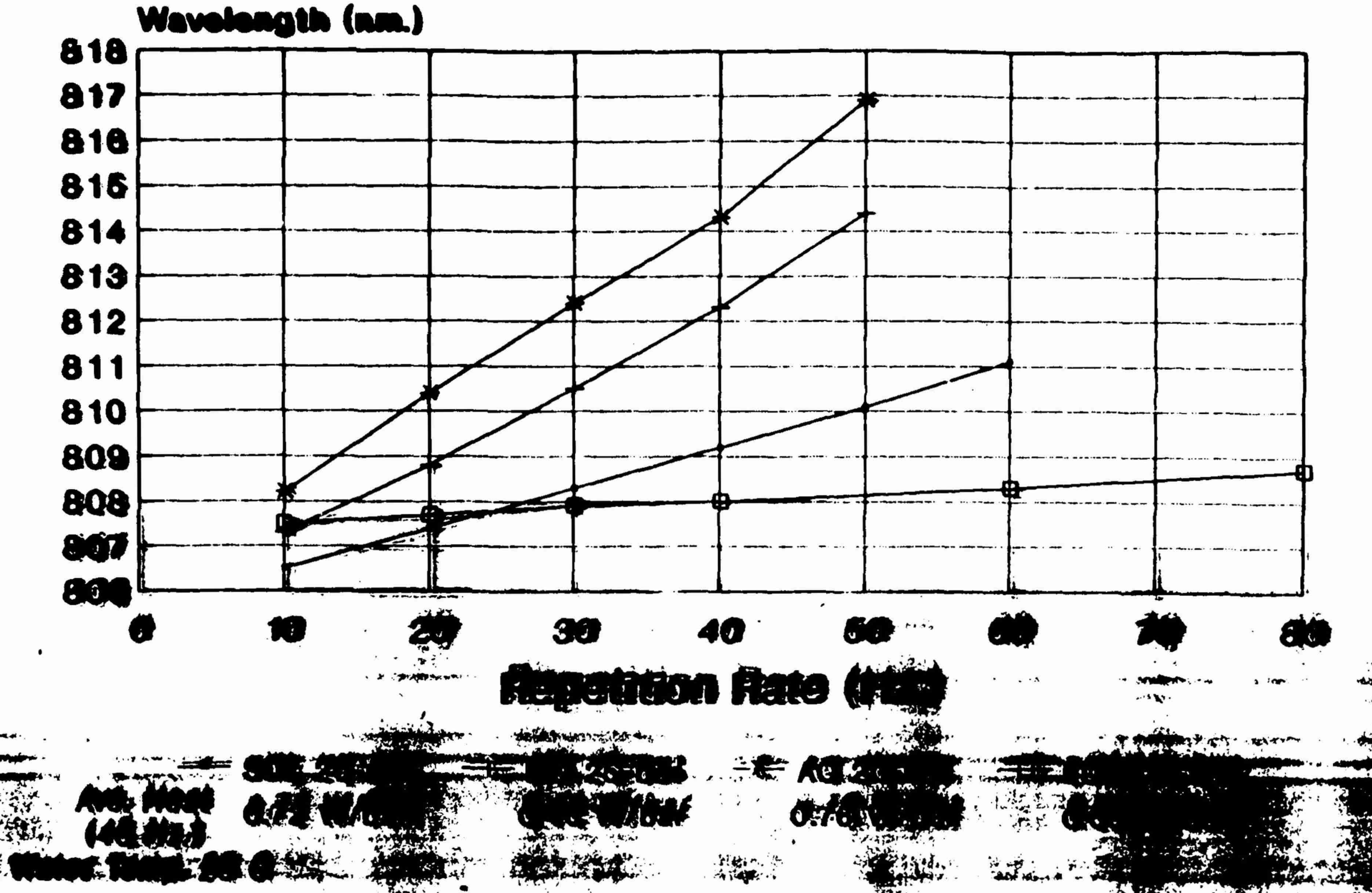

MDESC # 1-007 25-bar array

50 Amps

200 μS pulses

*1°C/div 10 HZ

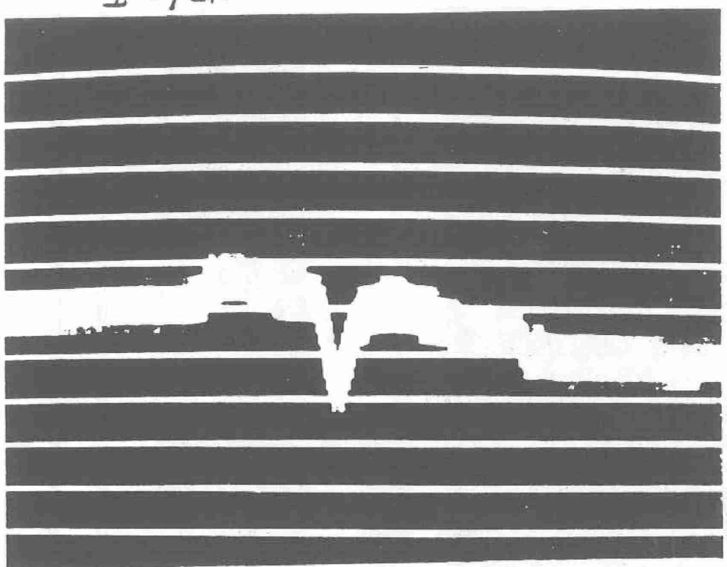

24°C 21.5°C 20.5°C

* 1°C/div 20 HZ

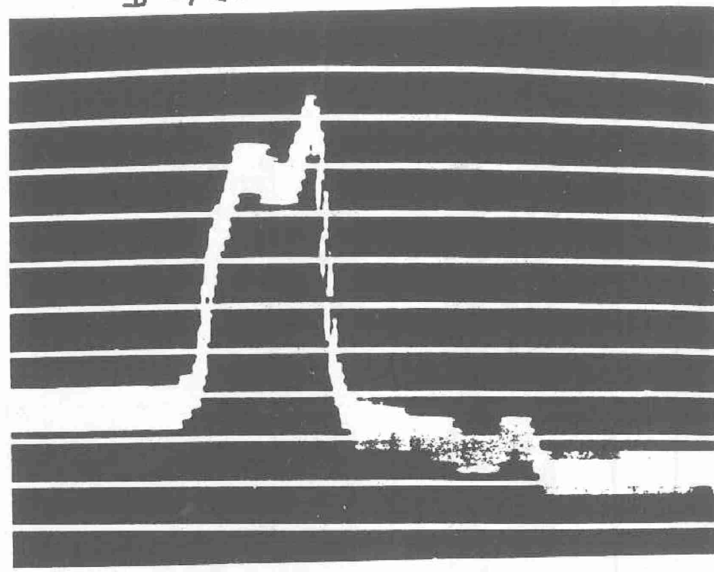

* 2°C/div 30 HZ

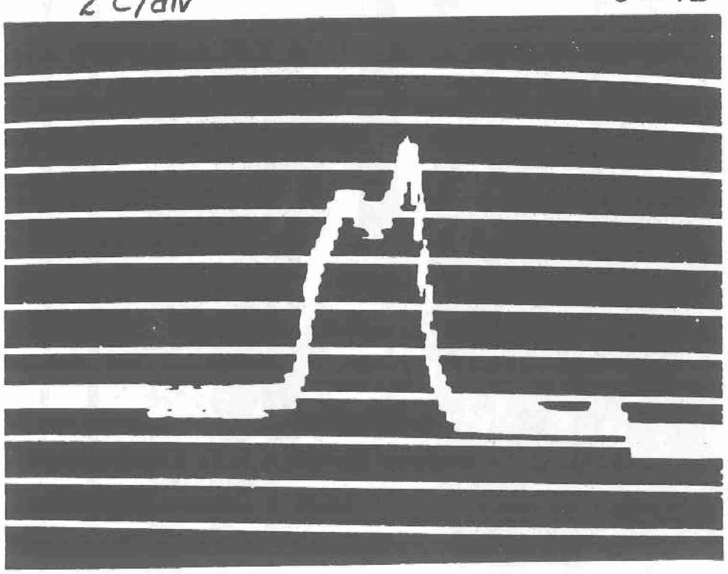

* 2°C/div 40 HZ

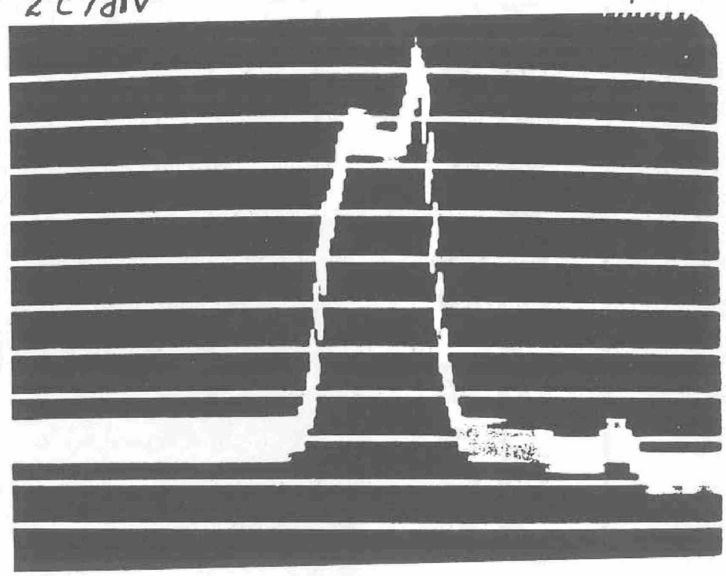

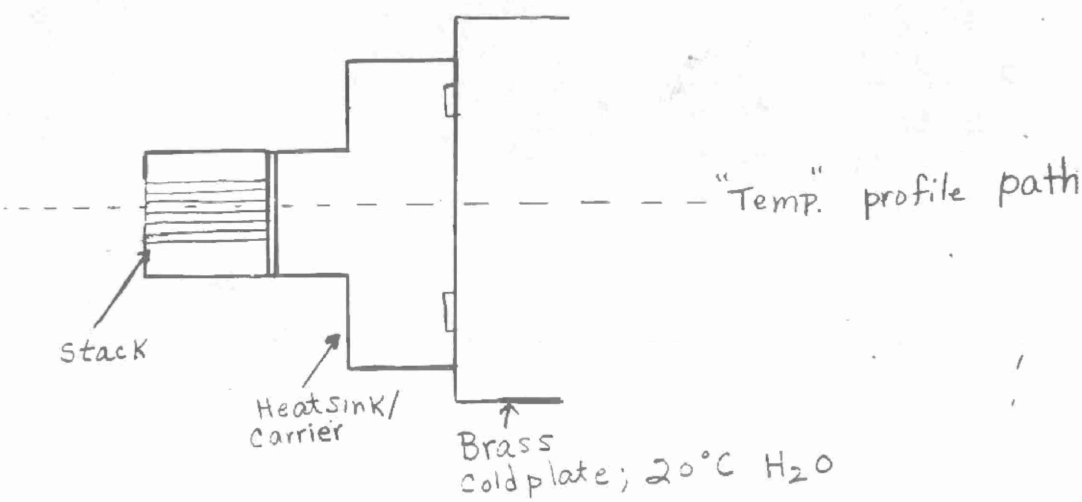

Intensity Noise and Phase Noise
in Semiconductor Lasers

George R. Gray
The Institute of Optics
University of Rochester

* Introduction
* Langevin Rate Equations
* Intensity Noise and Mode-Partition Noise
* Frequency Noise
* Optical Spectrum and Laser Linewidth
* Conclusions

Sources of Noise

Intrinsic Noise Sources

- Spontaneous emission
- Shot noise

Extrinsic Noise Sources

- Pump fluctuations
- Environmental fluctuations

- Extrinsic noise dominates in most lasers.
- Noise in semiconductor lasers dominated by spontaneous emission.

Two-Mode Theory

* Nearly-Single-Longitudinal Mode Lasers

* Two orthogonal polarizations

* Two stripes of a laser array

* Two competing directions in external cavity ring laser

Spontaneous Emission Noise

- Each spontaneously emitted photon perturbs the coherent field established by stimulated emission.
- Rate of spontaneous emission is relatively high ($\approx 10^{12}\ s^{-1}$) in semiconductor lasers.
- Phasor diagram shows induced intensity and phase fluctuations.

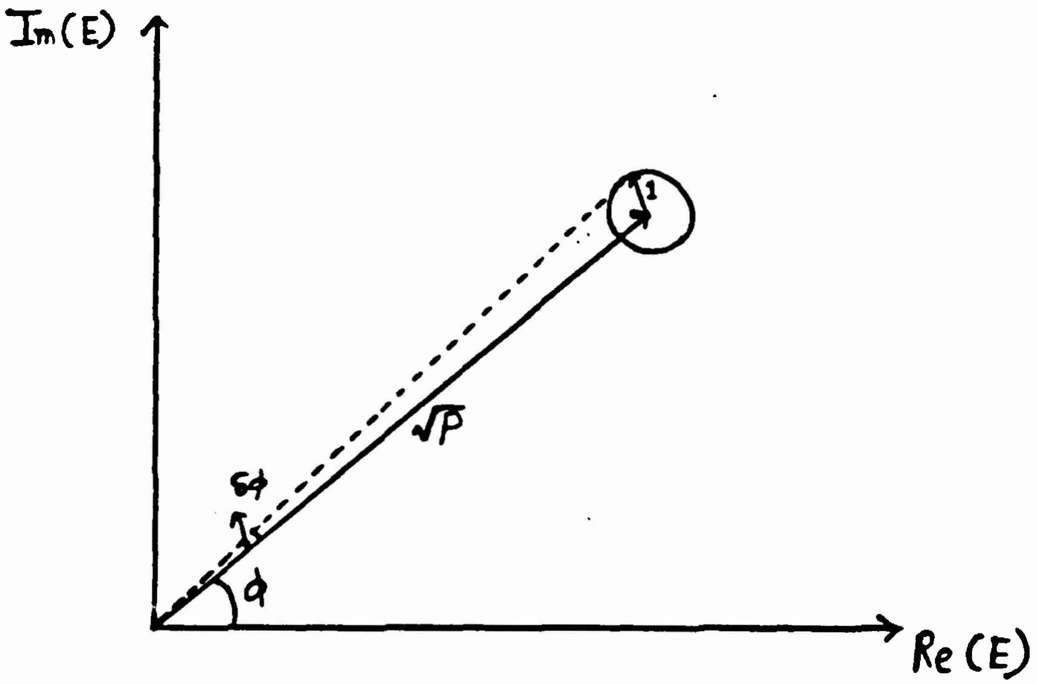

- Intensity and phase change randomly because of the uncertainty in phase of spontaneously emitted light.

Langevin Rate Equations

$$\frac{dP_i}{dt} = \left[G_i - \frac{1}{\tau_p} \right] P_i + R_{sp} + F_i(t)$$

$$\frac{d\Phi_i}{dt} = \frac{\alpha}{2} \left[G_i - \frac{1}{\tau_p} \right] + F_\phi(t)$$

$$\frac{dN}{dt} = \frac{I}{q} - \frac{N}{\tau_e} - \sum_i G_i P_i + F_n(t)$$

- Langevin Noise Sources

$$<F_i(t)> = 0$$

$$<F_i(t)F_j(t')> = 2D_{ij}\delta(t-t')$$

- Nonlinear Gain in Single Mode Lasers

$$G(N,P) = \frac{G_N(N-N_0)}{\sqrt{1 + P/P_s}}$$

- Nonlinear Gain for Two-Mode Laser

$$G_i(N,P_j) = G_N(N-N_0) - \beta_i P_i - \theta_{ij} P_j$$

Relative-Intensity Noise

$$\mathrm{RIN}(\omega) = \int_{-\infty}^{+\infty} \exp(-i\omega t) \frac{\langle \delta P(t)\delta P(t+\tau)\rangle}{\langle P\rangle^2} d\tau$$

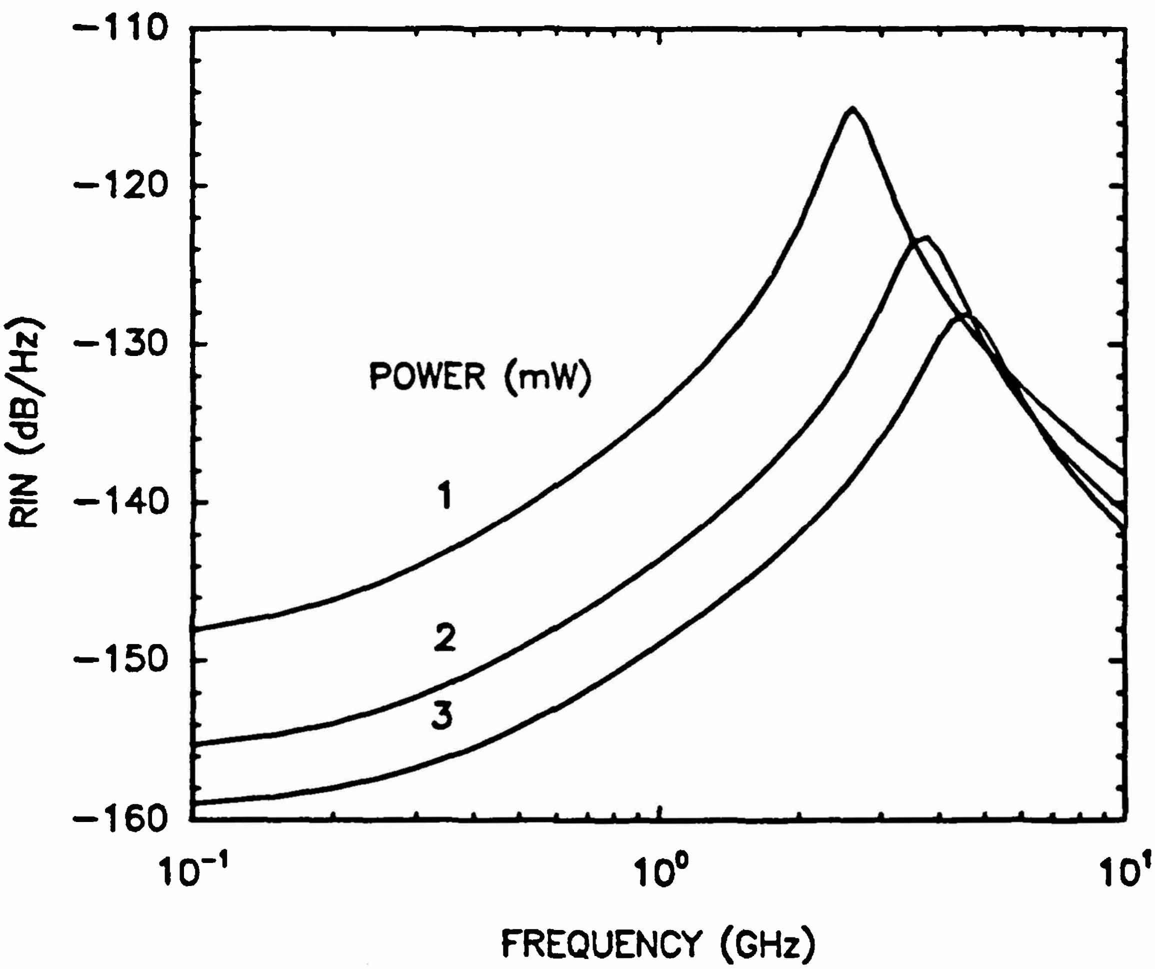

- RIN peaks at the relaxation-oscillation frequency Ω_r.

- $\Omega_r \quad \sqrt{\frac{G_N P}{\tau_p}}$, $\quad \Gamma_r \quad \frac{P}{4P_s\tau_p}$

- Nonlinear gain saturates the SNR to about 30dB

Mode-Partition Noise

- Intensity noise of the main mode is enhanced due to the presence of a relatively weak side mode.

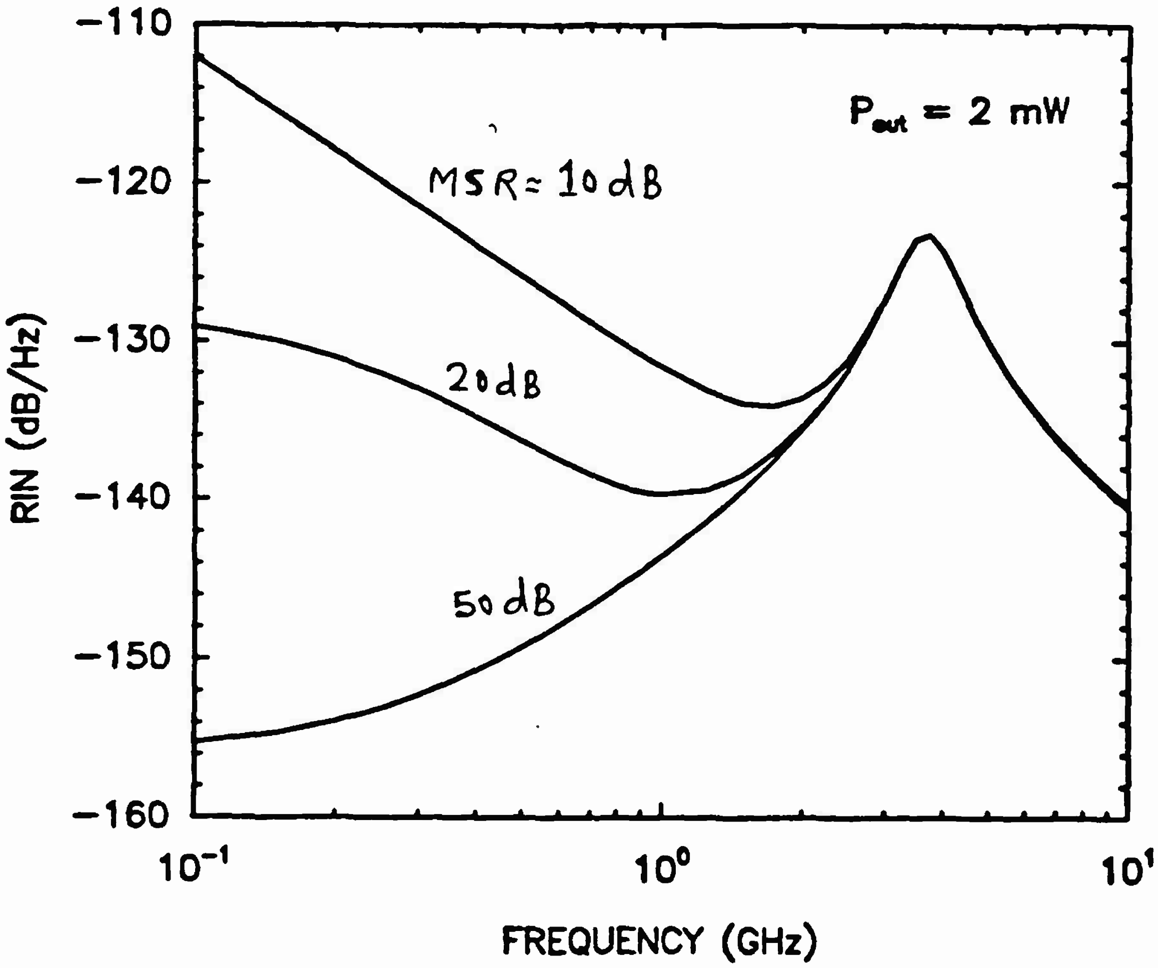

- Mode-suppression ratio: $\text{MSR} = \dfrac{\text{Main-mode power}}{\text{Side-mode power}}$

- Large increase in low-frequency noise (30-40 dB)

Increase in Total RIN due to Nonlinear Gain

- Cross Saturation by a weak side mode can also enhance the total low frequency RIN.

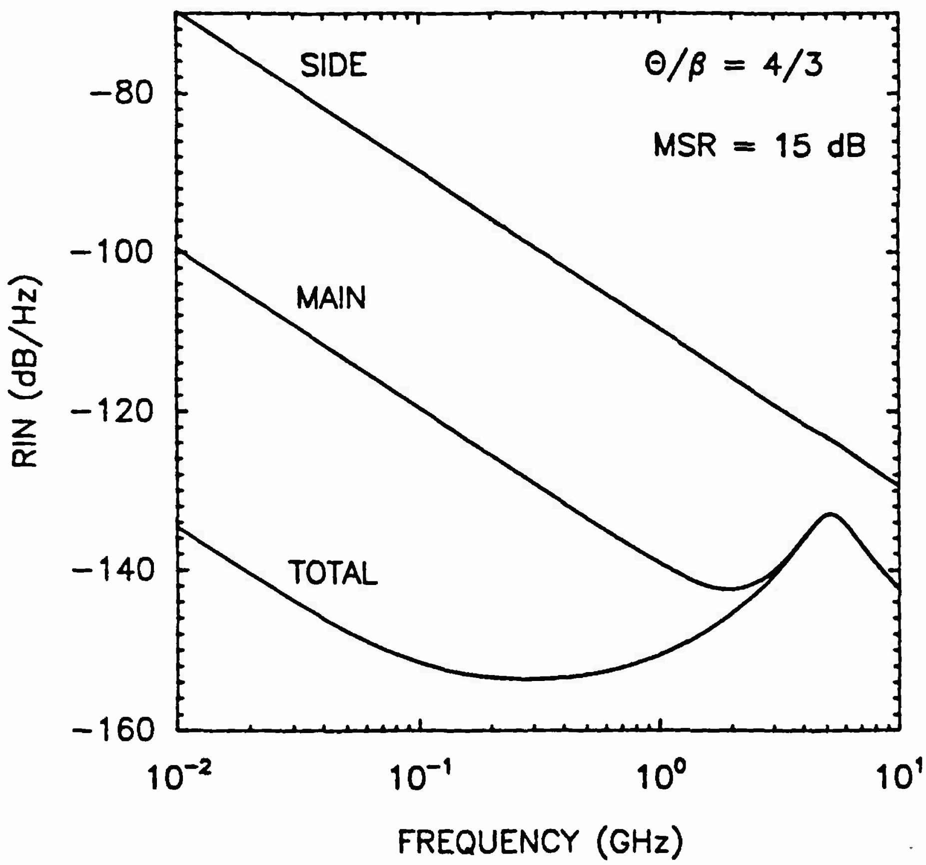

- If MSR degrades with increasing power, total SNR can actually worsen at high powers.

Phase Noise

- Frequency fluctuations: $\delta f = \frac{1}{2\pi}\frac{d\phi}{dt}$
- Frequency-noise spectrum (FNS)

$$S_f(\omega) = \int_{-\infty}^{+\infty} <\delta f(t)\delta f(t+\tau)> \exp(-i\omega\tau)\, d\tau$$

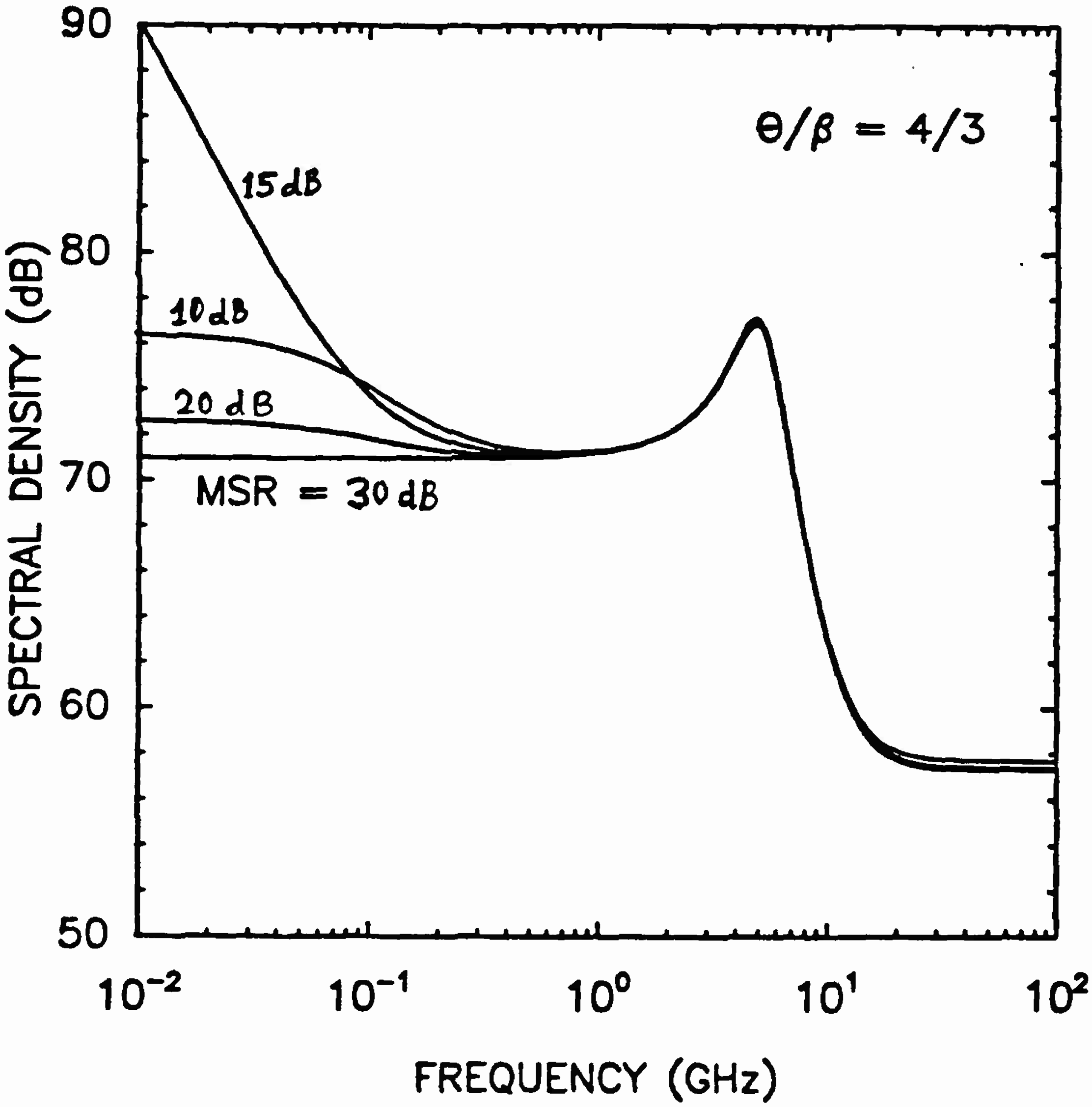

Optical Spectrum

$$S_E(\omega) = \int_{-\infty}^{+\infty} \langle \delta E(t)\delta E^*(t+\tau)\rangle \exp(-i\omega\tau)\, d\tau$$

- Relaxation oscillations appear as satellite peaks in the optical spectrum.

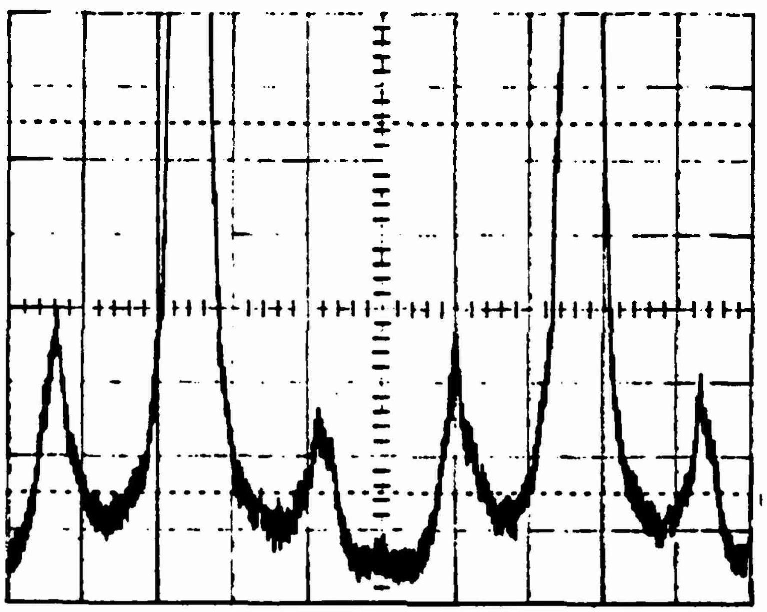

1.5 GHz/div.

- Asymmetry in the side bands is related to amplitude-phase coupling (α).

- Amplitude of side bands is $\approx$ 1% of main peak

Laser Lineshape at different powers

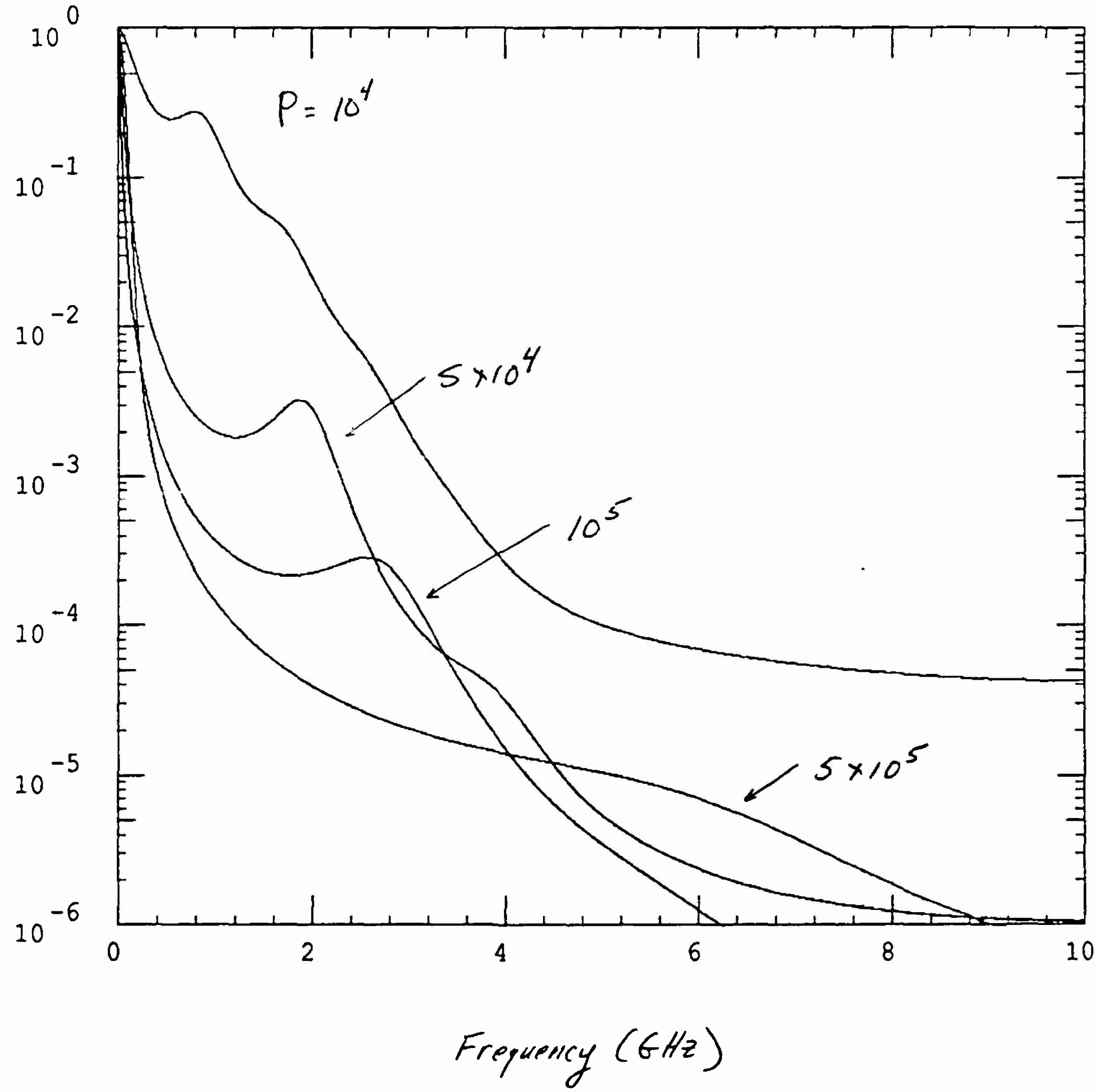

Laser Linewidth

- Single-mode lasers:

$$\Delta\nu = \frac{R_{sp}(1+\alpha^2)}{4\pi P}$$

- In practice, $\Delta\nu$ saturates at about 10 MHz (and often rebroadens) at power levels of 10-20 mW.

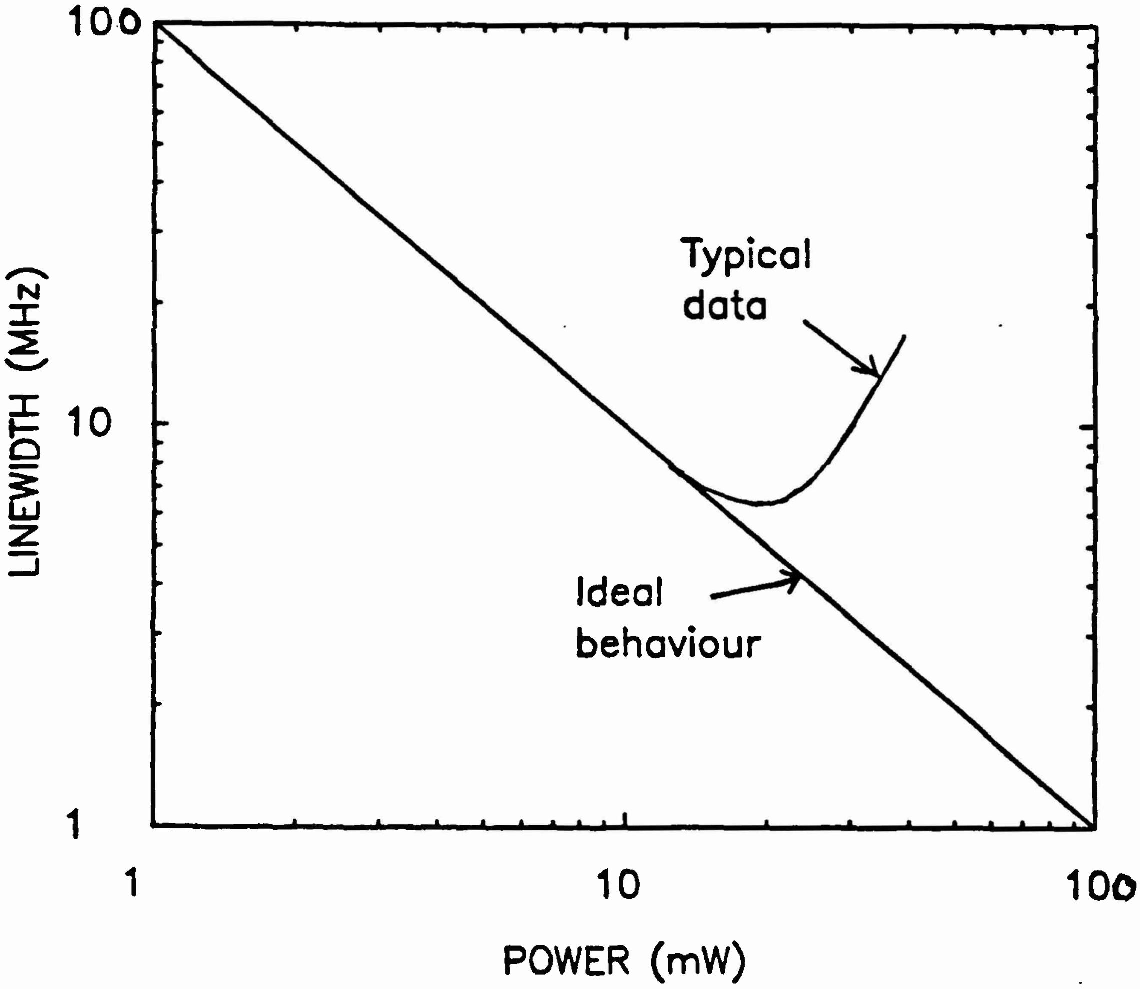

- Possible mechanisms: current fluctuations, 1/f noise, spatial hole-burning, intraband gain saturation, side-mode cross saturation

Side-Mode Cross Saturation

$$G_i(N,P_j) = G_N(N-N_0) - \beta_i P_i - \theta_{ij} P_j$$

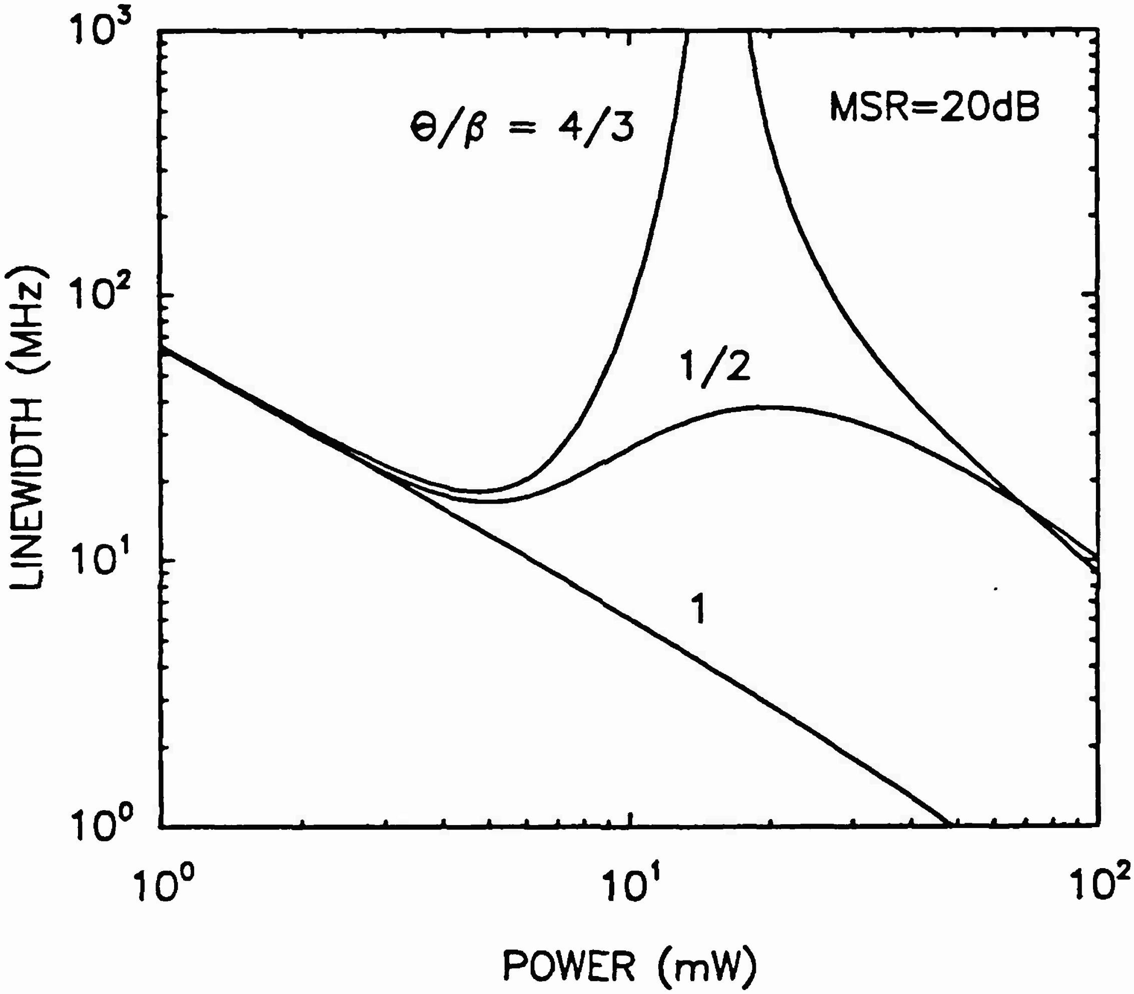

- Theory shows maximum rebroadening at particular side-mode power. For high power lasers, even a good MSR can allow for substantial side mode power.

$$S = \sqrt{\frac{R_{sp}}{2(\theta-\beta)}}$$

Conclusions

- Noise in semiconductor lasers dominated by spontaneous emission
- Both laser intensity noise and phase noise can be strongly affected by side modes.
- Mode-partition noise can increase the main-mode RIN; Cross saturation can enhance the total RIN.
- Side-mode cross saturation can also lead to saturation and rebroadening of the laser linewidth.

Acknowledgements: Govind Agrawal

CECOM CENTER FOR NIGHT VISION AND ELECTRO-OPTICS

DIODE-PUMPED SOLID-STATE LASER AMPLIFIERS

URI-ARO WORKSHOP

SEMICONDUCTOR LASERS FOR COMMUNICATIONS AND DIODE PUMPING

17 DECEMBER 1990

MOTIVATION

**HIGH EFFICIENCY, HIGH ENERGY
Q-SWITCHED LASERS**

ARRAY PROPERTIES

- HIGH PEAK POWER
- NARROW BANDWIDTH
- HIGH EFFICIENCY

MATERIAL PROPERTIES

- LONG FLUORESCENT LIFETIME - STORAGE EFFICIENCY
- INTERMEDIATE TO HIGH GAIN - EXTRACTION EFFICIENCY
- LARGE BOULES - HIGH DAMAGE THRESHOLD

COMPARISON OF Nd LASER MATERIALS

KEY FEATURES	YAG	YLF	G(S)GG
SIZES (CM DIAMETERS)	1.0	1.0	$\boxed{8.0}$
FLUORESCENCE LIFETIME (10-6 SECONDS)	232	$\boxed{480}$	240
EMISSION CROSS SECTION (10-19 cm2)	2.4	1.8 (pi) 1.2 (sigma)	1.2
INDEX OF REFRACTION	1.8	$\boxed{1.4}$	1.8
THERMAL CONDUCTIVITY	$\boxed{\text{HIGH}}$	MODERATE	MODERATE
THERMAL LENSING	HIGH	$\boxed{\text{LOW}}$	HIGH
THERMAL BIREFRINGENCE	HIGH	$\boxed{\text{LOW}}$	HIGH

BTI PRODUCIBILITY
SPECTRA DIODE LABS 10-BAR ARRAY # S032

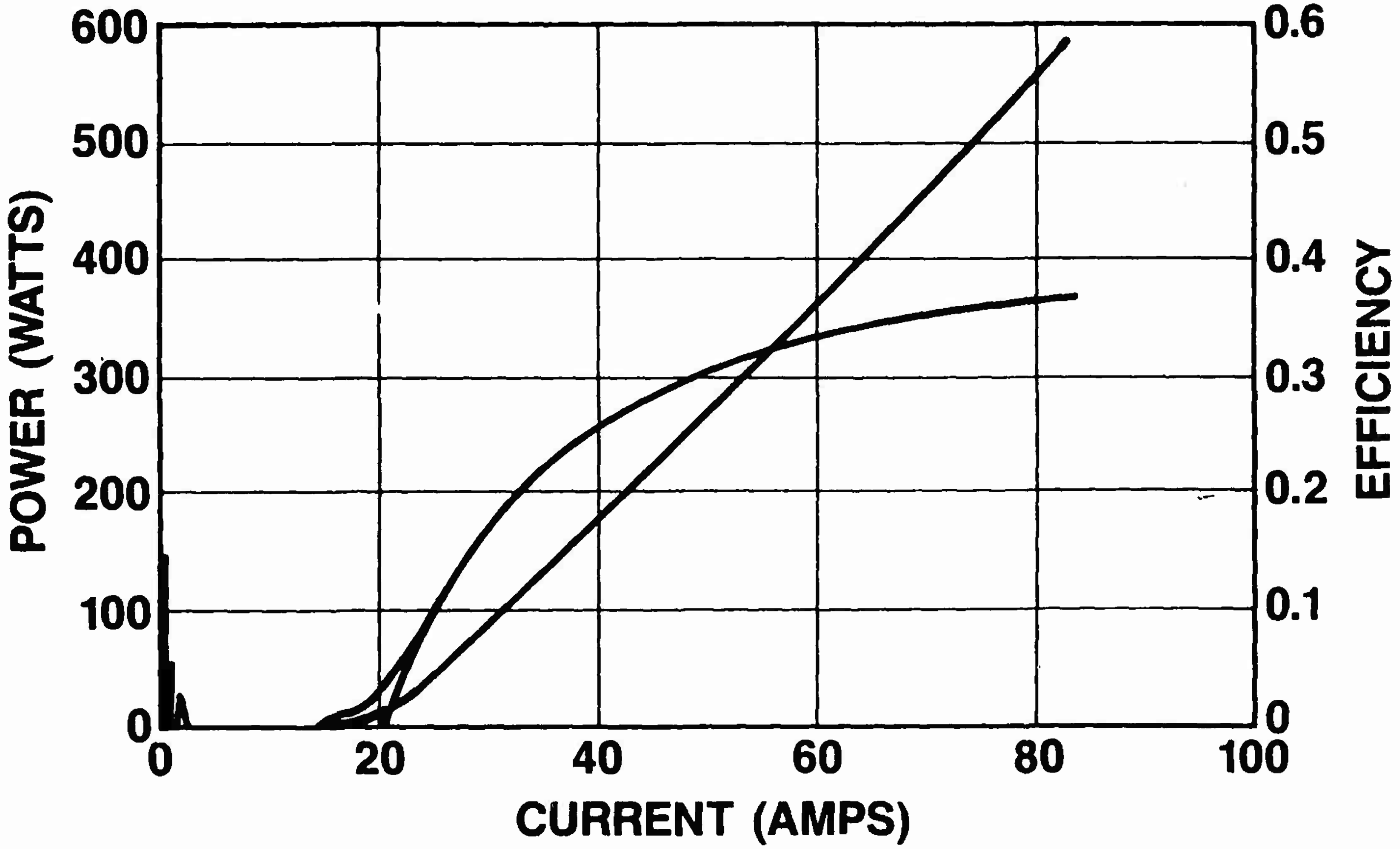

C2NVEO DATA

REF'D DIR; 6LC; FIL. G; HP w/.0217

Apparatus Diagram

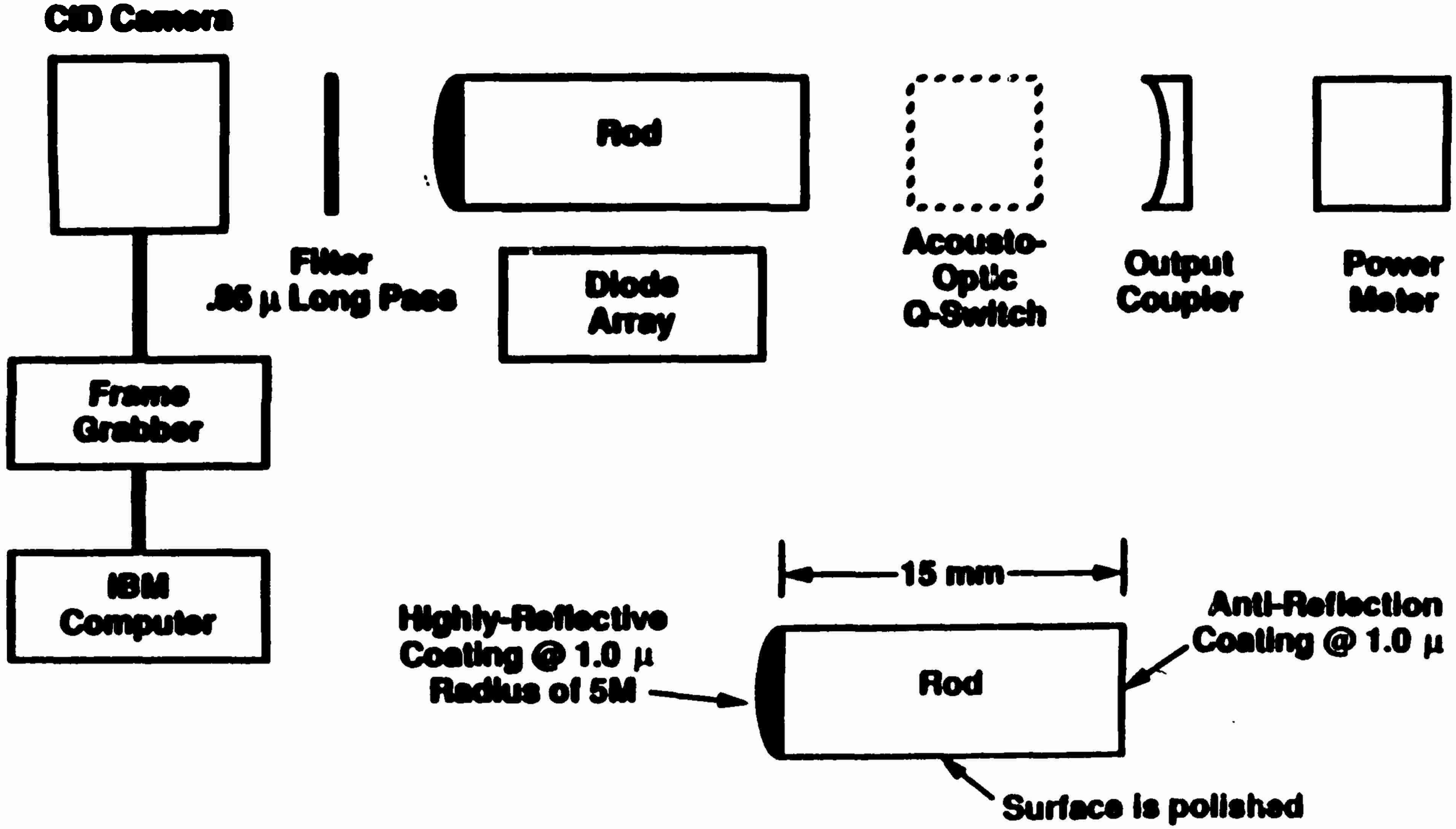

OUTPUT ENERGY AS A FUNCTION OF DIODE-ARRAY WAVELENGTH OR TEMPERATURE
INPUT ENERGY IS 100 MJ

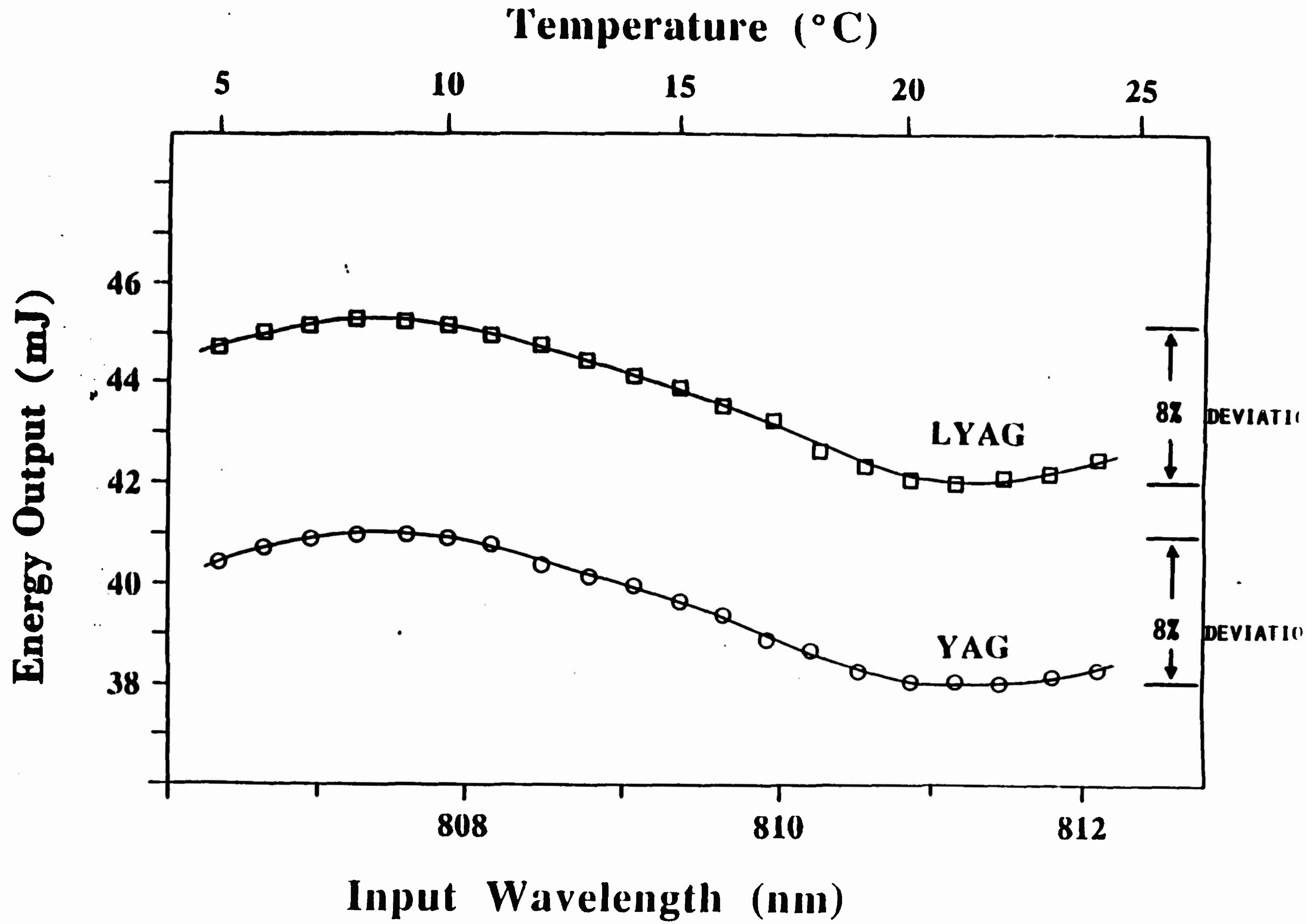

Nd: LYAG ABSORPTION SPECTRUM

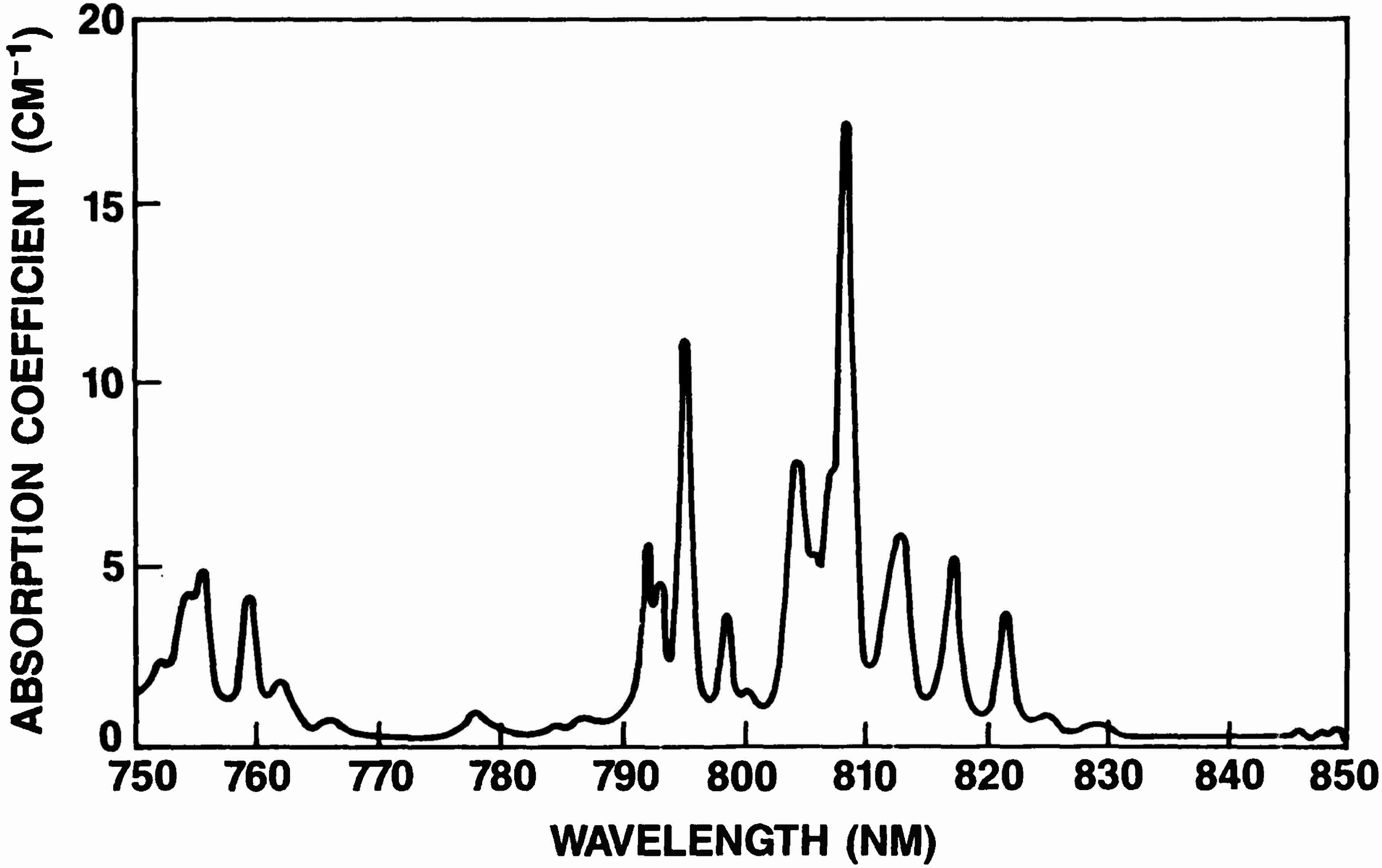

SIDE PUMPED YAG FLUORESCENT PROFILE

- 4 × 10 mm DIODE ARRAY
- 1/4 INCH DIAMETER YAG ROD
- BUTT COUPLED SIDE PUMPED
- AR/SILVERED ROD BARREL

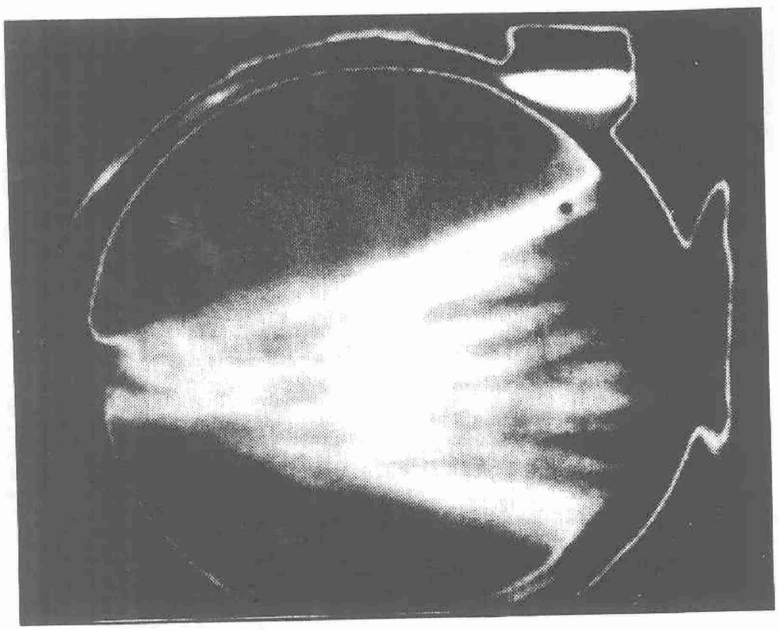

DIODE ARRAY TEMP. = 10°C
WAVELENGTH = 808 NM

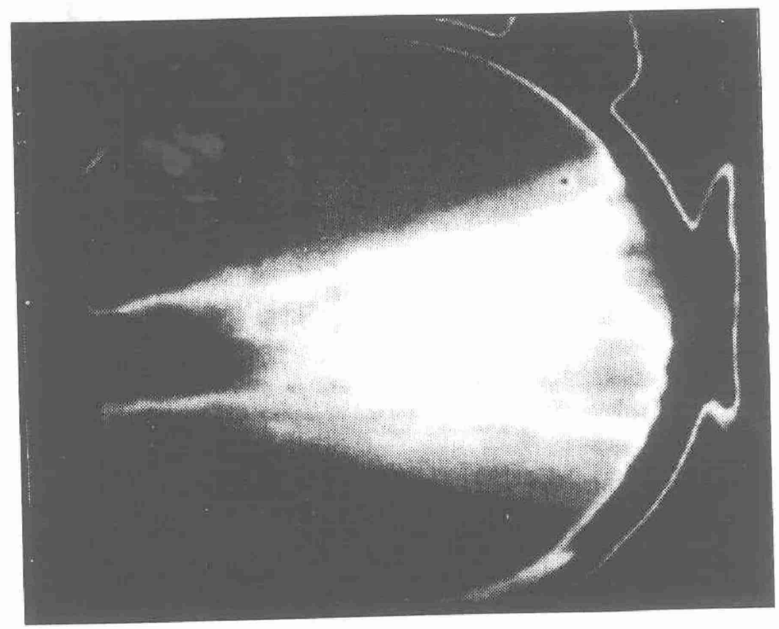

DIODE ARRAY TEMP. = 20°C
WAVELENGTH = 811 NM

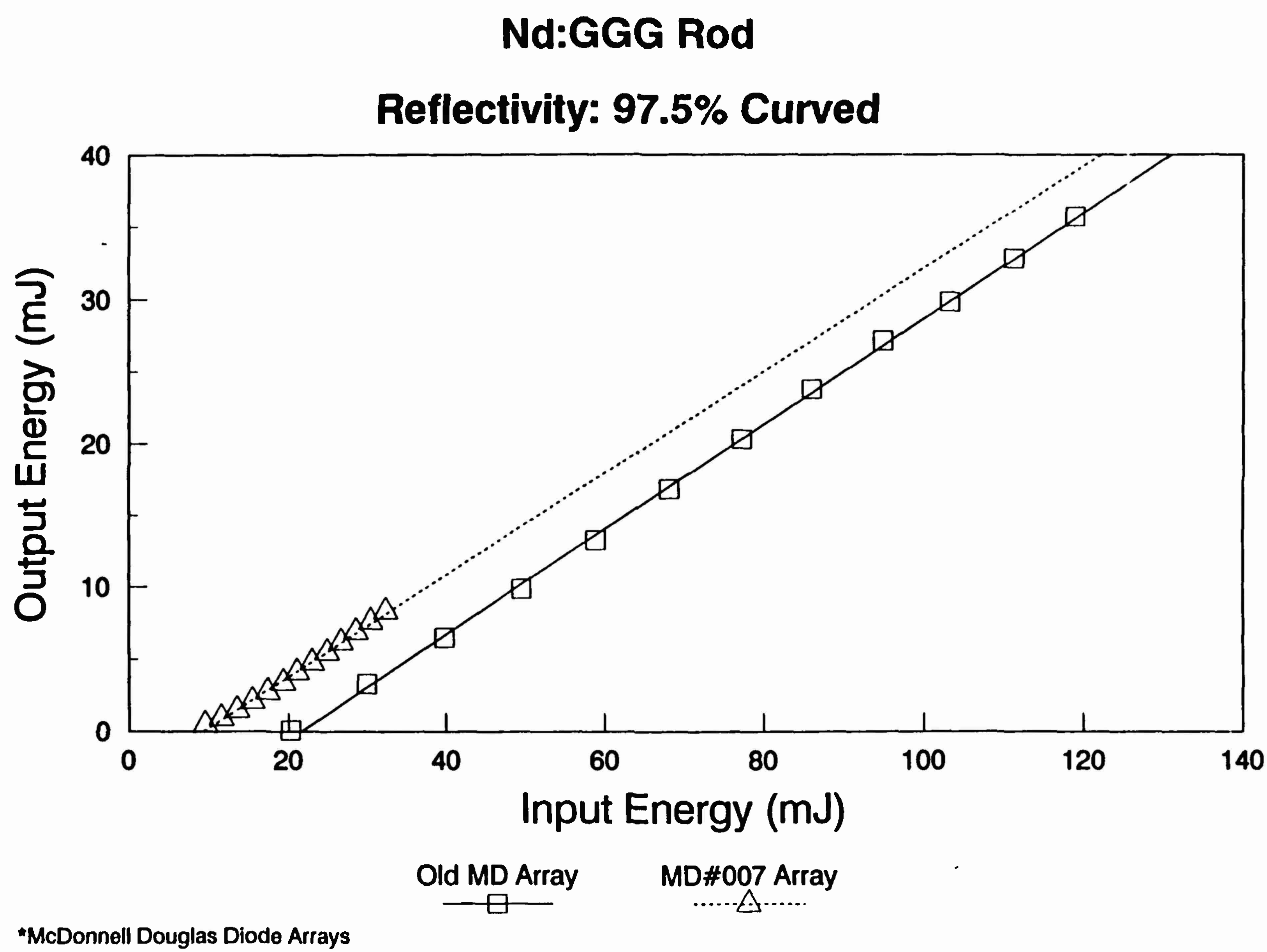
Nd:GGG Rod
Reflectivity: 97.5% Curved
Output Energy (mJ)
0
10
20
30
40
Input Energy (mJ)
0
20
40
60
80
100
120
140
Old MD Array
MD#007 Array
*McDonnell Douglas Diode Arrays

FIGURE 11

DIODE ARRAY PUMPED LASER EFFICIENCIES FOR RODS AND SLABS

MATERIAL	MEASURED SLOPE EFFICIENCY	ROUND-TRIP RESONATOR LOSS (FINDLAY-CLAY)
Nd:Lu:YAG ROD	50.3%	2.4%
Nd:YAG ROD	47.7%	2.8%
Nd:YLF ROD	42.9%	2.0%
Nd:GSGG ROD	41.5%	3.6%
Nd:BZAG ROD	22.8%	4.0%
Nd:YSAG ROD	9.2%	20.2%
Nd:YAG SLAB	40.1%	6.7%
Nd:GSGG SLAB	39.5%	2.0%
Nd:Cr:GSGG SLAB	32.5%	10.2%

AMPLIFIER GAIN EXPERIMENT

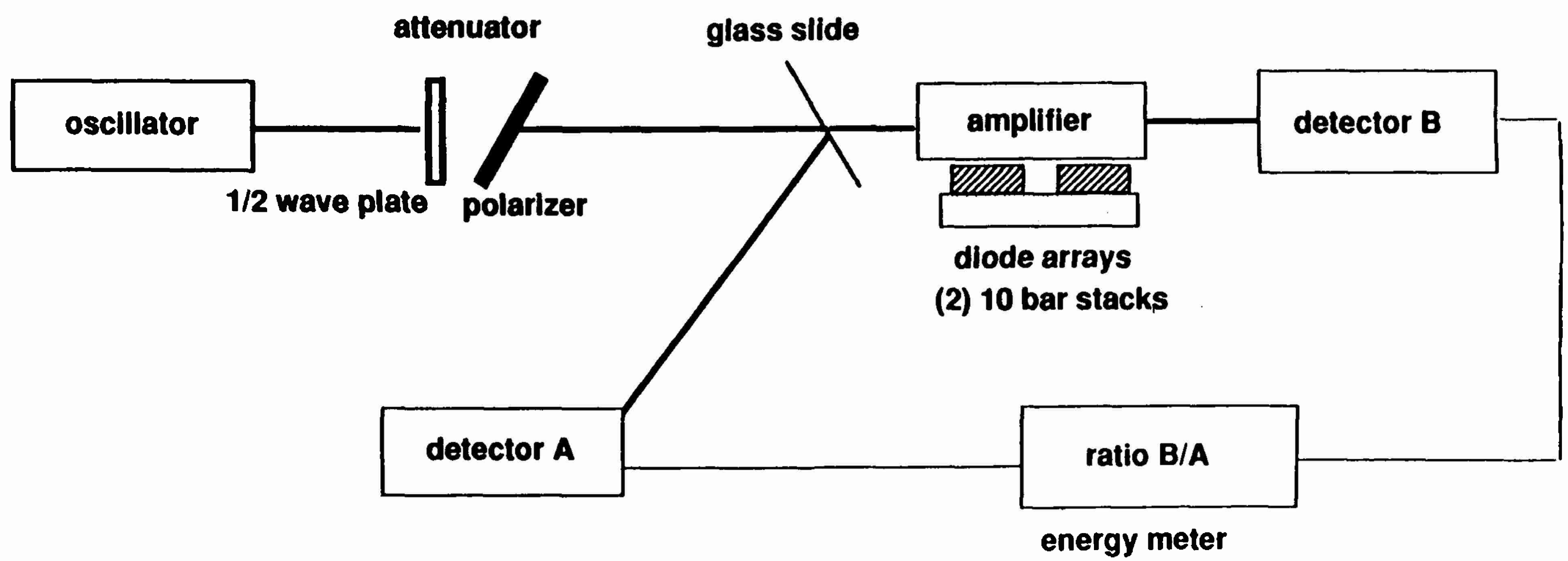

STORAGE EFFICIENCY

STORAGE EFFICIENCY = PRODUCT OF INDIVIDUAL EFFICIENCIES

$$\eta_{s} = \eta_{stokes} * \eta_{lifetime} * \eta_{coupling} * \eta_{absorption} * \eta_{quantum}$$

$$\eta_{stokes} = \frac{\text{pump photon energy}}{\text{lasing photon energy}}$$

$$\eta_{absorption} = \frac{\text{pump energy absorped}}{\text{pump energy injected}}$$

$$\eta_{lifetime} = \frac{\tau}{t}\left(1 - e^{\frac{-t}{\tau}}\right)$$

$$\eta_{quantum} = 1 - \text{loss from upper laser level}$$

$$\eta_{coupling} = \frac{\text{pump energy into laser material}}{\text{incident pump energy}}$$

STORAGE EFFICIENCY ANALYSIS

Nd:YLF

ARRAY PULSE = 460 mJ IN 500μs

EFFICIENCY FACTOR	EXPERIMENTAL	OPTIMIZED
STOKES	.76	.76
LIFETIME	.63	.63
QUANTUM	.9	.9
COUPLING & ABSORP	.54	.8
	.23	.34

MATERIAL COMPARISON

SMALL-SIGNAL SINGLE-PASS GAIN
PULSE DURATION 300 MICROSECONDS

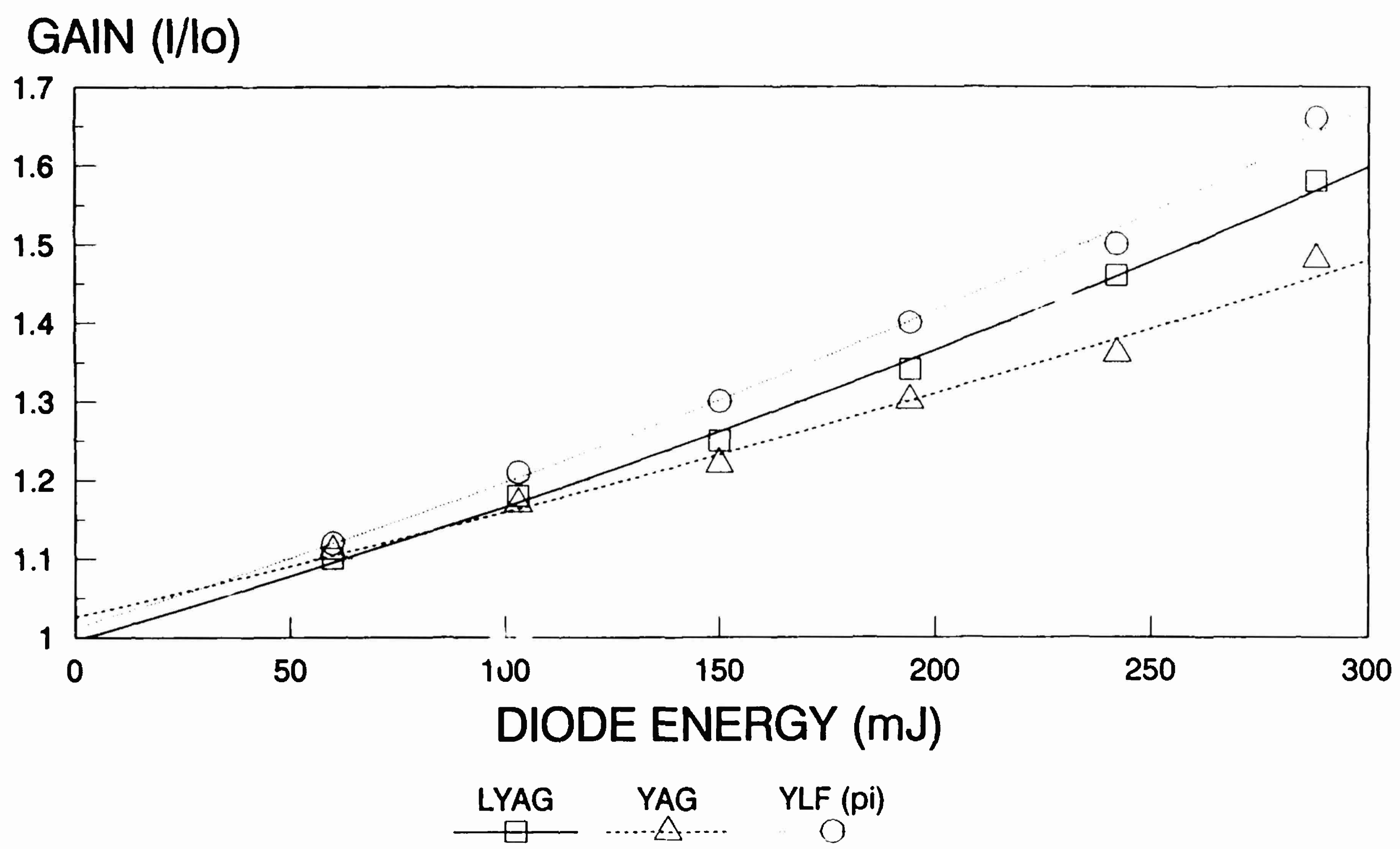

SUMMARY

- ALL MATERIALS EVALUATED PROVIDED >40% SLOPE EFFICIENCY IN LONG PULSE OSCILLATOR CONFIGURATION
- FOR HIGH PEAK POWERS, MATERIAL AND SPECTROSCOPIC PROPERTIES PLAY A MORE IMPORTANT ROLE FOR OBTAINING HIGH EFFICIENCIES
- Nd:YLF OUTPERFORMS OTHER MATERIALS FOR STORAGE EFFICIENCY DUE TO 2x LONGER UPPER STATE LIFETIME
- HIGH POWER ARRAYS PROVIDING 1.5KW/cm^2 WITH EFFICIENCIES OF 35% ARE READILY AVAILABLE
- HIGHER INTENSITY ARRAYS WOULD HAVE SIGNIFICANT IMPACT ON OVERALL LASER EFFICIENCY

FY 91 PLANS

- COMPLETE AMPLIFIER EXPERIMENTS TO IMPROVE DATA BASE FOR DIODE PUMPED DESIGN MODELS

  -measure absorption and coupling efficiencies of various materials with 5 and 10 bar arrays

- DIODE PUMP HEAD GEOMETRIES FOR PROVIDING UNIFORM PUMPING (NECESSARY FOR GOOD BEAM QUALITY) OVER A WIDE TEMPERTURE (TEMPER-TURE INSENSITIVE)

  -look at fluorescent profiles and measure small signal gain at various material absorption strengths

DIODE PUMPED RODS

DIRECT COUPLED

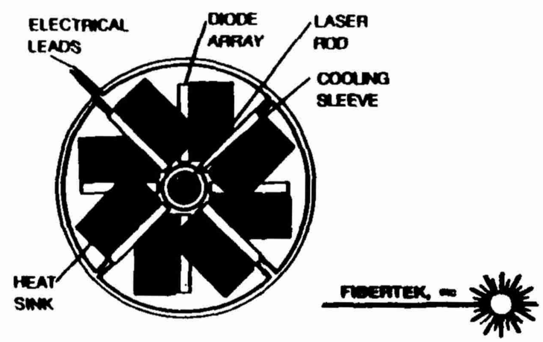

NON-IMAGING

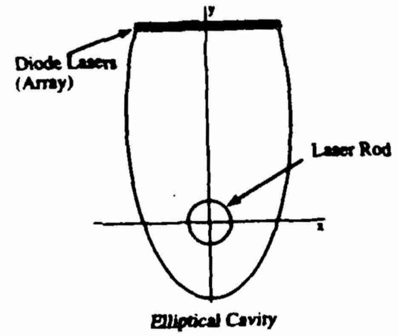

REFLECTIVE WAVEGUIDE

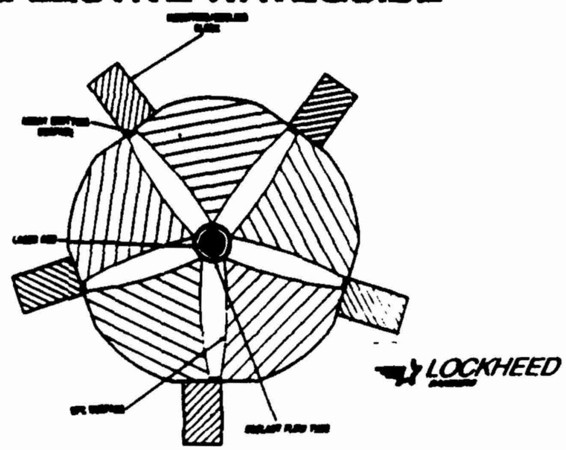

DIFFUSE

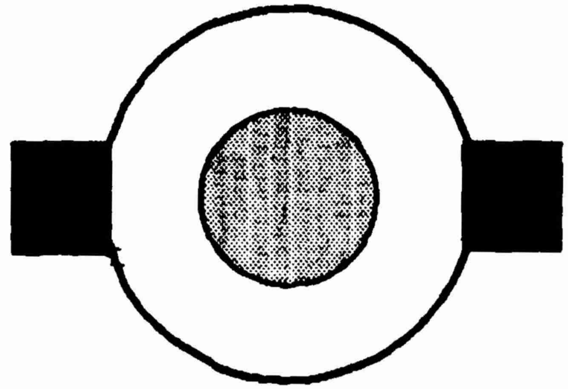

DIODE PUMPED SLAB LASER

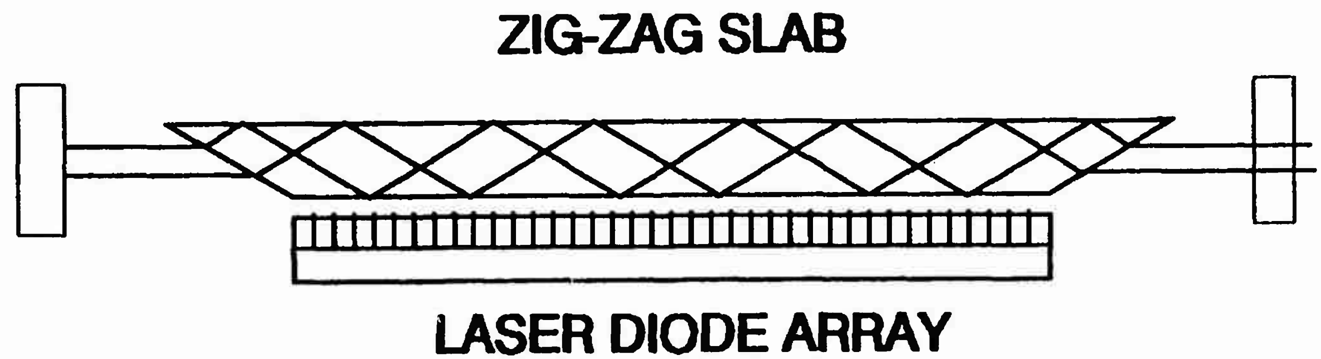

INHOUSE EXPERIMENTS

OSCILLATOR EXPERIMENTS - NINE Nd DOPED MATERIALS EVALUATED

- *ALL MATERIALS SHOWED GOOD PERFORMACE UNDER DIODE PUMPING*
- *ARRAY PUMP WAVELENGTH DOES NOT NEED TO BE ON PEAK ABSORPTION LINE*
- *DIODE WAVELENGTH WAS TUNED 6nm WITH ONLY 8% OUTPUT DEVIATION*

AMPLIFIER EXPERIMENTS - PROVIDE DATA BASE FOR MODELING

- *SHOWED EFFECTS OF ARRAY PEAK POWER ON EFFICIENCY*
- *SHOWED EFFECTS OF UPPERSTATE LIFETIME ON STORAGE EFFICIENCY*
- *MEASURE SMALL SIGNAL GAIN OF VARIOUS MATERIALS*

CENTER FOR OPTO-ELECTRONIC SYSTEMS RESEARCH
QUANTUM-WELL DYNAMICS

Subband Structure for Narrow, Coupled Quantum Wells

Mark L. Biermann and C. R. Stroud, Jr.

University of Rochester

Also acknowledge the assistance of
Christian Mailhiot

Theoretical Approach

1. Zone-center basis states from a pseudopotential calculation.

   *Use only material parameters and superlattice symmetry.

   *Effective masses are not assumed.

2. Use the k• p theory to calculate band structure.

   *Couple Γ_1 conduction and Γ_{15} valence bands to spinor. Treat explicitly.

   *Treat neighboring states in Lowdin Perturbation Theory.

   *Use normal component of current density operator for interface matching of bulk eigenfunctions.

See: Smith, D. L. and C. Mailhiot, Phys. Rev. B., 33, 8345-8372, (1986).

The System Studied:

Symmetric Coupled Quantum Wells, (SCQWs), well width W and barrier width B, as seen below.

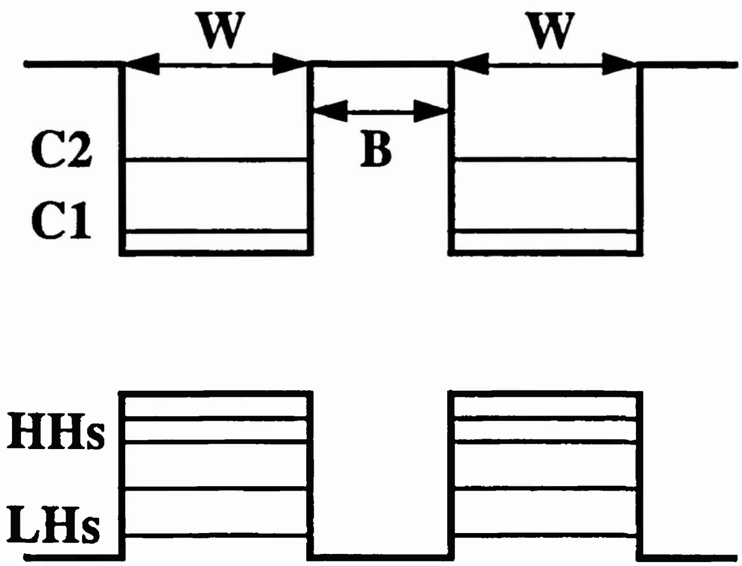

*Growth direction 100, room temperature

*Wells are GaAs layers ranging in width from 4 to 35 monolayers, 11.4 to 99.0 Å

*Barriers are $Al_{.3}Ga_{.7}As$ layers, 4 to 6 monolayers, 11.4 to 17.0 Å, thick

*Fourth layer of periodic structure is a thick AlGaAs layer to isolate SCQWs

*43% of bandgap offset goes to valence band

Valence Subband Energy Positions

The first three valence subbands are plotted against well width for fixed barrier widths of 4 and 6 atomic monolayers, 11.4 and 17.0 Å, respectively.

Hole Subbands, 11.4 Å barriers

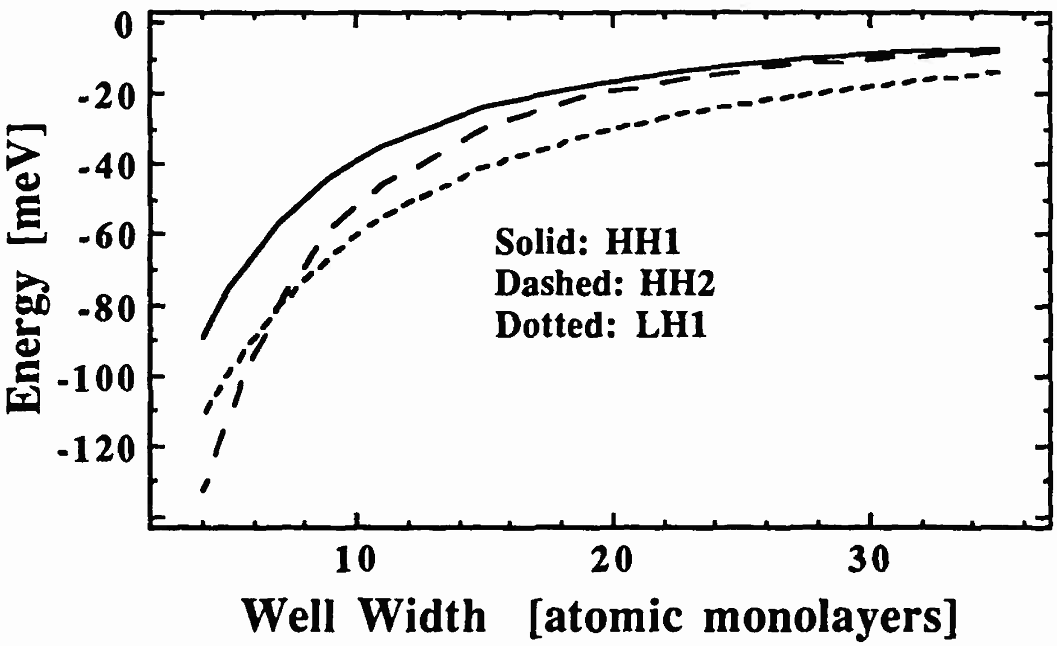

*LH1 crosses under HH2 for narrow wells, less than 7 monolayers, 19.8 Å

*Crossover observed experimentally. Could be useful in Quantum Confined Stark Effect devices or experiments

See: H. Kawai, J. Kaneko, N. Watanabe, J. Appl. Phys. 58, 1263 (1985).

valence subbands, cont.

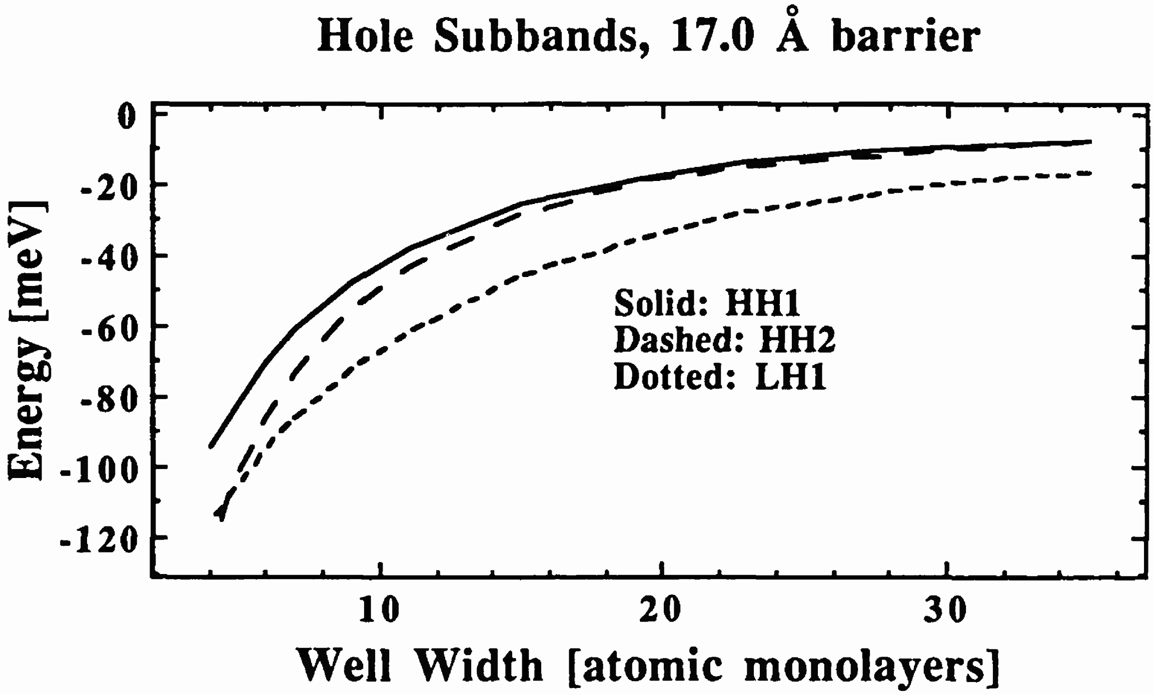

* HH1/HH2 splitting smaller due to thicker barrier

* LH1 crosses under HH2 at narrower well widths, less than 5 monolayers, 13.3 Å

* HH1 and HH2 are symmetric and anti-symmetric solutions arising from HH1 solution in single well

* HH1 and HH2 become degenerate for wide wells.

valence subbands, cont.

Difference Between HH2 and LH1

*Helpful to look at the difference between HH2 and LH1 in the crossover region

LH1 - HH2, Subband Separation

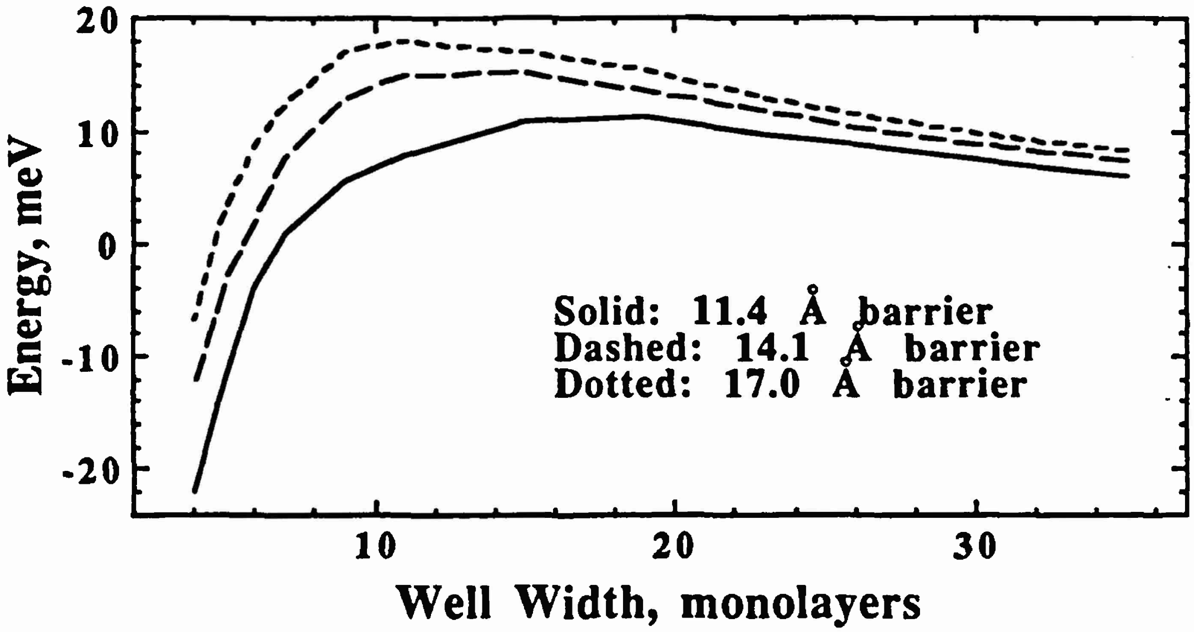

*Crossover occurs for wider wells as the barrier width decreases

*Amount of crossover, up to over 20 meV, can be large

Conduction Subband Energy Positions

The first two conduction subbands are plotted against well width for fixed barrier width of 4 atomic monolayers, 11.4 Å.

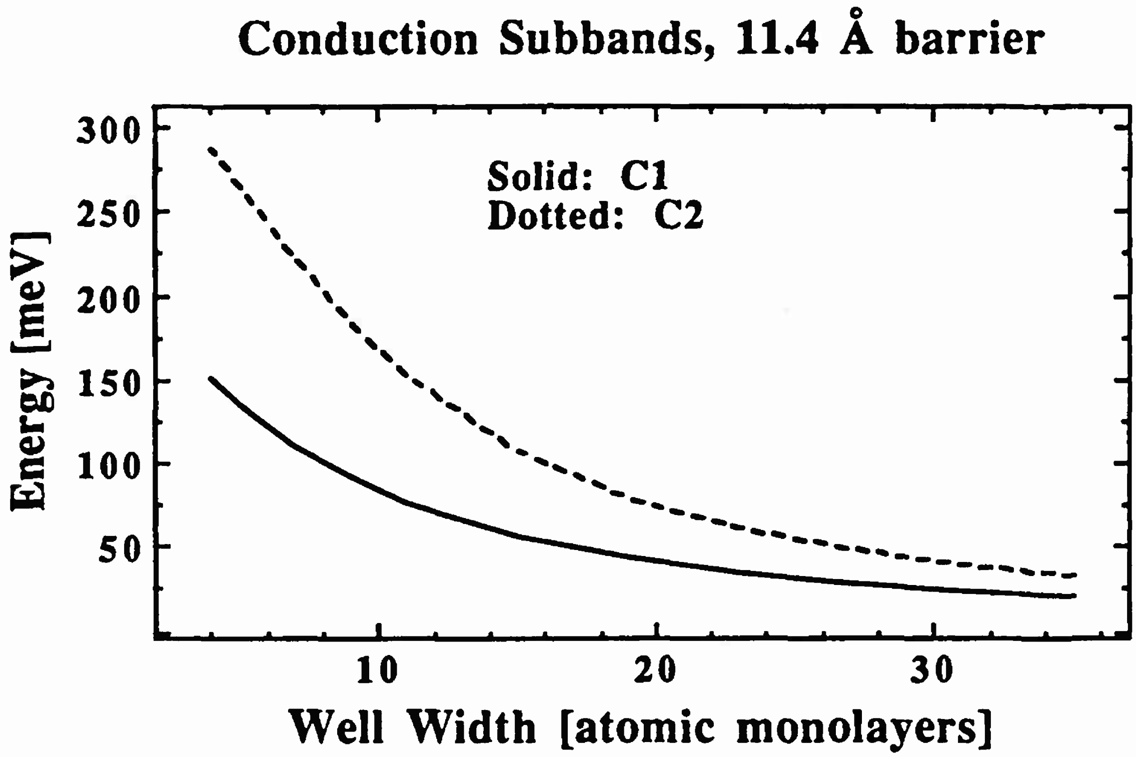

*First two subbands are the symmetric and antisymmetric solutions arising from the single well C1 subband

*Splitting is greater than in hole cases: electrons more strongly coupled due to smaller effective mass

SCQW Subbands Compared to Single Well Case

The first two subbands in the SCQWs split about the first single well state.

Valence Subbands: 4 monolayers, 11.4 Å, barrier

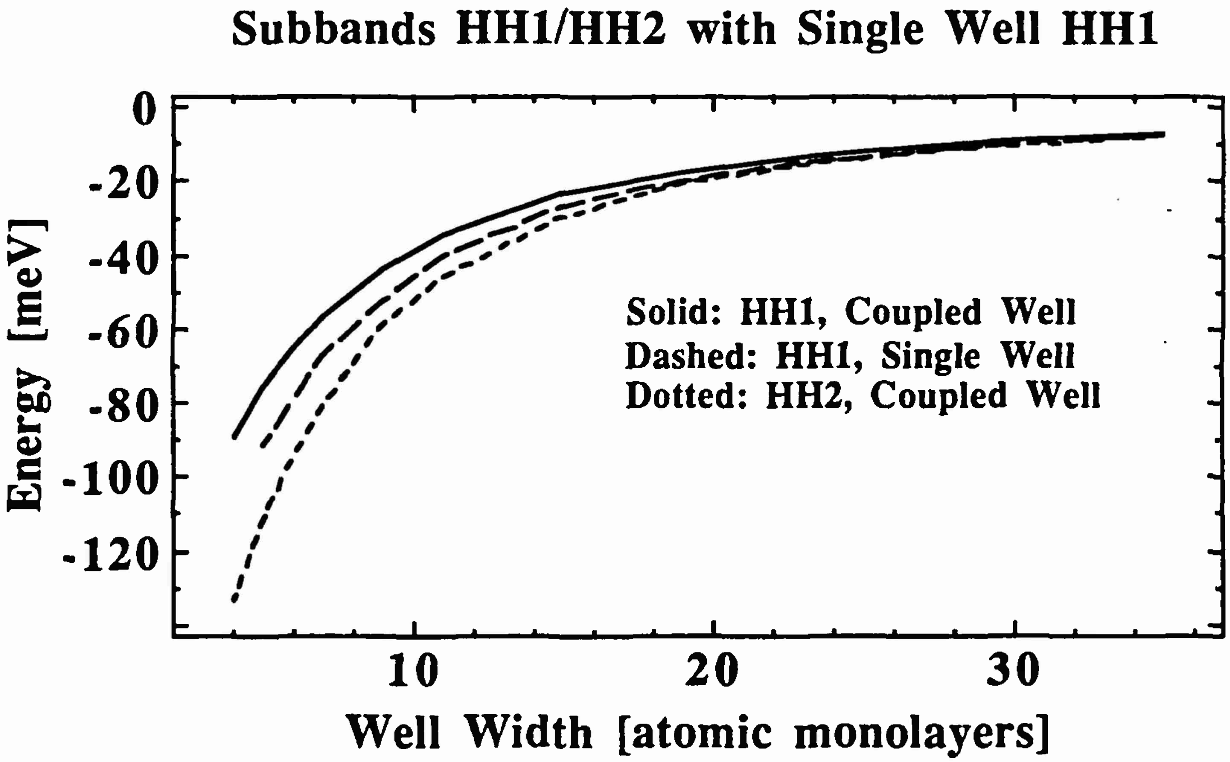

*Splitting is quite even about the single well state

Single well comparison, cont.

Conduction Subbands: 4 monolayers, 11.4 Å barrier

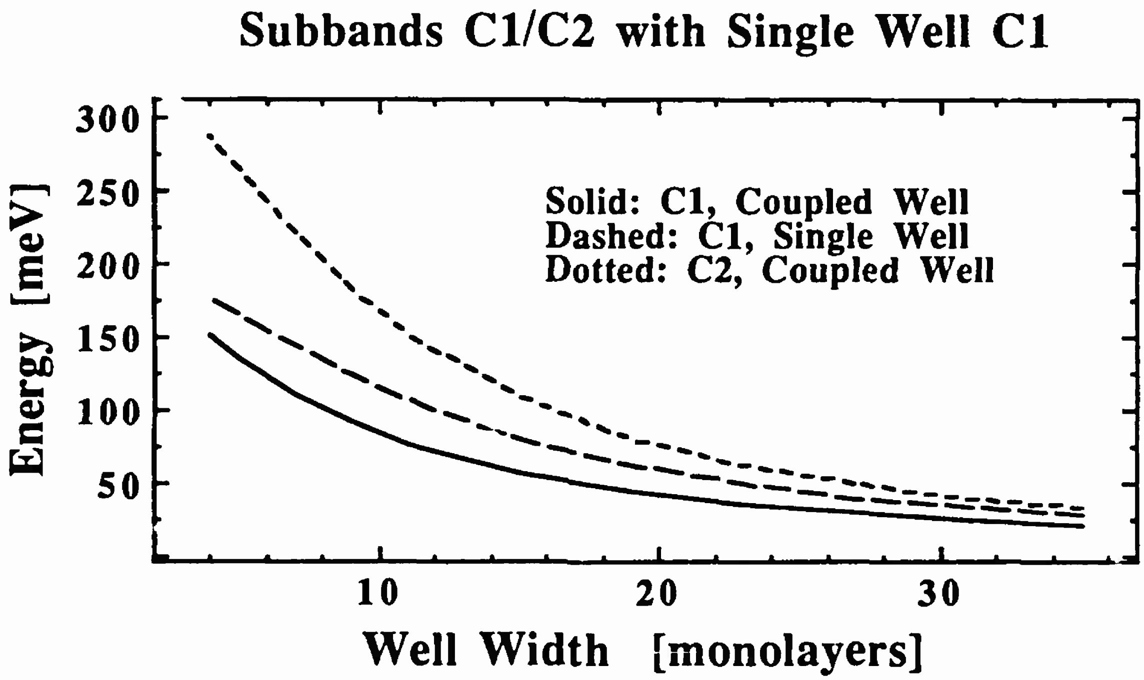

*Splitting is not even about single well state: can not assume equal splitting

*Coupled Well C1 behavior could be due to bulk bandedge

* Assumption of equal splitting is okay for wide wells and barriers

Subband Behavior as a Function of Barrier Width

Plot the position of the first two valence and conduction subbands as a function of barrier width for a fixed well width of 11 atomic monolayers, 31.1 Å.

Valence and Conduction Subbands:

HH1/HH2 Splitting vs. Barrier Width

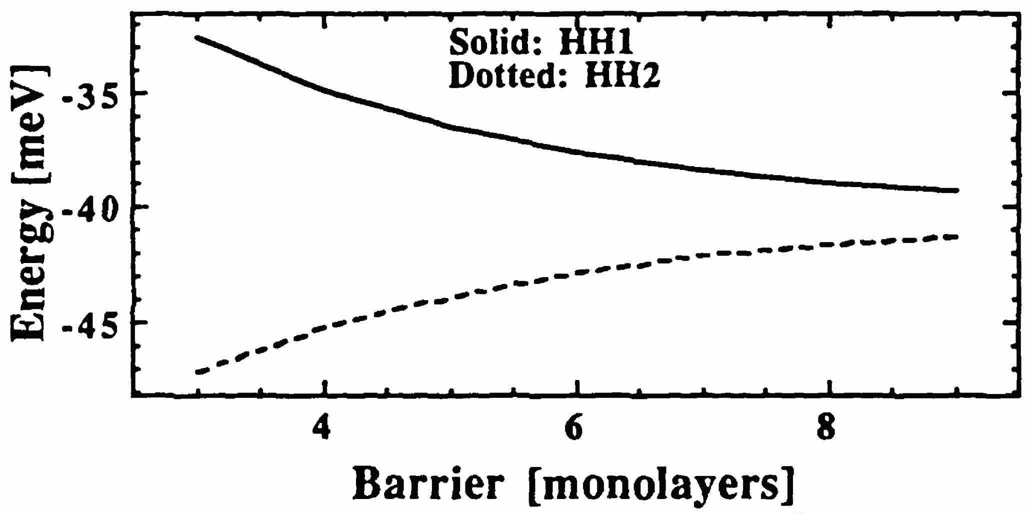

Barrier Width Behavior, cont.

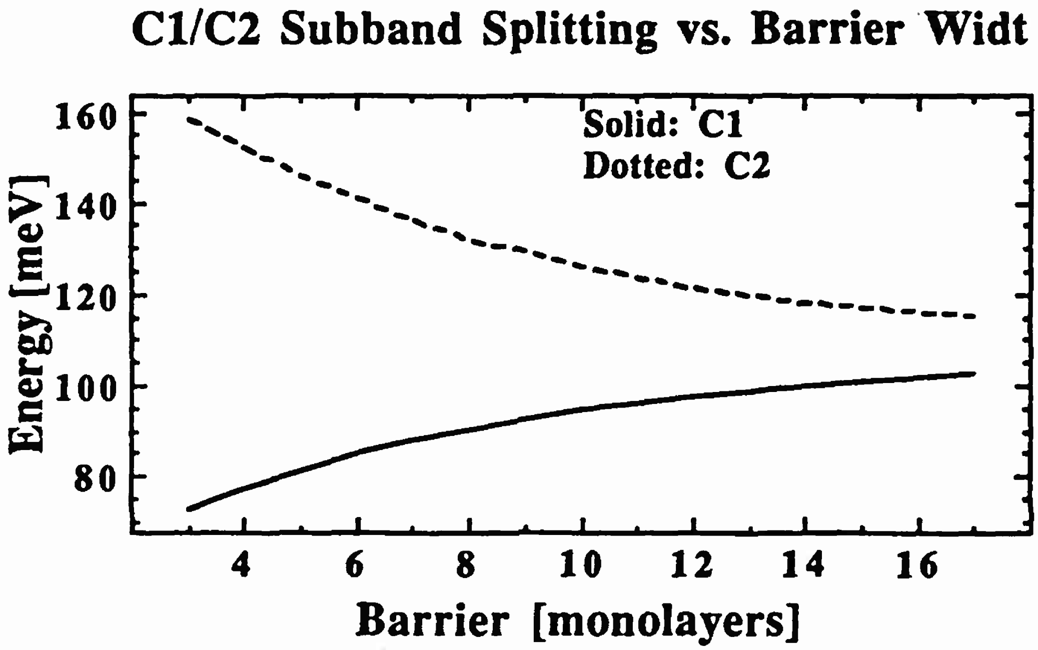

*Splitting is greater for the conduction states than for the valence states: follows from effective mass argument

*Functional form for both cases is quite simple: Use a simple fitting function?

Fitting Functions

It is seen that a simple function can be fit to the subband energy positions as a function of both well and barrier widths in SCQWs.

The functional form is:

$$D = \frac{A}{x^2} + \frac{B}{x} + C$$

where

D is the energy position
x is the well or barrier width
and A, B and C are system dependent parameters

*This function works well for the systems studied.

*It can also be applied to subband splittings since they are simply the difference between subband positions.

Fit to Valence Subbands

Plot the HH1 and LH1 subband energy positions for various well widths and a barrier width of 4 monolayers, 11.4 Å.

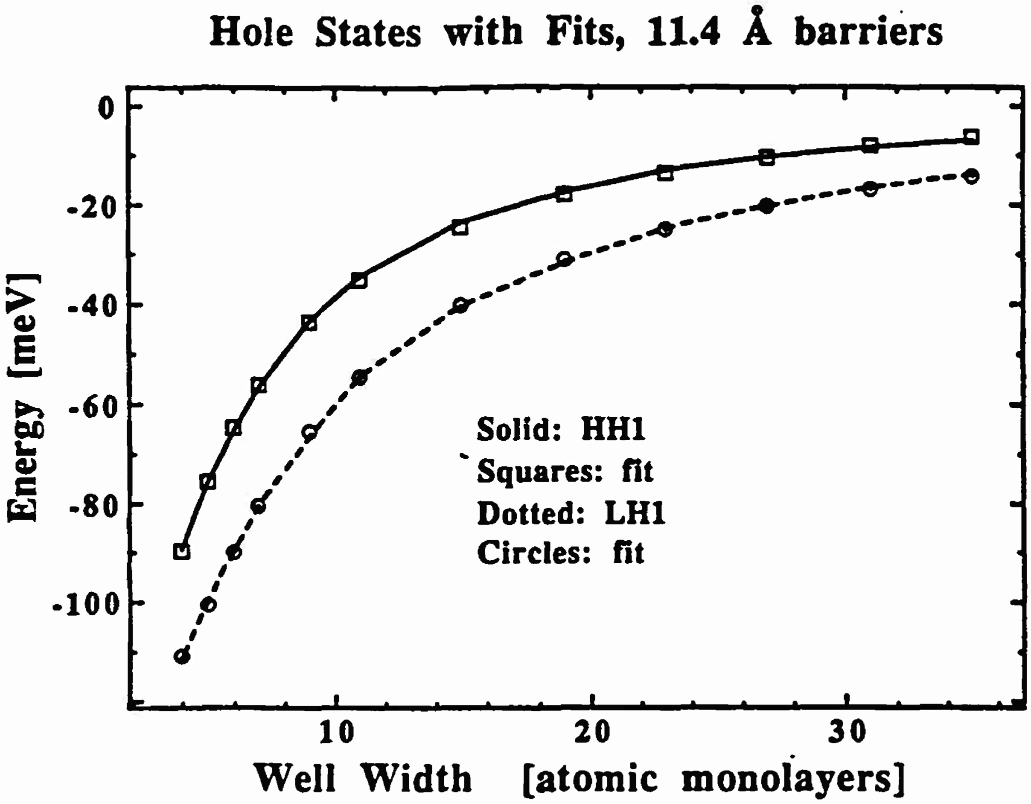

***Fit is excellent for both bands over entire region studied.**

Fit to Conduction Subbands

Plot the C1 and C2 subband energy positions for various well widths and a barrier width of 4 monolayers, 11.4 Å.

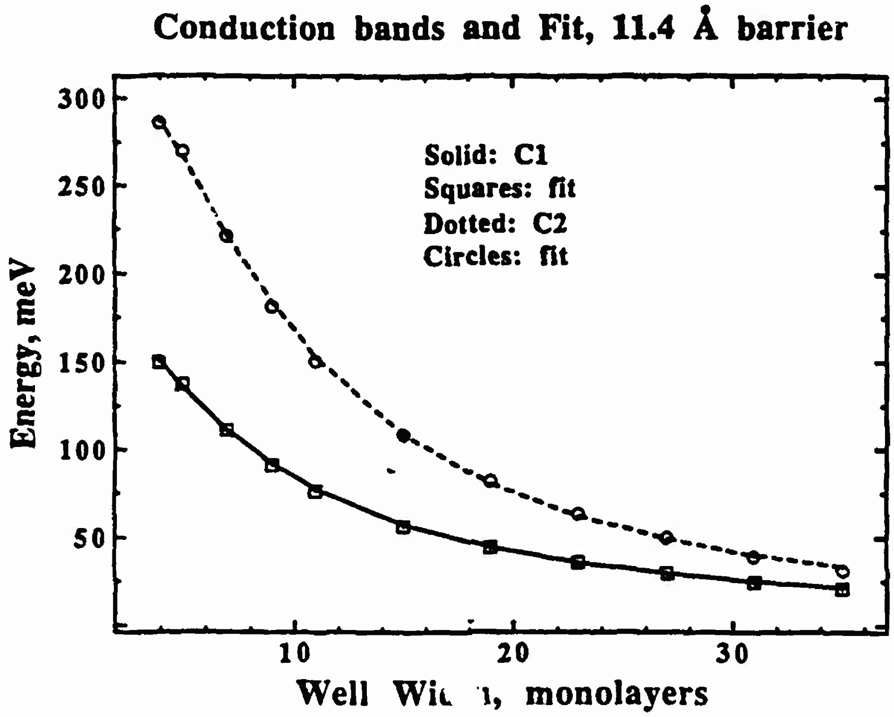

*Fit is quite good for the conduction bands also.

Fit as a Function of Barrier Width

The separation between the first two conduction states as a function of barrier width for a well width of 11 monolayers, 31.1 Å, is plotted along with the fit to it. The same functional form is used.

C1/C2 Splitting vs. Barrier, with Fit

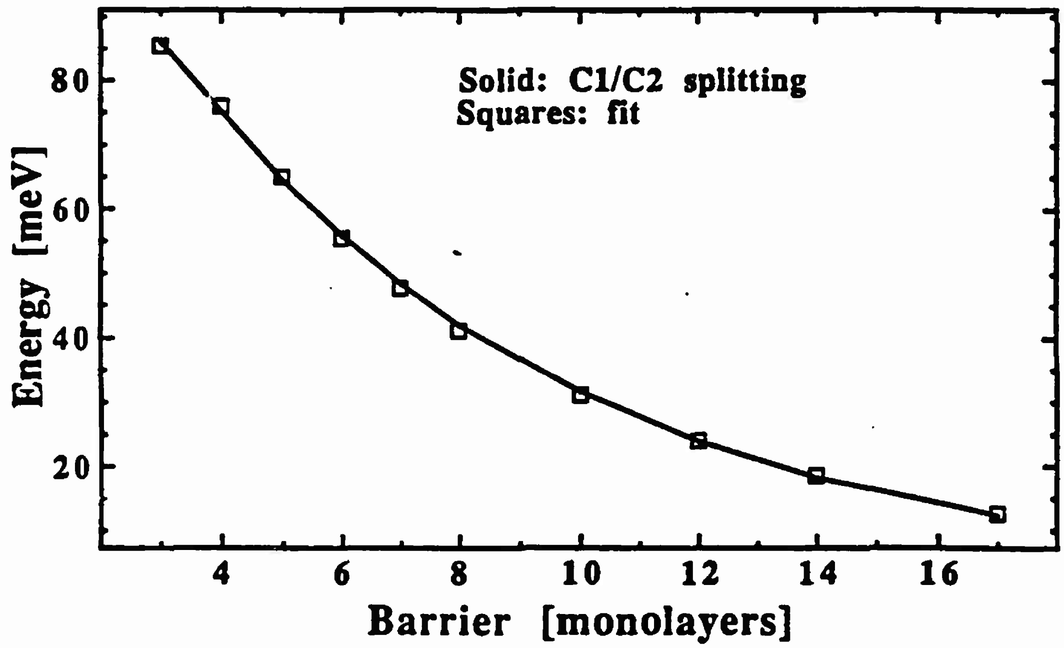

*Yariv, *et. al.*, found an exponential dependence on barrier width for the band splitting in a weakly coupled case. This case is strongly coupled.

See: A. Yariv, C. Lindsey, U. Sivan, J. Appl. Phys. 58, 3669 (1985).

Points to Note About Fitting Parameters

*The more strongly coupled subbands, conduction and light holes, have a larger inverse well width squared component.

*The more weakly coupled subbands, the heavy holes, are more linear in inverse well width.

*This is in agreement with the findings of Yariv *et. al.*, who found a linear dependence on inverse well width for a weakly coupled case.

$$D = \frac{A}{x^2} + \frac{B}{x} + C$$

Failure of the Fitting Function

The fit begins to fail in certain regions for the heavy holes. This can be explained in terms of a shift from the dominance of quantum confinement effects in determining subband location, to a region in which bulk material parameters play a larger role.

*Where quantum confinement is strong for all states, all subbands will have the same functional dependence.

*Heavy holes are the least strongly coupled due to large effective masses, so they should be the first to be more strongly affected by the bulk material.

*Fitting functions work well for light holes and electrons for well width of at least 100 Å, for these barriers, while the heavy holes go into a region where the bulk material effects are stronger: the fit begins to fail.

Summary

*Subband behavior for narrow, strongly coupled quantum wells is studied in detail.

*LH1 and HH2 subband crossover is seen at narrow well width: could be useful for Quantum Confined Stark Effect.

*Splitting of symmetric/antisymmetric states about single well state is not even for strongly coupled wells.

*Subband location and subband pair splitting can be given accurately using a simple fitting function.

*Fitting function has three system dependent parameters.

*Fitting function fails as quantum confinement gives way to the influence of the bulk material.

LIST OF ATTENDEES

4. LIST OF ATTENDEES

Name	Organization	Phone
Neil Bambha	CCNVEO	703-664-4766
David Caffey	CCNVEO	703-664-1431
Suresh Chandra	SAIC, CCNVEO	703-664-4766
J. A. Hutchinson	CCNVEO	703-664-5310
Vernon King	CCNVEO	703-664-1431
Bill Lyndon	CCNVEO	703-664-1431
Larry Merkle	CCNVEO	703-664-4766
Albert Pinto	CCNVEO	703-664-5310
C. Ward Trussell	CCNVEO	703-664-5310
Richard Utano	CCNVEO	703-664-4766
Bahram Zandi	CCNVEO	703-664-4766
Govind Agrawal	Optics, University of Rochester	716-275-4846
Mark Biermann	Optics, University of Rochester	716-275-8006
Thomas Brown	Optics, University of Rochester	716-275-7816
George Gray	Optics, University of Rochester	716-275-6892
Clifford Headley	Optics, University of Rochester	716-275-3459
Lisa Liou	Optics, University of Rochester	716-275-3459
Carlos Stroud	Optics, University of Rochester	716-275-2598
John Varriano	Optics, University of Rochester	716-275-2598
Gary Wicks	Optics, University of Rochester	716-275-4867